SLAM Method for A RFID Positioning System and A Low-cost IR Positioning System for The Indoor Mobile Robot

UNIVERSITY OF FUKUI

Abstract

Department of Advanced Interdisciplinary Science and Technology

Doctor of Engineering

SLAM Method for A RFID Positioning System and A Low-cost IR Positioning System for The Indoor Mobile Robot

by Jun Wang

In this article, contrary to the common visual sensors for the self-localization of the indoor mobile robot, we focus on utilizing the artificial landmarks and addressing the problem of the low-cost, stability and accuracy of the positioning system. Radio-frequency identification (RFID) and infrared (IR) LED systems have been used for the self-localization of the indoor mobile robot for a long time. RFID system uses an electromagnetic wave, which is robust against the influence of obstacles outside the RFID communication area or lighting conditions. Especially, comparing with the visual sensors, RFID system is robust against the data association errors. The IR system has the advantages of a stable signal, fast response, high confidentiality of information, and it is less affected by environmental change. Therefore, RFID and IR sensors are useful for the self-localization of an indoor mobile robot. However, RFID positioning system needs a large amount of preparation work, e.g., building a map of the IDs and the positions of the RFID tags and most IR-system-based self-localization approaches use a unique ID to encode the landmarks which means that some mobile robot localization techniques are inappropriate for a large indoor environment because of the limited availability of IDs and the associated high production cost.

In this work, we propose to use two novel simultaneous localization and mapping (SLAM) methods to replace the preparations of an HF-band RFID-based positioning system and a novel landmark arrangement to reduce the cost of the IDs and production cost of the IR-sensor-based positioning system. Because the tag detection of the HF-band RFID system does not follow the standard Gaussian distribution, the proposed SLAM methods use particles for the self-localization of the robot and landmark mapping. The novel landmark arrangement consisting of the IR LED arrays with unique ID-encoding capabilities based on a combination of different frequencies and the repeated ID-encoding LEDs to address the problems of limited IDs and production cost of the IR-sensor-based positioning system. Both positioning systems are verified by the experiments. The experimental results confirmed the validity of our proposed methods for both positioning systems.

Acknowledgements

I would like to thank my adviser, Professor Yasutake Takahashi for his support, his patient guidance, and constant encouragement throughout this work. I would like to thank Jian Mi, who helps me in life and research during my study aboard. I also want to thank all members of the laboratory for their helpful assistance and insightful comments. My sincere thanks also go to the teachers of Beijing Information Science & Technology University for giving me the opportunity to study abroad. My gratitude to Hirose International Scholarship Foundation for the financial support which gives me more time to invest in the study.

Last but not least, I would like to thank my family, especially my parents, my sister, and Weihua Zhu, who continually encouraged me on my academic path, and supported me in finishing this thesis.

Contents

List of Figures

List of Tables

List of Abbreviations

2D	**T**wo **D**imensional
3D	**T**hree **D**imensional
CCD	**C**harged **C**oupled **D**evice
CPU	**C**entral **P**rocessing **U**nit
EKF	**E**xtended **K**alman **F**ilter
FFT	**F**ast **F**ourier **T**ransform
HF	**H**igh **F**requency
IC	**I**integrated **C**hip
IR	**I**nfrared **R**adiation
LRF	**L**aser **R**ange **F**inder
MCL	**M**onte **C**arlo **L**ocalization
OOK	**O**n **O**ff **K**eying
PF	**P**article **F**ilter
PS	**P**article **S**moother
RBPS	**R**al **B**lackwellized **P**article **S**moothing
RFID	**R**adio **F**requency **ID**entification
RSS	**R**eceived **S**ignal **S**trength
SLAM	**S**imultaneous **L**ocalization **A**nd **M**apping
UHF	**U**ltra **H**igh **F**requency

Chapter 1

Introduction

With the development of intelligent robots, indoor mobile robots are being expected to perform more tasks. For safe and stable performance, one of the fundamental requirements for the indoor mobile robot is the localization technology. Indoor mobile robot estimates its position and orientation mainly based on the measurements obtained by the sensors which equipped on the robot and the prior knowledge such as an environment map or artificial landmarks [1][2][3][4]. The sensors used for the self-localization of indoor mobile robots are centered on laser range finders (LRFs) [5][6], ultrasonic sensors [7][8], Bluetooth [9][10], WiFi [11][12], magnetic sensor [13][14], visual sensors [15], the radio frequency identification (RFID) [16][17], and infrared (IR) sensors [18][19][20].

LRF and ultrasonic sensor based positioning systems have superiority of high accuracy and simple structures. However, the accuracy of both of these two types of sensors is easily affected by the unknown moving objects. The limitation of LRF to the transparent materials which are widely used in the current indoor environment also restricts its utilization. Although it is easy to integrate hardware of Bluetooth and WiFi into the mobile device, the energy and economic demands of Bluetooth infrastructure is high, and the localization accuracy based on WiFi is influenced by characteristics of transmitters and receivers and characteristics of the environment which influences on the radio signal propagation. The stability of the distributed magnetic filed is capable of keeping over a long period of time so that the magnetic sensor can be used for the localization of the indoor mobile based on a magnetic map. However, the practicality of the magnetic sensor for the self-localization is easily affected by

the magnetized materials. The self-localization of a mobile robot based on a visual sensor is realized without the environment alteration and is convenient for the interaction of human-computer. However, the practicality of the visual sensor is adversely affected by the environmental conditions and illumination changes.

The communication of the HF-band RFID system utilizes the electromagnetic induction. HF-band RFID system is capable of providing a precise and secure detection model. The communication of the IR system happens between the IR emitter and receiver. It supports a stable and fast signal transmission. Especially, the production cost of the IR system is commonly low which utilizes the cheap IR LEDs. Both the RFID and IR systems have the advantage of high information confidentiality and are less affected by environmental changes. These valuable characteristics are useful for the self-localization of the indoor mobile robot and prompted us to utilize an RFID system and an IR system to locate the robot. However, the RFID technology for the self-localization of the indoor mobile robot needs burdensome preparation work, such as measuring the tag positions and recording the tag IDs. Therefore, we propose two novel simultaneous localization and mapping (SLAM) methods [21][22][23][24][25][26] which is suitable to the RFID system detection model to achieve the robot self-localization and reduce the preparation work. In addition, most current IR-based positioning techniques only use unique IDs to encode the emitters for the self-localization of the indoor mobile robot. Because of the limitation of the available IDs and high system cost, this leads to some IR-based robot positioning systems are unsuitable for a large indoor environment. In this study, we propose a novel emitter arrangement for an IR-based indoor mobile robot self-localization system with the purpose of solving the difficulty of the limited available IDs and reducing the production and computational costs. In this chapter, a brief overview of two novel SLAM technologies based on RFID system and a positioning system based on the IR sensor is given to make clear the purpose of this dissertation.

1.1 SLAM Technology for HF-band RFID System

RFID system contains a reader/writer and an integrated circuit (IC) chip built-in tag. The information of the tag can be read and written by the antenna installed on the reader/writer. The communication between the reader/writer and tag using the electromagnetic wave is robust against the illumination conditions or the influence of the objects outside the communication range of the RFID system [27][28]. Therefore, RFID is capable of using for the self-localization of an indoor mobile robot [29][30][31][32]. For the self-localization of the indoor mobile robot based on the RFID system, the positions and ID information of the RFID tags are needed to be built in advance [16][33][34]. However, measuring the positions and recording ID information of the IC tags are time-consuming. Especially an RFID positioning system always needs a huge amount of tags to achieve an accurate estimation.

With the rapid development of self-driving, visual sensors and LiDAR devices based SLAM technologies are widely applied in outdoor environments. SLAM as the underlying technology can be used for performing the localization of the vehicle and building the environment map simultaneously [35][36][37]. SLAM method is also being expected to use for the indoor robots to make a safe and more intelligent performance. Landmark-based SLAM [38][39] utilizes the feature objects in the environment as landmarks and builds a landmark map while localizes the robot. The RFID IC tags in the environment can be used as the landmarks of the SLAM technology. Therefore, by using the landmark-based SLAM method, the robot is able of localizing itself without a prior knowledge of positions and ID information of the IC tags so that the labor and time costs can be reduced.

1.1.1 Particle Filter used for the Landmark Updating of The SLAM Method

FastSLAM [40][39] which using the Kalman filter to update the tag locations was utilized in an unknown indoor environment to achieve the self-localization

of the mobile robot and the localization of HF-band RFID tags simultaneously by Wang and Takahashi [41]. The RFID system with a small detection range obtained a good performance by using FastSLAM. The robot localization and tag location errors are within 3 cm. The antenna of the RFID reader used in [41] is very small so that 96 readers are needed to cover a wide detection range. A large number of RFID readers seriously increases the production cost of the system. The antenna with a large detection range is needed to reduce the number of the readers for a practical RFID system. However, the non-Gaussian detection model of the HF-band RFID system makes the Kalman filter is unsuitable for the estimation of the IC tag locations. This problem becomes obvious with the increase of the detection range. Moreover, the insufficient scalability of FastSLAM easily results in a failure in an environment with a greater number of landmarks.

Therefore, we propose the SLAM method of using the particle filter [42][43][44][45] for both the robot localization and the location of the IC tags. Particle filter does not need any parametric model so that it is suitable to the SLAM technology based on HF-band RFID system with the non-Gaussian detection model. Self-localization of the mobile robot is estimated by Monte Carlo localization (MCL) [46][47] method. A set of independent particle filters are used to the landmark mapping. Each detected IC tag is assigned with a particle filter which makes the proposed SLAM method is capable of achieving a good scalability for the environment with a great number of RFID tags.

1.1.2 Particle Smoother used for the Landmark Updating of The SLAM Method

Particle filter is suitable to the positioning system based on RFID with the non-Gaussian detection model. However, the shortage of the degeneracy problem of the particle filter possibly causes a large error for the SLAM method [48][49][50]. By adding a Gaussian random value to each particle for estimating the robot localization during the motion model updating step at each loop

of the SLAM procedure, the degeneracy problem of the robot particles can be avoided. However, the particles for estimating a stationary landmarks are updated within the states initialized at the first detection of this landmark by using the particle filter. The tag particles easily converge to a small number of particles at the resampling step and generate the degeneracy problem when using a RFID reader with a large detection range. This degeneracy problem of the particle filter for estimating the tag location easily leads to a wrong estimation. Especially, with the increase of the detection range of the RFID reader, the effect of the degeneracy problem of the particle filter for estimating the landmark becomes serious.

Therefore, a novel SLAM method is proposed to use the particle smoother [51][52][53] to update the landmark location. In this study, the fixed-lag smoothing method [54][55] is used for the particles for estimating the tag location. Each detected IC tag is updated by an independent particle smoother. By using the fixed-lag smoothing method, the particles for estimating a detected tag are updated by adding a Gaussian random value in the subsequent detection after the first detection of this tag. In addition to the states initialized at the first detection, novel states of the tag particles are generated by adding the Gaussian random value at the updating step. The position of the detected tag is updated based on both the historical and current states of the particles. The utilization of the particle smoother effectively suppresses the degeneracy of particles for estimating the location of IC tags and smooths the estimation when using an RFID reader with a large detection range. Self-localization of the mobile robot in this novel SLAM method also utilizes Monte Carlo localization method.

1.2 Self-localization Based on IR System

IR position systems for the indoor mobile robot mainly based on the devices of the IR emitter and receiver [56][57][58][59]. IR receiver always set on the robot to scan the IR signal transmitted from the emitter. Some researches positioned the IR emitters in the environment as the active landmarks and transmit the

encoded IR signal [60][61]. The robot estimates the position and orientation of the robot based on the signal information of the detection emitter through the receiver. Other researches utilize the IR light-reflecting materials as the passive landmarks [62][63]. Both an emitter and an IR camera receiver are integrated into the mobile robot. The emitter continuously transmits the IR signal to the environment. The signals transmitted to the IR light-reflecting materials are reflected and received by the IR camera. The robot recognizes the landmarks through the signals and locates itself based on the measurements with the detected landmarks.

The landmark used for current active or passive landmark-based IR self-localization systems is encoded by the unique ID. Because of the limitation of the valuable landmark IDs and the related high production cost, some IR-system-based localization systems are inappropriate for a large indoor environment. However, a mobile robot with the assistance function is expected to play a greater role in a large indoor environment, such as the hospital, large exhibition centers, large dining halls, and large sports complexes. Therefore, a novel landmark arrangement is proposed to support an adequate number of available IDs and reduce the production and computational costs for the IR-system-based self-localization system capable of being utilized in a large environment. Two types of the IR emitters are used as the active landmarks and applied to the novel landmark arrangement. The emitters are installed on the ceiling to minimize disturbance of the signals by obstacles. The first type of the emitter is a unique ID encoded IR LED array. The other is a repeated ID encoded IR LED. The ID of the IR emitter is driven by an on-off Keying (OOK) modulator [64][65] through a microcontroller. We use the frequency of the OOK modulator to encode the IDs of the IR emitters in this study. The unique ID is composed of multiple frequencies by a mathematical combination method. The repeated ID only contains a single frequency. Nine frequencies are supported to design the IDs in this research; however, 511 available IDs can be obtained by using the mathematical combination method. Using the repeated ID encoding emitter of the proposed emitter arrangement makes these available IDs can

be applied to a larger environment. Moreover, this novel arrangement of the landmarks is also suitable for an indoor mobile robot self-localization system with other-sensors-based landmarks.

Two receivers are set on the top of the mobile robot to detect the IR signals. The robot utilizes the detected IR signals to recognize the emitters and realize self-localization based on the measurements. Because of repeated IDs utilized in the emitter, a belief function is applied to compute a probability for each emitter with the detected repeated ID. The emitter with the largest belief value is considered as the detected emitter. The MCL method with this belief function is used to estimate the localization of the robot in this research.

Chapter 2

Related Work

2.1 SLAM based on Particle Method

In this dissertation, two novel SLAM technologies with the landmark updating respectively based on particle filter and particle smoother are proposed. Early landmark-based SLAM works with filter method were mainly based on the extended Kalman filter (EKF) [66][67][68]. In addition to the filter method, pose graph as a optimization method is widely used for the visual SLAM method. EKF SLAM as one of the early SLAM methods with filter method has obtained some successful applications. However, EKF SLAM is limited to the shortage of the computational complexity and the requirement of the Gaussian assumption. Murphy described that the method of using Rao-Blackwellized particle filters for solving the SLAM problem [69][70] is an effective approach. FastSLAM proposed by Montemerlo et al. utilized a Rao-Blackwellized particle filter to estimate the pose of the robot and a separate EKF to update the position of each landmark which improves the flexibility and reduces the computational complexity. However, these EKF-based SLAM methods assumed that the landmark detection could be modeled by a Gaussian model. Some sensors used for the SLAM technology do not follow the Gaussian model so that the estimation based on the EKF method becomes inaccurate and unstable.

2.1.1 Particle Filter used for SLAM Technology

Particle filter is based on the particles with the probability densities, which can be utilized to a non-linear/non-Gaussian state space model. Eliazar and Parr [71] proposed a particle filter-based SLAM method called DP-SLAM based on a laser detection model. DP-SLAM uses a particle filter to maintain a joint probability distribution of robot location and maps which effectively eliminates the accumulated errors of the map. Forster et al. [72] estimate the tag positions in a hybrid metric-topological map by particle filter with the received signal strength information from the sensor model.

Joho et al. [73] built a novel combined sensor model for the self-localization of a mobile agent and UHF RFID tag mapping by using the tag detection of the RFID system and the received signal strength. The map of the tags is built based on the assumption that the antenna set on the robot was known in advance. With the known locations of the RFID tags, the robot location can be estimated by using the same sensor model. The error of the tag locations is about 27 cm based on the predefined trajectory. Comparing with this research, the HF-band RFID system used in our research does not provide the received signal strength (RSS) information. Moreover, the self-localization of the robot and tag location are performed simultaneously in our research. The proposed sensor model for both estimations of the RFID locations and the robot poses provides us realize the SLAM study by the particle filter.

Deyle et al. [74] presented a mobile robot equipped with a UHF RFID reader with multiple antennas and utilizes a particle filter implementation for estimating the location of the RFID tags in the environment. A new particle filter framework is developed for estimating the distance and bearing of the UHF RFID tag respected to the reader which positioned on the robot by incorporating with RF signal propagation models. A mean range error of 690 mm and a mean bearing error of 6.1 degrees are presented over the distances of the robot to tag over 4 m based on the proposed method in [74]. The localization system used in our research is based on an HF-band RFID system. The detectable range of the HF-band RFID system is shorter than the UHF-band RFID system. It makes the

accuracy of the HF-band RFID system higher than UHF-band RFID system. According to the experiment results, our proposed method based on an HF-band RFID system obtained more accurate results. Especially, we applied the particle filter based landmark updating in the SLAM study without an RFID signal propagation model.

2.1.2 Particle Smoother Used for SLAM Technology

Particle filter can be utilized for the landmark estimation of the SLAM based on the HF-band RFID system with the non-Gaussian detection model within a certain detection range. However, the degeneracy problem of the particle filter for estimating the tag location becomes serious with the increase of the detection range. Because of this disadvantage of the particle filter, a particle smoother is proposed to estimate the position of each landmark in this study. We used the fixed-lag smoothing algorithm proposed by Kitagawa [54] to update the landmark location. The computational cost of the fixed-lag smoothing method which based on the storing state vector is almost the same as the particle filter. An additional requirement of this method is a little memory for storing the historical states of the particle. The fast computation of the fixed-lag smoothing method makes the proposed SLAM be capable of performing in real time.

Berntorp and Nordh proposed to utilize the Rao-Blackwellized particle smoothing (RBPS) for occupancy-grid based SLAM with an ultrasound sensor [75]. The authors implemented an RBPS for jointly estimating the position of the robot and the map. A more effective map model incorporates the uncertainty of the measurements was used in this approach. The proposed method was verified on a Lego Mindstorms mobile robot which has low-performance motors, with a low-cost ultrasonic range finder. The experimental results show that the smoothing gives a substantial robustness improvement and increased predictability of the proposed algorithm. However, each particle contains an estimate of the entire map in [75], thus it is of significant size. The computational demands then using smoothing are also greater than for filtering by using the method. This means that for larger maps, the memory requirements and the

computational cost will be a problem. In our proposed method, each landmark is updated by a set of particles with the fixed L-lag smoothing method. The computational cost of this method is almost the same as the particle filter. The only requirement is a little memory for storing the particles.

Clark et al. developed the random finite set approach to SLAM by introducing forward-backward smoothing in order to refine the vehicle trajectory [76]. The algorithms are implemented with sequential Monte Carlo and Gaussian mixture techniques. The proposed method was evaluated in a simulated environment with a range and bearing detection model. In this scenario, the uncertainty in the distribution on the vehicle position grows as the vehicle traverses the path until the loop is closed, and the uncertainty decreases at this point. By smoothing backwards at times just prior to the loop closure, a significant reduction is achieved in the estimated vehicle position. Comparing with [76], we proposed to use the smoother to refine the estimation of the landmark. Our proposed method is capable of using for the non-Gaussian RFID detection model.

2.2 IR-sensor-based Self-localization System

IR sensor has been widely used for the indoor positioning system. Some IR passive landmark based self-localization systems were developed for the indoor mobile robot. The Hagisonic StarGazer localization system [77] has been widely used for the researches and sold as a commodity. Ul-Haque et al. [78] evaluated the Hagisonic StarGazer localization system and point out this system to be reliable, stable and, accurate. Oh et al. [62] also evaluated this localization system. Several types of errors are found in the experiments. They utilized an optimal arrangement of landmarks and an EKF to improve the accuracy. The passive landmarks used in the Hagisonic StarGazer localization system are easily installed and inexpensive. An HLD1-L 4x4 grid passive landmark used in this system is approximately $3.52. However, the localization sensor of the

Hagisonic StarGazer localization system costs nearly $1,400 which is unsuitable for an environment with multiple mobile robots. Moreover, the Hagisonic StarGazer localization system offers only thousands of unique IDs leads to it is not appropriate to a large-scale environment, whereas our proposed system is able of supporting more unique IDs. Especially, our proposed system utilizes repeated IDs encoding landmarks in the environment.

Most of the active IR landmark-based localization systems utilize the emitter as the active landmark. Krejsa and Vechet [60] used IR beacons and a scanner realize the self-localization of the indoor mobile robot. The IR beacons are placed in the environment with known positions. The scanner is placed around the robot with 16 receivers to cover the entire range of 360 degrees. The self-localization of the mobile robot was estimated by the EKF method based on the measurements of the scanner. Hijikata et al. [18] proposed an indoor self-localization system by using the IR LEDs as the landmarks and a CCD camera to observe the IR LEDs. The IR LEDs are observed as bright spots by using the CCD camera with the optical filter. The self-localization problem is solved with the nonlinear least squares method. This system is light because it only needs several LEDs and a CCD camera. The proposed system is easily installed in the environment and needs low production cost. Jungyun Bae et al. [19] designed a mobile robot localization system based on the coded IR light. Several IR LEDs coed by unique IDs are put on the ceiling. The robot activity area is divided into several sections by the combination of different ID encoding LEDs. The robot can roughly estimate itself by identifying these unique sections. They also presented an algorithm that combines both the dead-reckoning and the detected IR signal to improve the accuracy of the estimation.

Comparing these approaches with our proposed method, we make a more delicate treatment of the IR signal by using the RSS method to obtain a more accurate result. Especially, some IDs are repeatedly used in the environment so that the production costs are reduced.

Gorostiza et al. [79] tried to use the receiver which positioned on the ceiling as the landmark to estimate the position of the mobile robot. An emitter was

set on the top of the robot and continuously transmits the modulated IR signal. The distance between the receiver and emitter could be calculated based on the phase-shift. Therefore, the position of the robot was estimated by hyperbolic trilateration method. The precision of this system is below 10 cm based on the experiment results. The limitation of available IDs is solved by placing the receiver in the ceiling other than utilizing the emitter as the landmark. However, the communication cost between the robot and backstage controller increases when multiple robots operation in the workspace. Moreover, the receiver commonly complex than the emitter which makes the production cost of the system proposed in [79] increases obviously in a large environment.

Chapter 3

SLAM Method utilizing Particle Filter for Landmark Updating on RFID System

This chapter introduces the SLAM method with particle filter based landmark updating in detail. To make the article concise, we refer to it as PF-SLAM in the following description. First, the RFID system used in our study is presented in Section 3.1. In Section 3.2, FastSLAM based on RFID system is briefly reviewed. In Section 3.3, the proposed SLAM algorithm is explained and compared with FastSLAM in computational efficiency. The results of PF-SLAM from simulations and the real experimental environment are shown in Sections 3.4 and 3.5. Last, summaries are drawn in Section 3.6.

3.1 RFID Positioning System for Indoor Mobile Robot

The communication of the HF-band RFID system [80][81] utilizes the electromagnetic induction. Although the communication range of the HF-band RFID system is shorter than the UHF-band RFID system [82][83], the communication of the HF-band RFID system is robust against the influences between the antenna and tags. This character makes the landmark detection of the SLAM work reliable and precise.

Figure 3.1 shows the RFID system used for the SLAM work with an indoor mobile robot. Eight RFID readers are installed on the bottom of the mobile

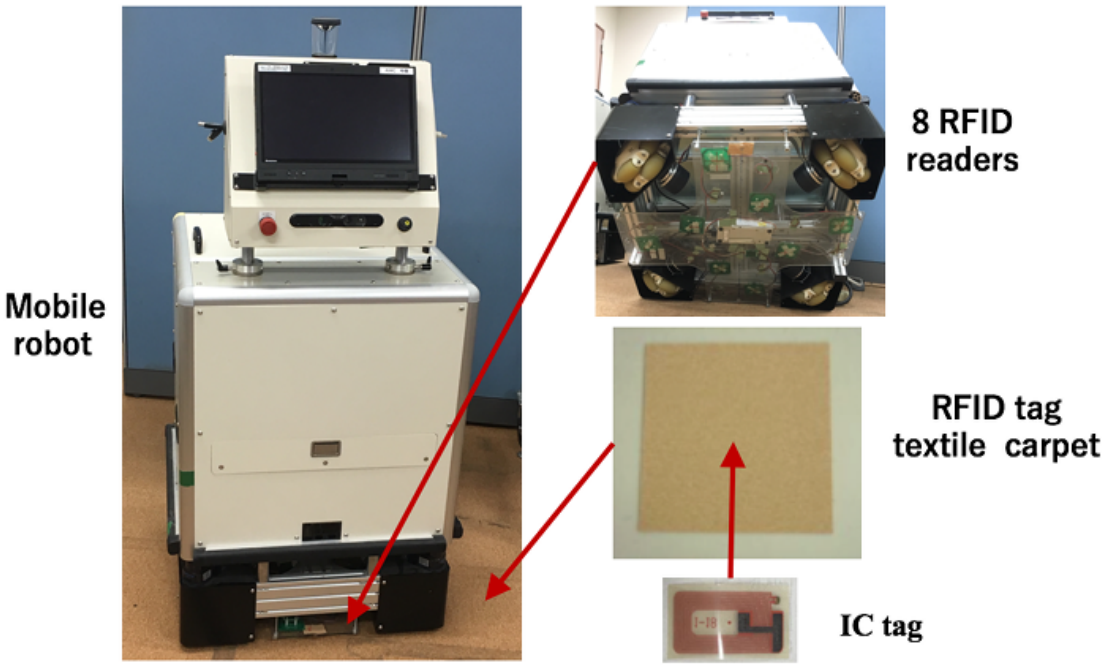

FIGURE 3.1: RFID system used for an indoor mobile robot.

robot. The detection range of the RFID reader in this study is 60 $\times$ 60 mm^2. The RFID tags are embedded in the floor carpet. One RFID tag is presented in Figure 3.1 and the size of this RFID tag is 10 $\times$ 20 mm^2. Each RFID tag has a unique ID so that the detection of RFID tags more reliable. Two types of carpets with densities of 100 tags/m^2 and 16 tags/m^2 are spread on the floor. The ideal configures of 8 RFID readers and two types of RFID tags are shown in Figure 3.2. However, it is difficult to position the RFID readers and tags precisely as Figure 3.2 shows. Therefore, they are installed with unavoidable errors in practical environment. In this study, the IDs and associated positions of the tags are unknown for the robot. The robot detects the RFID tags by using the RFID readers. The mobile robot self-localization is achieved and modified based on the RFID tags and the locations of the RFID tags are updated simultaneously during the robot movement.

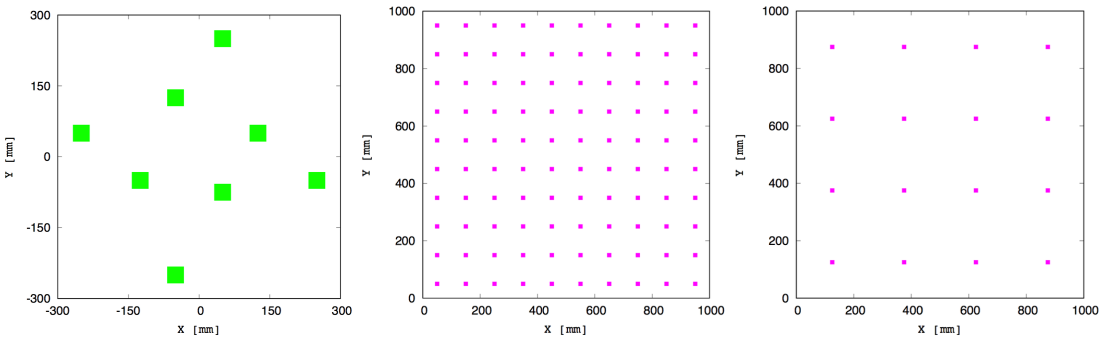

(a) Configuration of the RFID readers (b) Configuration of the RFID tags with 100 tags/mm^2 (c) Configuration of the RFID tags with 16 tags/mm^2

FIGURE 3.2: Configurations of RFID readers and tags.

3.2 FastSLAM for RFID system

From a probabilistic perspective, the SLAM problem can be written in the factored form:

$$p(\boldsymbol{x}_{1:t}, \boldsymbol{m} \mid \boldsymbol{z}_{1:t}, \boldsymbol{u}_{1:t}, \boldsymbol{n}_{1:t}) = p(\boldsymbol{x}_{1:t} \mid \boldsymbol{z}_{1:t}, \boldsymbol{u}_{1:t}, \boldsymbol{n}_{1:t}) p(\boldsymbol{m} \mid \boldsymbol{x}_{1:t}, \boldsymbol{z}_{1:t}, \boldsymbol{u}_{1:t}, \boldsymbol{n}_{1:t}) \quad (3.1)$$

where $\boldsymbol{x}_{1:t}$ is the path of the robot, $\boldsymbol{m}$ is the map built during the movement, $\boldsymbol{z}$ means the observation, $\boldsymbol{u}$ is the robot control, and $\boldsymbol{n}$ is the index of the detected landmark.

FastSLAM utilizes a particle filter to estimate the robot paths of the first term in the posterior in Equation. (3.1). A separate estimator is used to locate the position $p(\boldsymbol{m}_n \mid \boldsymbol{x}_{1:t}, \boldsymbol{z}_{1:t}, \boldsymbol{u}_{1:t}, \boldsymbol{n}_{1:t})$ for each landmark in $\boldsymbol{m}$. Each particle in FastSLAM is of the form

$$\boldsymbol{y}_t^{[i]} = < \boldsymbol{x}_t^{[i]}, \omega^{[i]}, \mu_{1,t}^{[i]}, \Sigma_{1,t}^{[i]}, ..., \mu_{N,t}^{[i]}, \Sigma_{N,t}^{[i]} > \quad (3.2)$$

where $\boldsymbol{y}_t^{[i]}$ is the combined state vector of the robot pose and the map. ω^i is the importance weight of particle $[i]$. $\mu_{n,t}^{[i]}$ and $\Sigma_{n,t}^{[i]}$ are the center vector and the covariance matrix of the Gaussian distribution of the landmark n, respectively.

The posterior of the FastSLAM is transformed to:

$$p(\boldsymbol{y}_{1:t} \mid \boldsymbol{z}_{1:t}, \boldsymbol{u}_{1:t}, \boldsymbol{n}_{1:t}) = p(\boldsymbol{x}_{1:t} \mid \boldsymbol{z}_{1:t}, \boldsymbol{u}_{1:t}, \boldsymbol{n}_{1:t}) \prod_{n=1}^{N} p(\boldsymbol{m}_n \mid \boldsymbol{x}_{1:t}, \boldsymbol{z}_{1:t}, \boldsymbol{u}_{1:t}, \boldsymbol{n}_{1:t}) \quad (3.3)$$

N is number of the landmarks set in the environment.

The position parameters of the landmarks are updated by an EKF. Figure 3.3(a) shows a likelihood model belongs to a Gaussian distribution. The detection model of a general range and bearing sensor always follows this distribution. However, the detection model of the HF-band RFID system is close to a step function. The likelihood model of the RFID system with the size of 60 $\times$ 60 mm^2 is shown in Figure 3.3(b). It does not belong to a Gaussian distribution. The detection model of the RFID antenna with the size of 60 $\times$ 60 mm^2 or larger is unsuitable to be modeled as a Gaussian distribution. Therefore, Kalman-filter-based FastSLAM is not appropriate to the SLAM task based on the RFID system with a large antenna.

3.3 SLAM Method utilizes Particle Filters for The Robot and Landmark Localization

Because of the non-Gaussian detection, particle filter is proposed to estimate the RFID tag location. Each detected tag is updated by an independent particle filter. The pose of the mobile robot is also estimated by a particle filter. A total of $1 + N$ independent particle sets are utilized for the proposed SLAM method. One particle set is used for estimating the self-localization of the mobile robot and N particle sets are utilized for updating the locations of N detected tags. Each robot particle is of the form

$$\boldsymbol{x}_t^{[i]} = <^{w} \boldsymbol{x}_t^{[i]}, \omega_{r,t}^{[i]} > \quad (3.4)$$

where ${}^{w}\boldsymbol{x}_t^{[i]}$ is the position and orientation of particle $[i]$ in the world coordinate at time t and $\omega_{r,t}^{[i]}$ represents the importance wight of robot particle $[i]$. Each tag

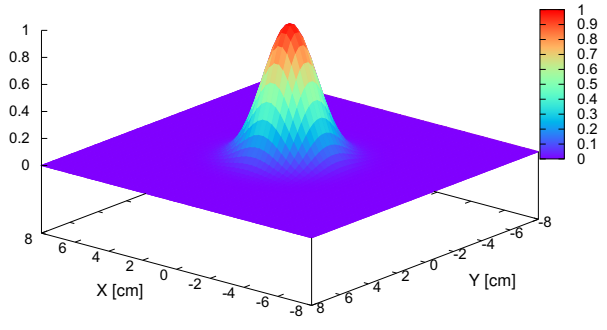

(a) Gaussian distribution

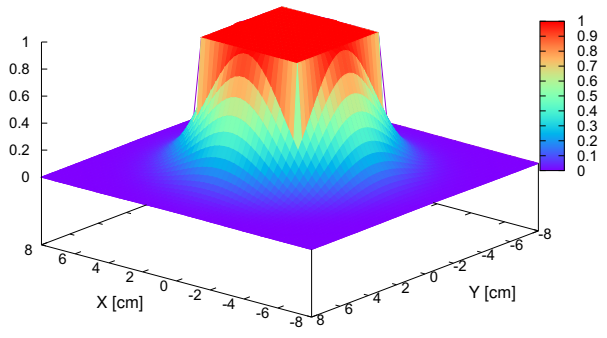

(b) Non-Gaussian distribution

FIGURE 3.3: Distributions of the likelihood with (a) Gaussian model and (b) non-Gaussian model.

particle is of the form

$$\boldsymbol{m}_{n,t}^{[j]} = <^{w} \boldsymbol{m}_{n,t}^{[j]}, \omega_{n,t}^{[j]} > \tag{3.5}$$

where ${}^{w}\boldsymbol{m}_{n,t}^{[j]} = ({}^{w}x_n, {}^{w}y_n)$ presents the location of tag n in the world coordinate system. $[j]$ is the index of the tag particle. The importance weight of tag particle $[j]$ is represented by $\omega_{n,t}^{[j]}$.

Algorithm 1 presents the PF-SLAM algorithm utilizes independent particle filters for both the self-localization of the robot and landmark updating. The robot starts with a known position and orientation. The particles for estimating

Algorithm 1: PF-SLAM:

Initialization of the robot particle set $\boldsymbol{S}_{r,t} = (\boldsymbol{x}_t^{[1]}, \boldsymbol{x}_t^{[2]}, \cdots, \boldsymbol{x}_t^{[I]})$
for $i = 1$ to I **do**
  Robot particles are updated by the motion model:
  ${}^{w}\boldsymbol{x}_t^{[i]} = MotionModel({}^{w}\boldsymbol{x}_{t-1}^{[i]})$
end for
if landmark n is detected **then**
  if landmark n never seen before **then**
    Initialize a new tag particle set $\boldsymbol{S}_{n,t} = (\boldsymbol{m}_{n,t}^{[1]}, \boldsymbol{m}_{n,t}^{[2]}, \cdots, \boldsymbol{m}_{n,t}^{[J]})$
  else
    for from $j = 1$ to J **do**
      Update $\omega_{n,t}^{[j]}$ for each particle in $\boldsymbol{S}_{n,t}$
    end for
  end if
  for from $j = 1$ to J **do**
    Create particle $[k]$ with probability $\propto w_{n,t}^{[j]}$
    Add $\overline{m}_{n,t}^{[k]}$ to $\boldsymbol{S}_{n,t}$
  end for
  for from $i = 1$ to I **do**
    Update $\omega_{r,t}^{[i]}$ based on the likelihood function
  end for
end if
for from $i = 1$ to I **do**
  Create particle $[o]$ with probability $\propto w_{r,t}^{[i]}$
  Add $\overline{x}_{r,t}^{[o]}$ to $S_{r,t}$
end for
Return $\boldsymbol{S}_{r,t}$, $\boldsymbol{S}_{n,t}$

the robot localization are initialized around the start point. These robot particles are updated by the motion model at each loop of the SLAM procedure. The motion model used in this study is expressed as

$$ {}^{w}\boldsymbol{x}_{r,t} = {}^{w}\boldsymbol{x}_{r,t-1} + V\Delta t + \epsilon\Delta t, \quad \epsilon \sim N(0,\sigma) \tag{3.6} $$

where $V = (v_x, v_y, \omega)$ and Δt are the velocity of the robot and the period between times $t-1$ and t, respectively. $N(0,\sigma)$ denotes the Gaussian distribution with the standard deviation σ.

When a tag is detected by an RFID reader, the robot recognizes this tag if seen before by its ID firstly. If never detected before, a novel tag particle set is assigned to this tag for estimating its position. The tag particles are initialized around the area of the reader that detected this tag and assigned with an importance weight value 1. Otherwise, the importance weights of these tag particles are updated based on the likelihood function. The likelihood function is associated with the HF-band RFID detection model. Particles in the detection area have the same possibility as the real tag location as shown in Figure 3.3(b). The likelihood function is defined as a piecewise function as

$$ \omega = \begin{cases} 1, & \text{if } |e_x| < \sigma \; and \; |e_y| < \sigma \\ \beta \exp\left(-\frac{1}{2\sigma^2}\boldsymbol{e}^{\mathrm{T}}\boldsymbol{e}\right), & \text{else} \end{cases} \tag{3.7} $$

where $\boldsymbol{e} = (e_x, e_y)^{\mathrm{T}}$. $e_x = {}^{r}x_n - {}^{r}x_b$ and $e_y = {}^{r}y_n - {}^{r}y_b$. $({}^{r}x_n, {}^{r}y_n)^{\mathrm{T}}$ means the location of the detected tag n in the robot coordinate. $({}^{r}x_b, {}^{r}y_b)^{\mathrm{T}}$ presents the location of reader b that detects tag n in the robot coordinate. σ is set at 30 and β is a constant. $||$ is the symbol of the absolute value. The positions of the RFID readers can be calculated through configure of the readers as shown in Figure 3.2(a). At the resampling step, a new distribution of the detected tag particles is generated according to the importance weights obtained by Equation (3.7). The position of the detected tag is estimated based on the new distributed tag particles.

Then, the position and orientation of the robot are estimated by using the

updated tag location. The importance weights of the robot particles are also updated by Equation (3.7). In this step, ${}^{r}\boldsymbol{x}_n$ is known and used as the observation value. After the importance weight of each robot particle is updated, the resampling is executed. A new distribution of the robot particles are obtained. Finally, the position and orientation of the robot is estimated by using the updated robot particle set.

Figure 3.4 shows the procedure of the PF-SLAM based on the RFID system. Particles around the center of the robot are used for estimating the self-localization of the mobile robot. These particles are always updated by the motion model during the movement. When the robot detects a new tag, a new tag particle set is assigned to estimate the tag location. These tag particles are randomly distributed in the detection range of the reader with importance weights 1 in the beginning. As shown in Figure 3.4(b), if this tag is detected again, another detection area of the reader is defined. The importance weights of some particles in the area of first detection but outside the area of second detection are updated with smaller values. These particles are transformed into particles with larger importance weights at resampling step. A more accurate area for the detected tag is achieved based on second detection. The particles for estimating the localization of the mobile robot are also updated after the estimation of the detected tag. A more accurate estimation of the robot localization can be obtained with the decrease of the possible area of the detected tag. The feasible area of the detected tag becomes much smaller with multiple detection by the mobile robot at additional location as shown in Figure 3.4(c). A greater accuracy of the tag location is obtained. The accuracy of the robot localization also improves.

This hypothesis is evaluated in a simulation by moving the robot in a random method to detect a tag at more locations. The accuracy of the tag estimation is recorded during the detection. The evolution of the error of the tag estimation against the detection times is shown in Figure 3.5. The error of the estimation decreases with the increases of the detection times which proves the validity of the hypothesis mentioned above. Even though the converge of the

tag particles becomes difficult after the 65 detection times, the accuracy is sufficient for the estimation of the tag locations.

3.3.1 Comparison between FastSLAM and PF-SLAM

The computation efficiency of the proposed PF-SLAM is compared with FastSLAM. Equation (3.2) presents the form of the particle in FastSLAM. If M_f particles and N landmarks are used in FastSLAM, a memory size of $O(M_f N)$ is needed. The forms of the robot particle and tag particle in PF-SLAM are defined in Equations (3.4) and (3.5). If we use M_p robot particles and J tag particles for each landmark. The proposed SLAM method needs a memory size of $O(M_p + JN)$. Because the scale of the possible area for the robot localization is much larger than that of a tag localization, the number of the robot particles M_f and M_p are always much larger than the number of the tag particles J. This makes the increase rate of $O(M_f N)$ is larger than $O(M_p + JN)$ with the increase of the detected tags. In this study, we set $M_f = M_p = 500$ and $J = 100$. When $N \geq 2$, the memory size $O(M_f N)$ is larger than $O(M_p + JN)$. Taking into account the parameters inside the particle, three robot localization parameters, one importance weight, two mean parameters, and three covariance parameters of the tag position, in total $(3 + 1 + 2 + 3)M_f$ parameters are needed to update for FasrSLAM when a tag is detected. However, our proposed method requires $(3+1)M_p+(2+1)J$ parameters (three position parameters and one importance weight for each robot particle and two position parameters and one importance weight for each tag particle). Substituting the values of the robot and tag particles used in this study into the formula, 4500 and 2300 parameters need to be updated for FastSLAM and PF-SLAM, respectively. Moreover, PF-SLAM becomes much faster than FastSLAM with the increase of the number of robot particles. The superiority of the proposed SLAM method is also correct for the mobile agent in 3D space. For a mobile agent in 3D space, $(6+1+3+6)M_f$ parameters (six robot position parameters, one importance weight, three mean parameters, and six covariance parameters of the tag position) are required for FastSLAM, and $(6+1)M_p+(3+1)J$ parameters (six position parameters and one

importance weight for each robot particle and three position parameters and one importance weight for each tag particle) are needed for PF-SLAM method, respectively. If we also use the values of $M_f = M_p = 500$ and $J = 100$, 8000 and 3900 parameters are required for FastSLAM and PF-SLAM, respectively. The calculation cost of FastSLAM is also larger than the proposed SLAM method.

The efficiency of the proposed method in computation cost is evaluated in a simulation by using a PC with a 2.6 GHz CPU. The RFID tag in the environment is set with a density of 100 tags/m^2. FastSLAM is also evaluated in the same simulation environment. Both two SLAM methods are evaluated under two conditions. Firstly, we compared the time costs by using PF-SLAM and FastSLAM of an update against the increase of the particles for estimating the robot localization. The robot moves on a predetermined trajectory with different numbers of the robot particles. The average time cost of an updating of the SLAM procedure is calculated. The numbers of the particles are set from 100 to 4000. The results of an updating using FastSLAM and the proposed SLAM method with different robot particles are presented in Figure 3.6. The time cost for both SLAM methods increases with the number of the particles for estimating the robot localization increases. However, the average time cost of an updating using PF-SLAM always less than FastSLAM.

The time cost of FastSLAM can be reduced by using fewer particles. However, reducing the number of particles affects the accuracy of FastSLAM. We investigated the influence of the number of particles on the accuracy of the proposed SLAM method and FastSLAM. Two SLAM methods were tested on a predetermined trajectory with different particles for estimating the self-localization of the robot. The error data obtained by using the proposed SLAM method and FastSLAM are presented in Figure 3.7. Our proposed SLAM obtained a stable and accurate estimation even using a small number of particles. The errors of the robot and tag localization by using FastSLAM have large changes with the increase of the particle numbers. FastSLAM obtained large errors by using a small number of particles. The accuracy of FastSLAM tends to stable and accurate as the number of particles increases. However, the errors obtained by

FastSLAM also larger than the proposed SLAM method. According to Figures 3.6 and 3.7, FastSLAM can obtain an accurate estimation at the expense of the time cost. Our proposed can get a more accurate result with less time cost.

Then, the time costs by using PF-SLAM and FastSLAM with an update against the increase of the number of the detected tags are surveyed. 500 particles for estimating the robot localization in FastSLAM and PF-SLAM method are set in the test. The robot using two SLAM methods run on the same trajectory. The average time cost for each RFID tag is calculated during the movement. Figure 3.8 shows the results of the average time costs of using PF-SLAM method and FastSLAM with an updating against the detected tag increases. The time cost using FastSLAM increases obviously with the increase of the detected tags. However, the time cost using the proposed SLAM method mostly has no alteration. Each tag is estimated by an independent particle filter so that the time cost of the updating is not affected by the increase of the detected RFID tags. The tag particles take a long time for the initialization than the updating time of the subsequent detection. The undulating of the results in Figure 3.8 is because of some tags only detected with single time which requires initialization and the average time cost of these tags becomes longer than that of the tags with multiple detection times.

3.4 Simulation Experiment

PF-SLAM was tested in a simulated environment. Eight HF-band RFID readers are installed on the bottom of the mobile robot as the configure shown in Figure 3.2(a) and two types of RFID-tag textiles with densities of 100 tags/m^2 and 16 tags/m^2 are set in the environment. The detection range of the RFID reader is set at 60 $\times$ 60 mm^2. The predetermined trajectory and a random trajectory are used to evaluate the proposed SLAM method. The estimated path of the robot can be easily compared with the predetermined trajectory. The random trajectory is much longer and more complex than the predetermined trajectory.

Running on the random trajectory is capable of evaluating the stability and sustainability of the proposed SLAM method. Moreover, the tag can be detected by the robot in more locations to improve the accuracy of the tag and robot localization. To show the superiority of PF-SLAM, FastSLAM was also tested in the same simulated environment. At last, the kidnapping problem of the mobile robot using the proposed SLAM method is also discussed.

3.4.1 Predetermined Trajectory Experiment

The simulated and environments with the density of 100 tags/m^2 and 16 tags/m^2 are presented in Figure 3.9. The predetermined trajectories are rectangular trajectories also shown in Figure 3.9. The robot run along the predetermined trajectories three times. The path of the robot and the detected tags are recorded during the movements. The proposed SLAM method and FastSLAM are evaluated on these two trajectories. We assigned 500 particles for estimating the mobile robot self-localization and 100 particles for the tag location to PF-SLAM and 500 particles to FastSLAM. To avoid a lengthy article, we only show the figures of the results on the RFID-tag textile with a density of 16 tags/m^2 in this chapter. The date of the results both on the density of 100 tags/m^2 and 16 tags/m^2 is listed in the table.

Figure 3.10 shows the results achieved by PF-SLAM and FastSLAM. The tag positions estimated by both methods are correctly estimated. However, the route estimated by FasSLAM presents some deviations as shown in Figure 3.10(c). The route of the mobile robot estimated by our proposed method almost overlaps with the trajectory.

Table 3.1 lists the average errors of the position and orientation of the mobile robot and the errors of the detected tag location during the movements on the predetermined trajectory. PF-SLAM and FastSLAM obtained an accurate estimation in the environment with the density of 16 tags/m^2. The distance errors of the tag and robot localization are about 35 mm for both SLAM methods. However, the robot runs in the environment with the density of 100 tags/m^2

detects more tags than 16 tags/m^2. Using FastSLAM, the errors increase obviously in the environment with the density of 100 tags/m^2. The distance errors of the robot and tag localization are about 62 mm by using FastSLAM. The distance errors obtained by our proposed method also maintained at 35 mm. According to the error data summarized in Table 3.1, our proposed SLAM method obtained more stable and accurate estimations.

TABLE 3.1: Errors of the robot and tag localization utilizing two SLAM methods on the predetermined trajectory in the simulated environment.

Density	Method	Robot localization				Tag localization		
tags/m^2		x [mm]	y [mm]	θ [rad]	dr [mm]	x [mm]	y [mm]	dt [mm]
16	FastSLAM	27.6	24.0	0.022	36.6	19.0	28.9	34.6
16	PF-SLAM	20.8	25.8	0.015	33.1	26.7	23.1	35.3
100	FastSLAM	44.4	43.7	0.031	62.3	44.7	33.2	55.7
100	PF-SLAM	23.2	23.9	0.011	33.3	25.7	24.1	35.2

3.4.2 Random Trajectory Experiment

The accuracy of the robot self-localization and tag locations can be improved by letting the robot detect the tags in more additional locations as introduced in Section 3.3. In this experiment, the robot run along a random trajectory. The random trajectory is much longer and more complex than the predetermined trajectory to make the robot is capable of detecting the tags in more locations. The assignments of the particles in both SLAM methods are same as Section 3.4.1. The results using the proposed SLAM method and FastSLAM are shown in Figure 3.11. Figures 3.11(a) and 3.11(b) present the path of the robot and tag locations estimated by using PF-SLAM. The path of the robot and the locations of the tags estimated by PF-SLAM mostly overlap the ground truth. Our proposed SLAM method exhibits an accurate estimation for the robot and tag localization. The robot path and tag locations estimated by FastSLAM are shown in Figures 3.11(c) and 3.11(d). The results estimated by FastSLAM drastically deviate from the ground truth. The superiority and validity of the proposed SLAM method show obviously on a longer trajectory.

TABLE 3.2: Errors of the robot and tag localization utilizing two SLAM methods on the random trajectory in the simulated environment.

Density tags/m^2	Method	Robot localization				Tag localization		
		x [mm]	y [mm]	θ [rad]	dr [mm]	x [mm]	y [mm]	dt [mm]
16	FastSLAM	122.0	72.6	0.076	142.0	147.0	71.3	163.4
16	PF-SLAM	10.8	26.8	0.006	28.9	9.3	26.9	28.5
100	FastSLAM	47.5	57.9	0.019	74.9	52.0	45.6	69.2
100	PF-SLAM	20.3	37.1	0.003	42.3	13.6	23.4	27.1

The error data generated by using PF-SLAM and FastSLAM on the random trajectory are listed in Table 3.2. The errors obtained by FastSLAM increase obviously than the results on the predetermined trajectory. The average distance errors of the robot localization and tag locations are 70 mm in the environment set with the density of 100 tags/m^2. Moreover, the distance errors of the robot and tag localization utilizing FastSLAM increase to 140 and 160 mm in the environment set with the density of 16 tags/m^2, respectively. However, comparing with the errors obtained by FastSLAM, the errors obtained by PF-SLAM are much smaller. PF-SLAM method also presents a better performance than FastSLAM on the random trajectory. Especially, comparing with the results on the predetermined trajectory, the accuracy of the tag locations are improved which sustains the hypothesis that the uncertainty of the estimation could be decreased by detecting the tag in more different locations when using the particle filter to estimate the tag location.

3.4.3 Kidnapping Experiment

We also tested the proposed SLAM with the kidnapping experiment which evaluates the ability to recover the accurate estimation from failures. The robot is moved to another place where the tags have been detected during the movement without the update of the motion model. The procedure of the kidnapping is shown in Figure 3.12. Figure 3.12(b) shows the error of the self-localization of the robot during this procedure. According to Figure 3.12(a), before kidnapped at point B, the robot moved from point A to B. The robot is

kidnapped to point C where the robot has been without any information. Figure 3.12(b) shows a drastic increase in the robot localization error. This happens at the time when the robot is kidnapped. Figure 3.12(a) shows some incorrect estimations happened at the beginning when the robot kidnapped to point C. These incorrect estimations are marked by the black coils. However, the robot is capable of recognizing the kidnapping and supporting an accurate estimation rapidly as presented in Figure 3.12(a). Then, the robot obtains an accurate localization as before the kidnapping and moved from point C to D successfully. This result demonstrates the validity of PF-SLAM for the kidnapping problem. The performance of the proposed SLAM in this experiment indicates its ability to deal with the kidnapping problem.

3.5 Real Environment Experiment

PF-SLAM was also evaluated by a mobile robot in the real environment set with the RFID tags. The mobile robot and the RFID system used in the experiments are introduced in Section 3.1. The experimental environments are set with two types of HF-band RFID tag with densities of 100 tags/m^2 and 16 tags/m^2. PF-SLAM is also tested on two types of trajectories: the predetermined trajectory and unpredetermined trajectory. The movement of the robot on the trajectories is manual control. FastSLAM is also tested in the same experiments and compared with our proposed SLAM method. Especially, the validity of the proposed SLAM is also tested under different speeds of the mobile robot on the predetermined trajectory. The number of the particles used in FastSLAM is set at 500. PF-SLAM utilizes 500 robot particles to estimate the self-localization of the mobile robot and 100 tag particles to estimate the location of each detected tag.

3.5.1 Predetermined Trajectory Experiment

The predetermined trajectories in the environments with densities of 16 tags/m^2 and 100 tags/m^2 are shown in Figure 3.13(a) and 3.13(b), respectively. The robot

runs on each predetermined trajectory three times. The velocity of the robot is set at 100 mm/s. The estimated path of the robot and locations of the detected tags by the proposed SLAM method and FastSLAM in the environment with 16 tags/m^2 are shown in Figure 3.14. Figures 3.14(a) and 3.14(b) show the path of the robot and positions of the tag estimated by our proposed method basically coincide with the predetermined trajectory and the actual positions of the tags. However, the path of the robot estimated by FastSLAM deviated from the predetermined trajectory, and the tag localization also incurred some inaccurate estimation.

It is difficult to compare the estimated position of the mobile robot at every position with the predetermined trajectory in the real experiment. To obtain the quantified evaluation, we set eight predetermined points on each trajectory to evaluate the accuracy for the robot localization by using the proposed SLAM method and FastSLAM. The eight points for two predetermined trajectories are presented in Figures 3.15(a) and 3.15(b), respectively. The robot run on the predetermined trajectory and remained at each of the eight points for 5 seconds when it passed by to record adequate estimated position data. The estimated position and orientation of the robot are compared with the positions of the eight points. The average errors of the self-localization of the robot at eight points and tag locations by using PF-SLAM and FastSLAM are listed in Table 3.3. Because the noise in the real environment, the errors also happened in the ground truth. Therefore, the error of the orientation in real environment is account to two decimal places. The proposed SLAM obtained good performances on the predetermined trajectories. The average distance errors of the mobile robot and tag localization are about 20 mm and 40 mm in the environment with 16 tags/m^2, respectively. The results of PF-SLAM in the environment with 100 tags/m^2 become more accurate. The distance errors of the localization of the robot and tag are about 15 mm and 38 mm. However, the errors generated by FastSLAM are twice times than that achieved by PF-SLAM in the same experimental situations. In the real experimental environment, the proposed PF-SLAM method also achieved more accurate estimations than FastSLAM.

Both of our proposed SLAM method and FastSLAM obtained a better self-localization performance in the experimental environment with 100 tags/m^2 than 16 tags/m^2. In the real environment, the noise mostly comes from the motor which is accumulated during the movements of the robot. The error accumulated by the motor can be reduced by using the measurements of the tags. Running in the environment with 100 tags/m^2, the tags can be frequently detected by the robot. The accumulated motor errors are modified frequently. However, more motor errors are accumulated during the movements of the robot in the environment with 16 tags/m^2. Therefore, the accuracy of the self-localization of the robot becomes better in the environment with 100 tags/m^2.

TABLE 3.3: Errors of the robot and tag localization utilizing two SLAM methods on the predetermined trajectory in a real environment.

Density tags/m^2	Method	Robot localization				Tag localization		
		x [mm]	y [mm]	θ [rad]	dr [mm]	x [mm]	y [mm]	dt [mm]
16	FastSLAM	49	28	0.06	56	72	56	91
16	PF-SLAM	17	12	0.01	21	35	23	42
100	FastSLAM	28	40	0.03	49	55	45	71
100	PF-SLAM	10	10	0.01	15	26	27	38

3.5.2 Predetermined Trajectory Experiment with Different velocities

In Section 3.5.1, the velocity of the robot is set at 100 mm/s. We also evaluated the performance of PF-SLAM with faster velocities in this study. The speeds are set from 200 mm/s to 400 mm/s. The robot runs on the predetermined trajectory in the environment with 16 tags/m^2. Figures 3.16(a) to 3.16(f) show the results achieved by PF-SLAM with different velocities of the robot. The estimated paths of the robot and tag positions with three faster robot velocities overlap with the ground truth. The accuracy of PF-SLAM is not affected by the faster velocities. The proposed SLAM method is capable of using for a faster velocity of the robot.

3.5.3 Random Trajectory Experiment

The accuracy of the tag locations can be improved by letting the robot run on a random trajectory by using the proposed SLAM which has been demonstrated in the simulated environment. We also evaluated PF-SLAM on a random trajectory to make the robot detect the tags in more locations in the real environment,. Moreover, FastSLAM is also tested on a random trajectory to make a comparison with the proposed SLAM. The results obtained by FastSLAM and our proposed SLAM in the environment with 16 tags/m^2 are presented in Figure 3.17. The path of the robot and the tag locations estimated by PF-SLAM are shown in Figures 3.17(a) and 3.17(b), respectively. The orientation of the robot is set at 0 deg during the movements. The path of the robot estimate by PF-SLAM remains straight indicates that the estimation of the robot orientation is accurate. The tag locations estimated by PF-SLAM overlap with the actual tag positions as shown in Figure 3.17(b). Therefore, the proposed SLAM method obtains a good performance on the random trajectory. Figure 3.17(c) shows the path estimated by FastSLAM and the curved path indicates some errors incurred in the orientation estimation. Furthermore, the range of the actual trajectory in Y direction is 2000 mm to 4000 mm. However, the path estimated by FastSLAM has a large deviation in Y direction. The positions of the tags estimated by FastSLAM also greatly deviate from the actual positions as shown in Figure 3.17(d).

To evaluate the proposed SLAM method on the random trajectory, we also used the eight marked points in the real experimental environment to calculate the accuracy of robot self-localization. The robot also remained at each point 5 seconds when the robot passed by and collected the position and orientation data as Section 3.5.1. The collected data is compared with the positions of the marked points. Table 3.4 lists the errors obtained by PF-SLAM and FastSLAM in the robot and tag localization. The average distance errors of the robot self-localization by utilizing PF-SLAM are 25 mm in the environment with 16 tags/m^2 and 100 tags/m^2. The average distance errors of the tag position by using PF-SLAM method are 26 mm and 22 mm, respectively. The accuracy of

the tag location by using the proposed SLAM is improved on the random trajectory. However, FastSLAM achieves large errors in the localization of the robot and tag on a random trajectory.

TABLE 3.4: Errors of the robot and tag localization utilizing two SLAM methods on the random trajectory in a real environment.

Density	Method	Robot localization				Tag localization		
tags/m^2		x [mm]	y [mm]	θ [rad]	dr [mm]	x [mm]	y [mm]	dt [mm]
16	FastSLAM	24	115	0.03	117	26	141	143
16	PF-SLAM	15	19	0.01	25	14	22	26
100	FastSLAM	31	56	0.01	64	30	46	55
100	PF-SLAM	17	17	0.02	24	14	18	22

According to the results obtained by using the proposed SLAM method in the real environment, the accuracy of PF-SLAM is sufficient to the self-localization of the robot and the tag locations. Especially, the RFID tags are installed in the carpets. The tag positions used as the ground truth are measured by hand in the case of invisible so that there are also some inevitable errors in the measurements. Comparing with the results obtained by FastLSAM, the superiority of PF-SLAM is demonstrated in the real environment.

3.6 Summaries

In this study, we attempted to use the RFID system for realizing the localization of the mobile robot. However, a large amount of preliminary works are needed for the RFID system based localization, for instance, the recording of the RFID tag ID and the measurements of the tag coordinates. SLAM technology is capable of reducing these preliminary works and finishing the self-localization of the robot and building a map of the RFID tags. The non-Gaussian detection model of the RFID reader makes the classical FastSLAM with kalman filter based landmark updating is not suitable. Therefore, a novel SLAM method using the independent particle filters for estimating the position and orientation of the mobile robot and the tag locations was proposed in this study. The

algorithm of the proposed SLAM method was explained in detail. The difference between the proposed SLAM and FastSLAM was also discussed. The proposed SLAM method and FastSLAM were evaluated in simulated and real experimental environments. The validity of PF-SLAM and superiority to FastSLAM were demonstrated in the experiments by using the RFID system with the non-Gaussian detection model.

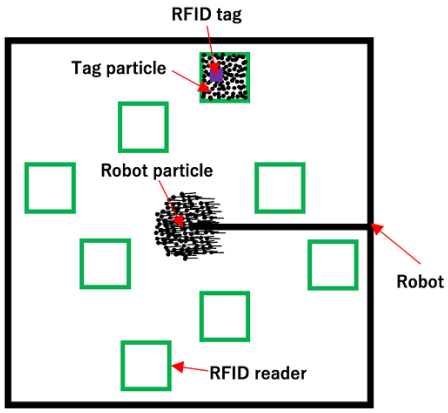

(a) First detection

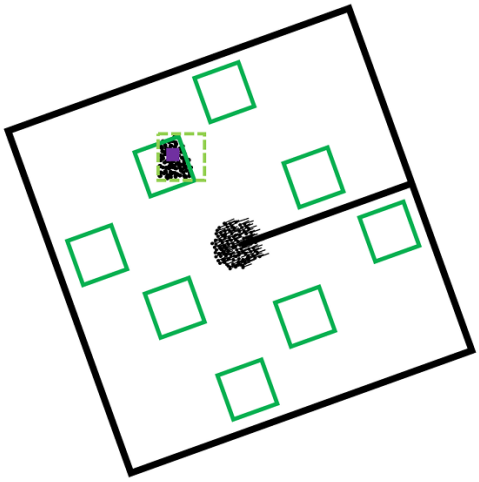

(b) Second detection

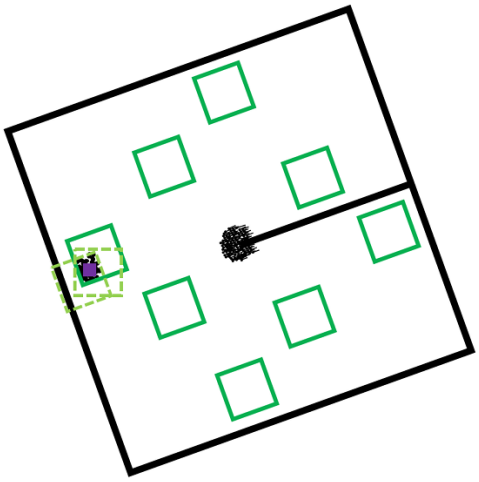

(c) Third detection

FIGURE 3.4: Procedure of the PF-SLAM based on the RFID system.

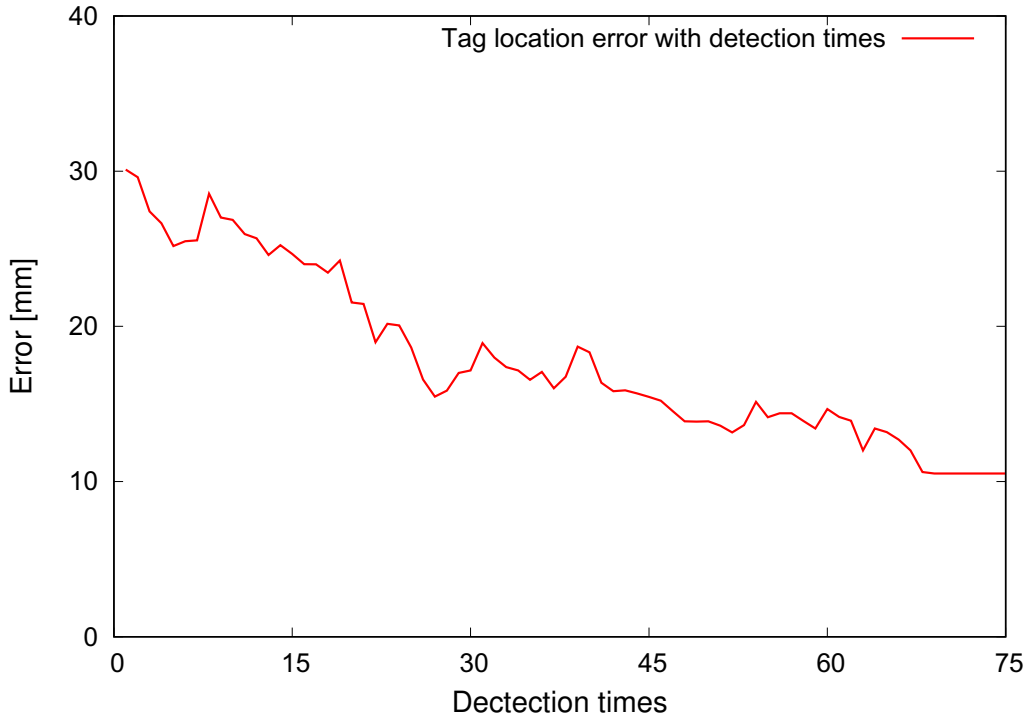

FIGURE 3.5: Tag location error versus the detection time.

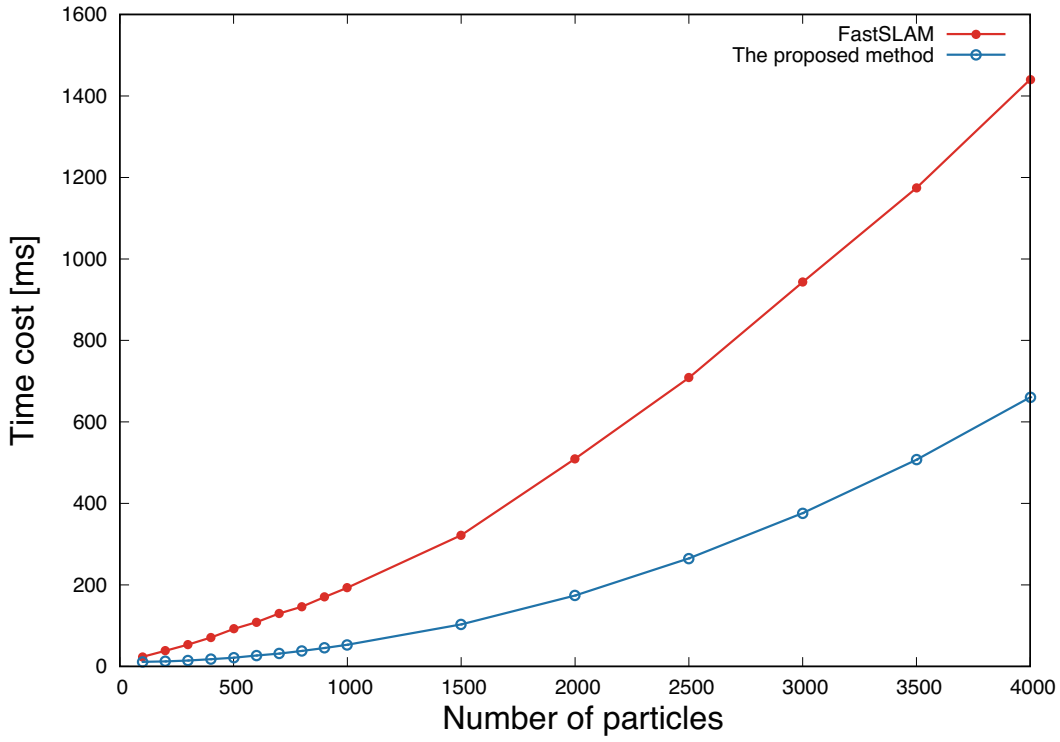

FIGURE 3.6: Time cost of an updating of the SLAM methods as the number of robot particles increase.

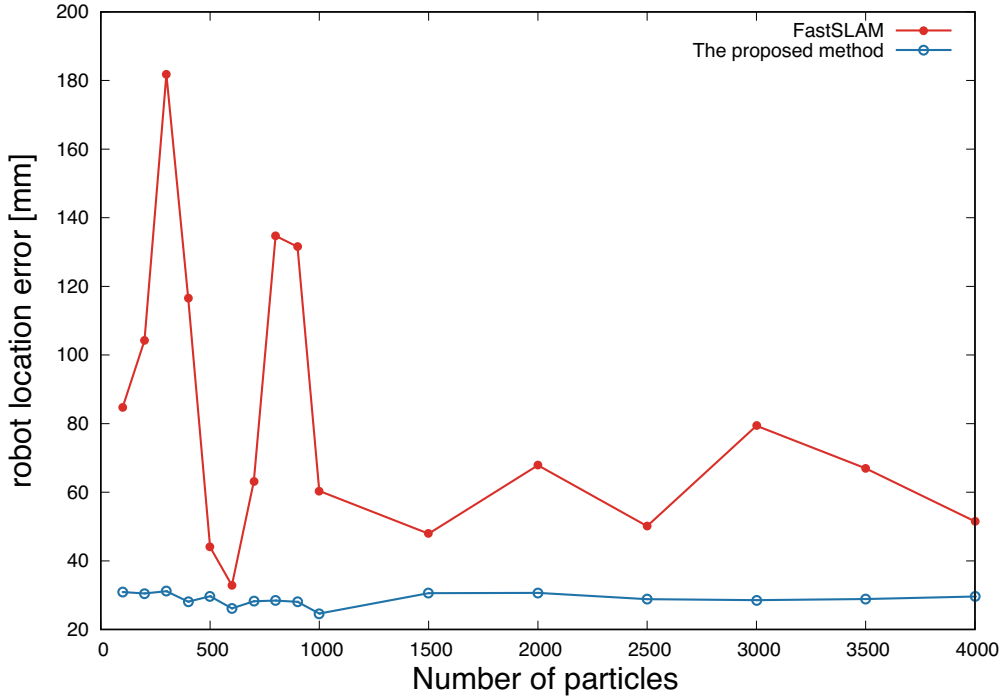

(a) Errors of the robot localization

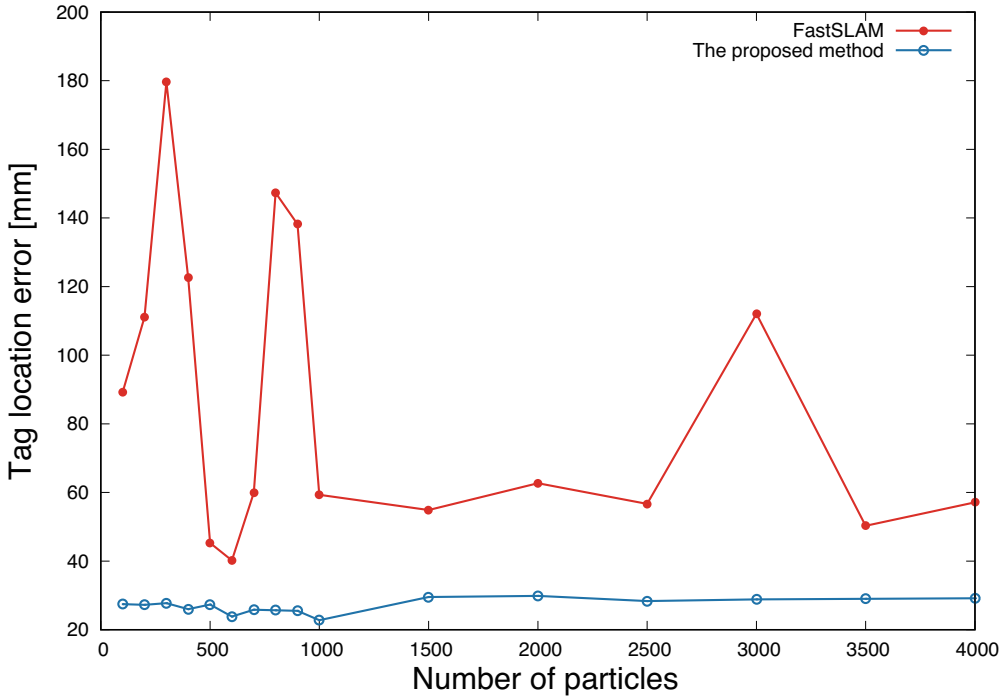

(b) Errors of the tag localization

FIGURE 3.7: Average errors of the robot and tag localization with different numbers of robot particles: average errors of the (a) robot localization and (b) tag localization against the number of the robot particles.

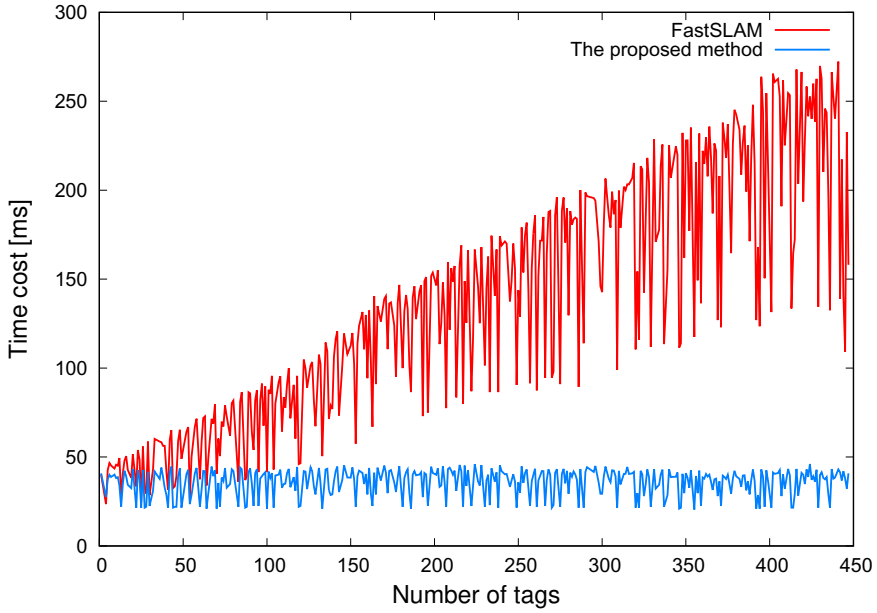

FIGURE 3.8: Time cost of an updating of the SLAM methods along with the increase of the detected tags.

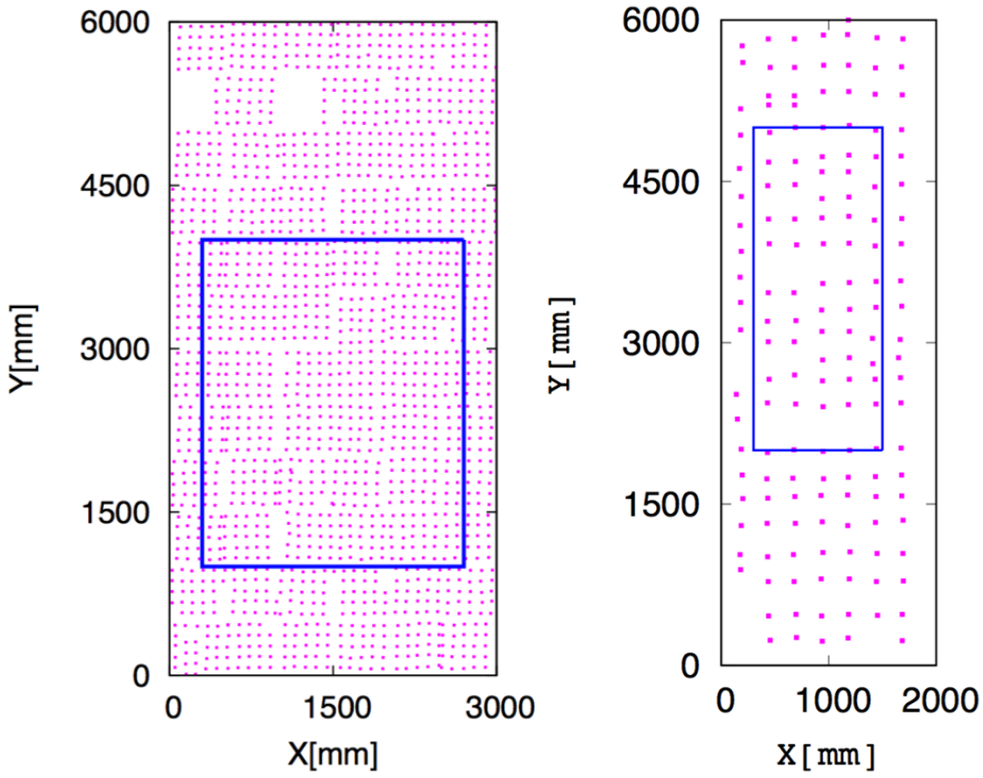

(a) 100 tags/m^2 (b) 16 tags/m^2

FIGURE 3.9: Simulated experimental environments: the RFID tags are indicated by the purple points, and the predetermined trajectories are indicated by the blue lines.

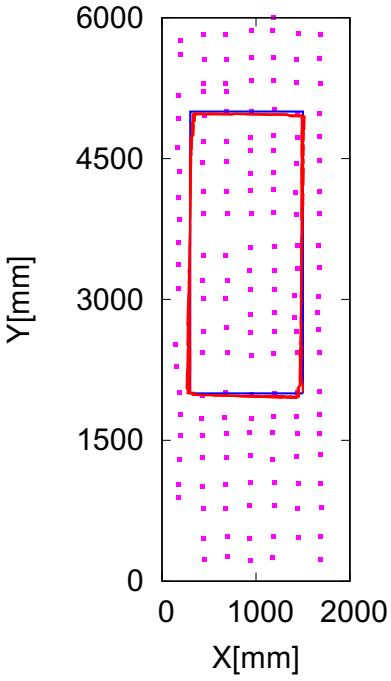

(a) Path estimated by PF-SLAM

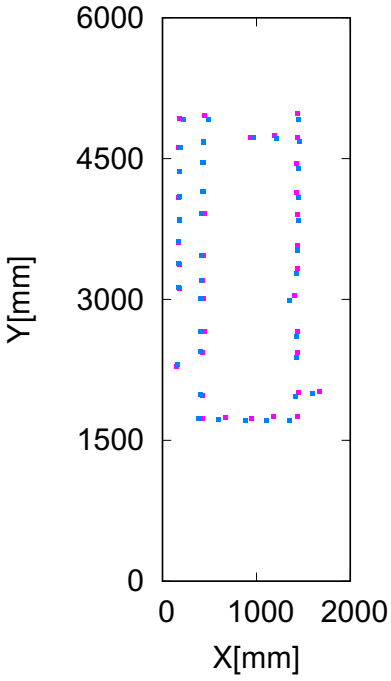

(b) Tag locations estimated by PF-SLAM

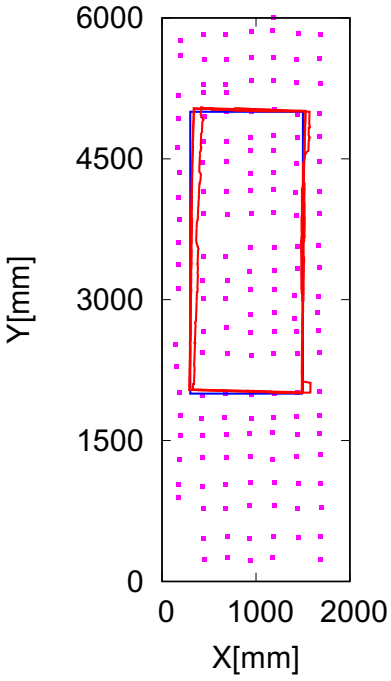

(c) Path estimated by FastSLAM

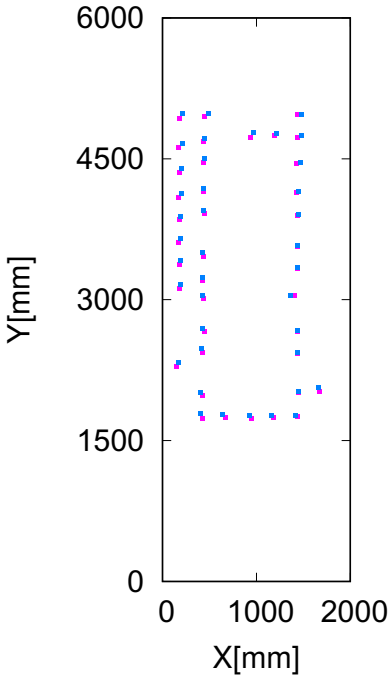

(d) Tag locations estimated by FastSLAM

FIGURE 3.10: Results obtained by PF-SLAM and FastSLAM on a predetermined trajectory in the simulated environment. (a) and (c) show the path of the robot estimated by PF-SLAM and FastSLAM (red lines), respectively. (b) and (d) show the tag locations estimated by PF-SLAM and FastSLAM (green points), respectively.

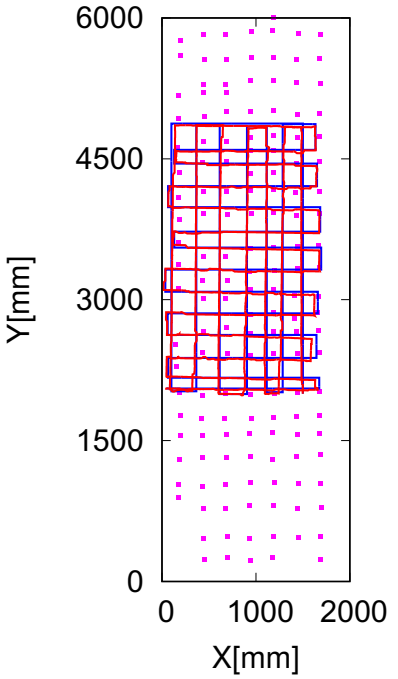

(a) Route estimated by PF-SLAM

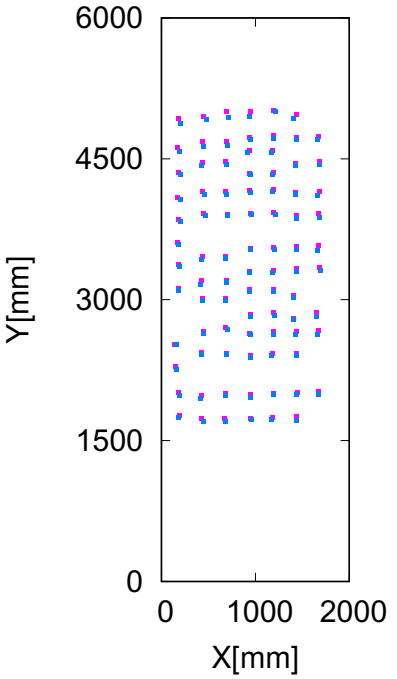

(b) Tag positions estimated by PF-SLAM

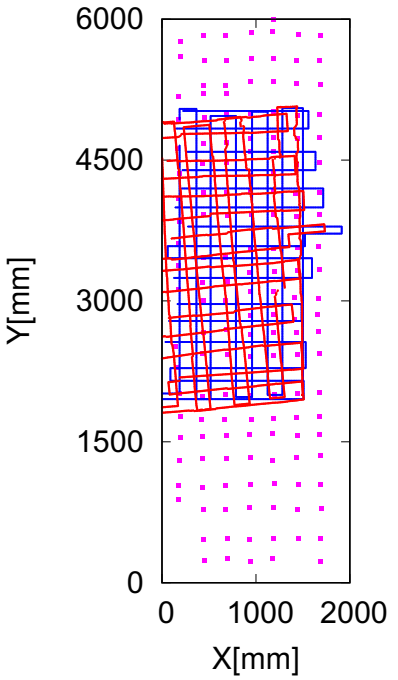

(c) Route estimated by FastSLAM

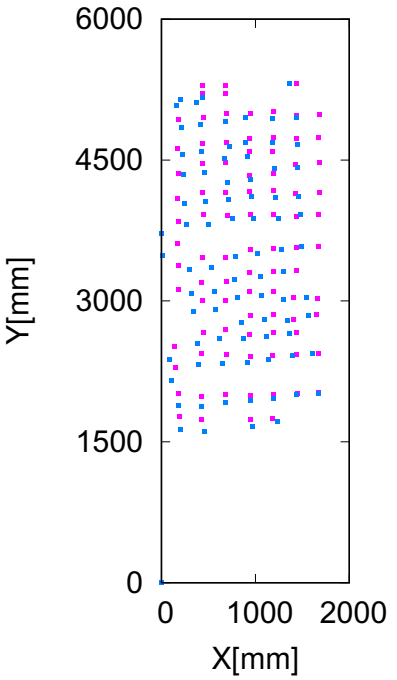

(d) Tag positions estimated by FastSLAM

FIGURE 3.11: Results obtained by PF-SLAM and FastSLAM on a random trajectory in the simulated environment. (a) and (c) show the path of the robot estimated by PF-SLAM and FastSLAM, respectively. (b) and (d) show the tag locations estimated by PF-SLAM and FastSLAM, respectively.

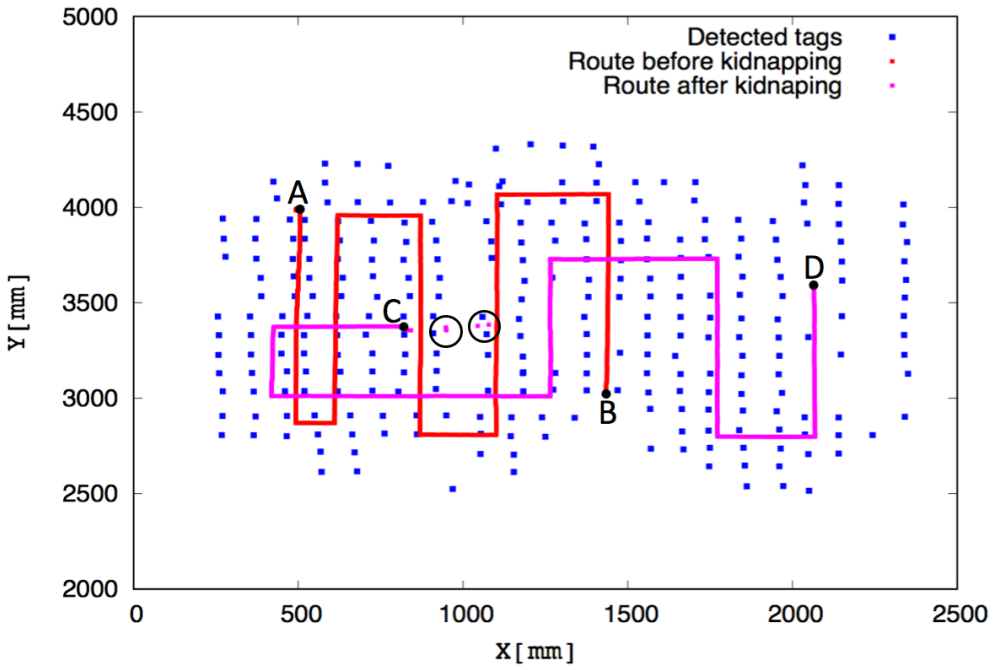

(a) Path estimated by PF-SLAM

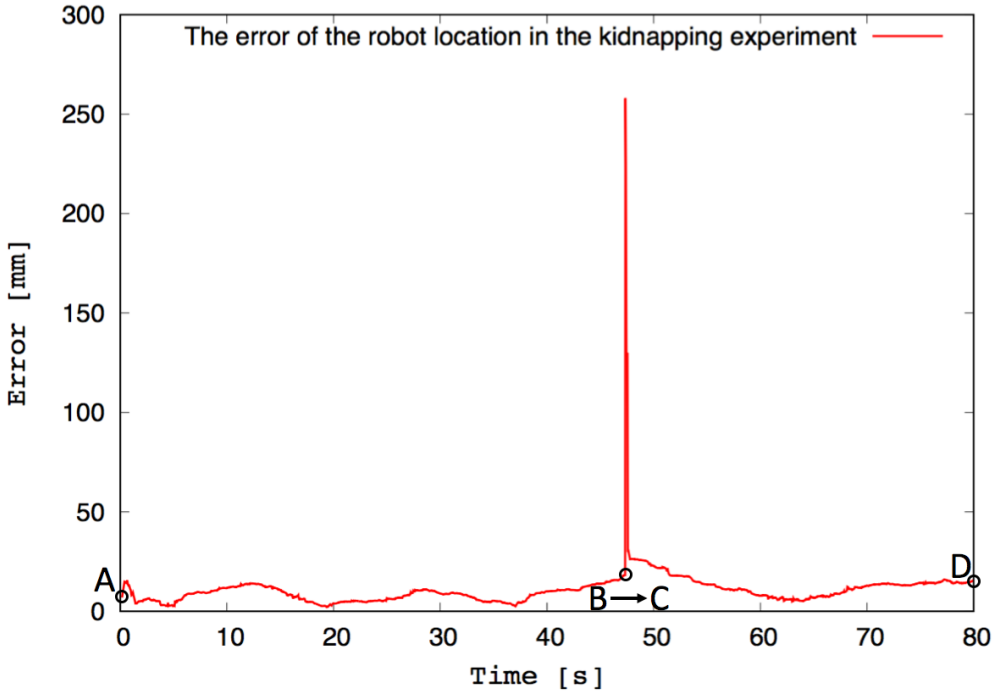

(b) The robot localization error

FIGURE 3.12: Results achieved by PF-SLAM in the kidnapping experiment.

(a) Experimental environment with 16 tags/m^2

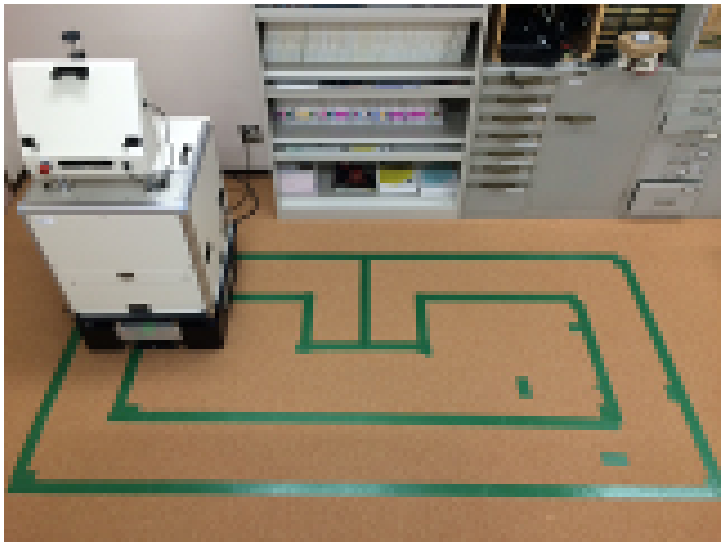

(b) Experimental environment with 100 tags/m^2

FIGURE 3.13: Experimental environments with 16 tags/m^2 and 100 tags/m^2 (green lines are the predetermined trajectory).

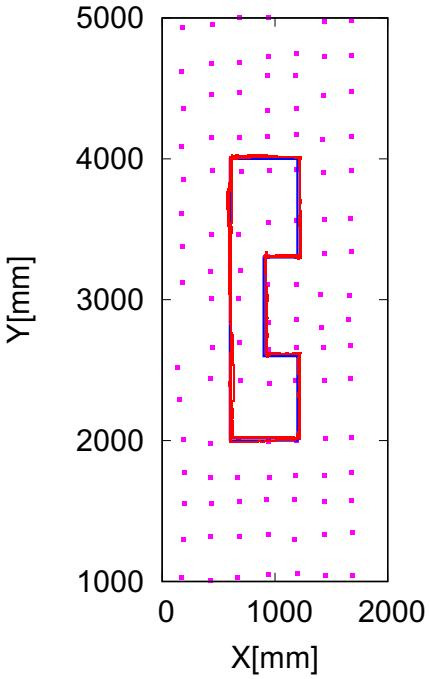

(a) Path estimated by PF-SLAM

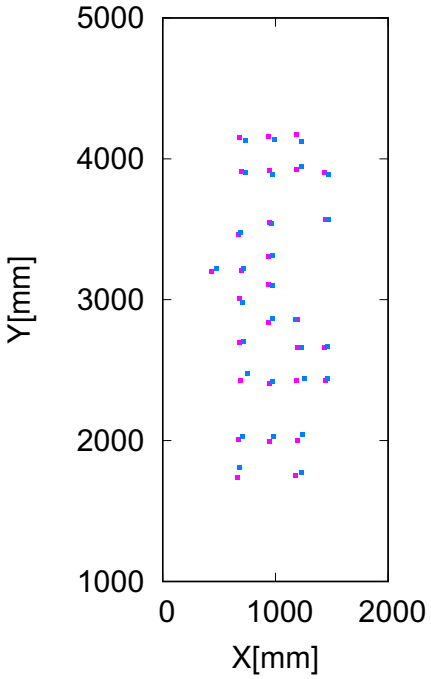

(b) Tag locations estimated by PF-SLAM

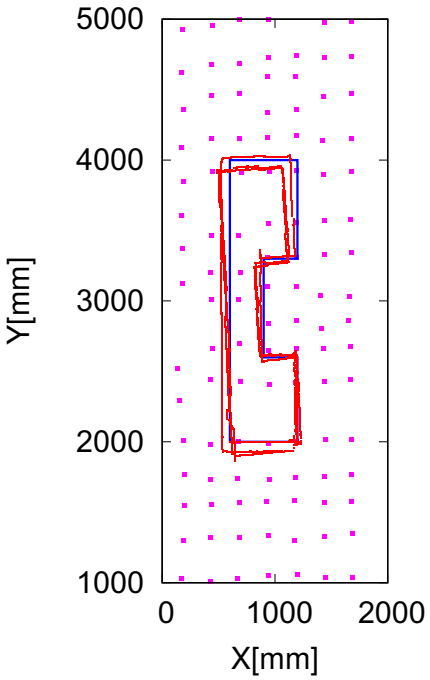

(c) Path estimated by FastSLAM

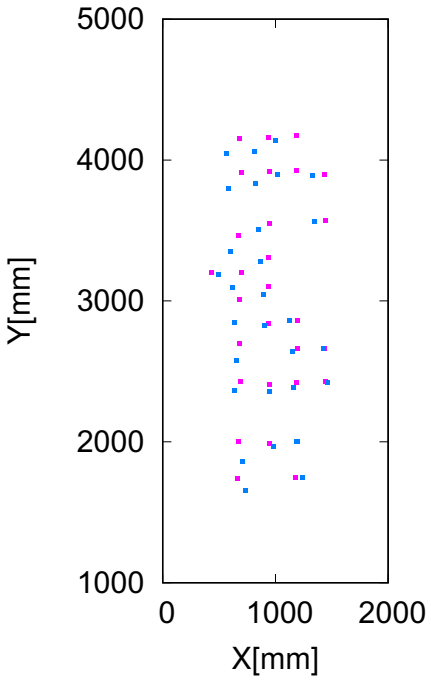

(d) Tag locations estimated by FastSLAM

FIGURE 3.14: Results obtained by PF-SLAM and FastSLAM on a predetermined trajectory in the real environment. (a) and (c) show the path of the robot estimated by PF-SLAM and FastSLAM, respectively. (b) and (d) show the tag locations estimated by PF-SLAM and FastSLAM, respectively.

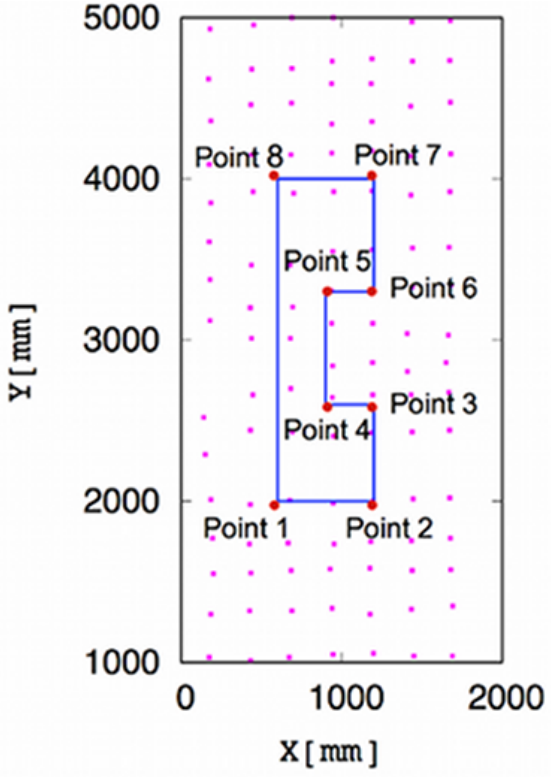

(a) Assignment of the predetermined trajectory and tags

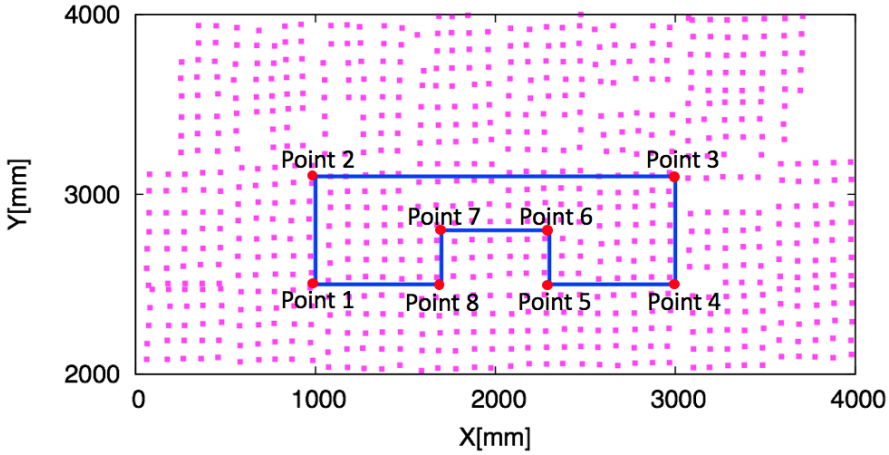

(b) Assignment of the predetermined trajectory and tags

FIGURE 3.15: Eight points used in experimental environments with 16 tags/m^2 and 100 tags/m^2 (eight selected spots are indicated by the red points).

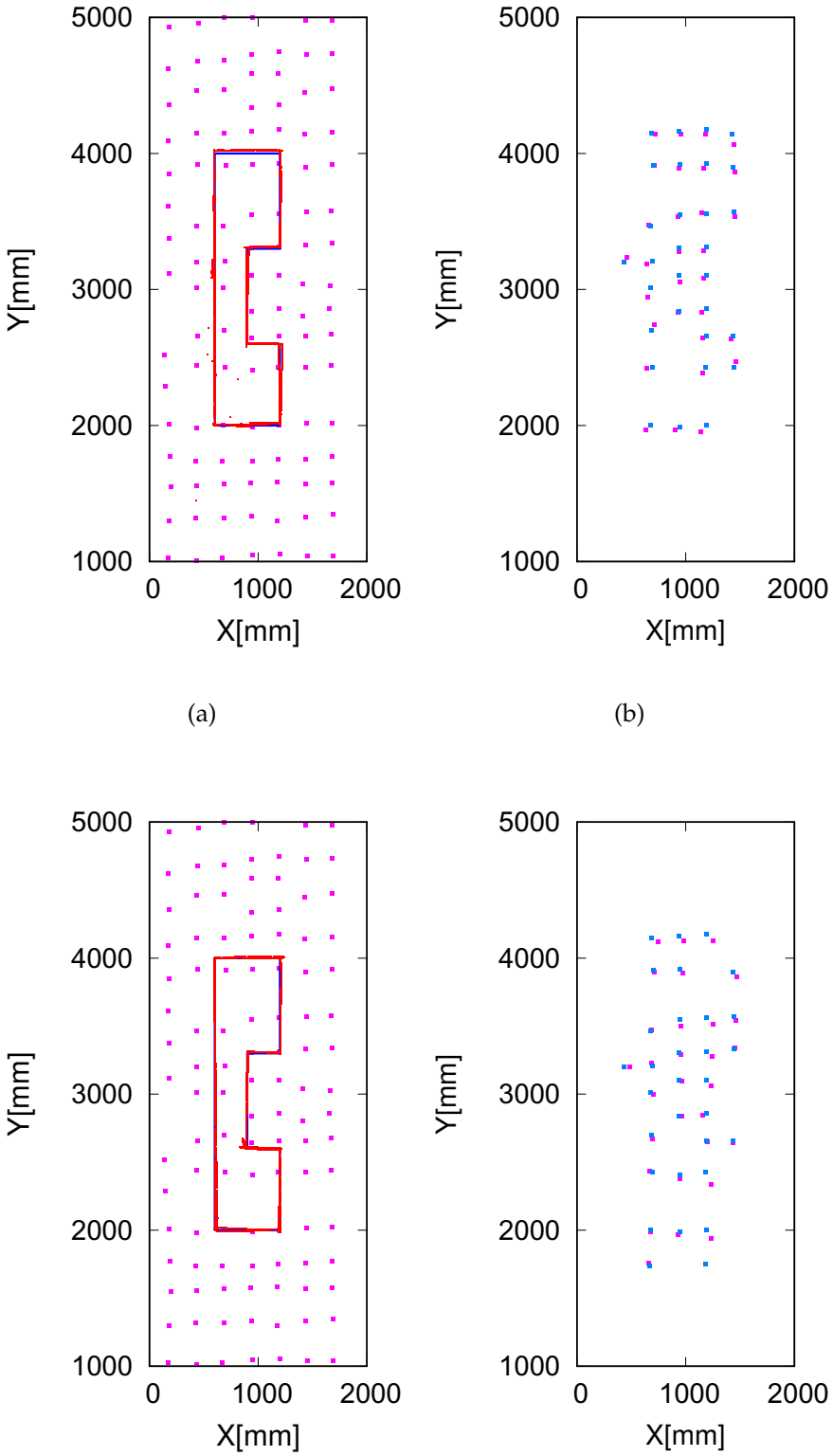

FIGURE 3.16: Results obtained by PF-SLAM at different velocities. (a), (c) and (e) show the estimated path of the robot at velocities of 200 mm/s, 300 mm/s and 400 mm/s, respectively. (b), (d) and (e) present the estimated tag locations at velocities of 200 mm/s, 300 mm/s and 40 mm/s, respectively.

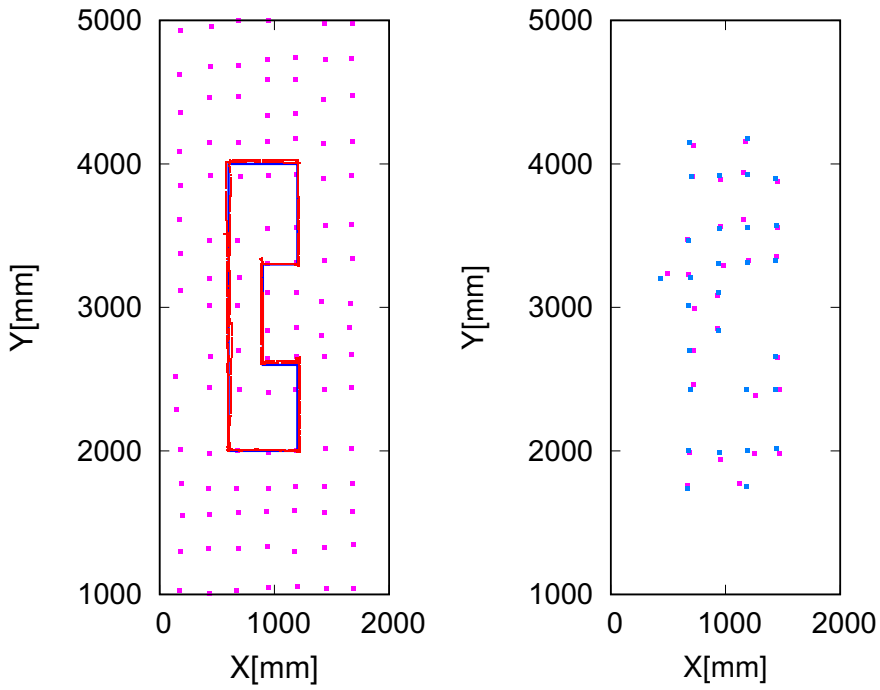

(e) (f)

FIGURE 3.16: Results obtained by PF-SLAM at different velocities. (a), (c) and (e) show the estimated path of the robot at velocities of 200 mm/s, 300 mm/s and 400 mm/s, respectively. (b), (d) and (e) present the estimated tag locations at velocities of 200 mm/s, 300 mm/s and 400 mm/s, respectively.

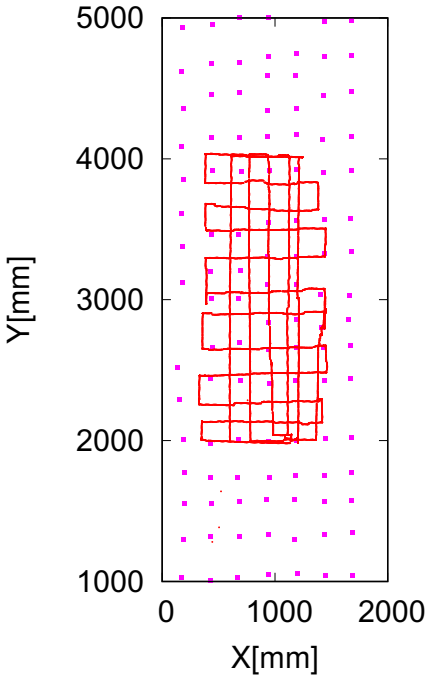

(a) Path estimated by PF-SLAM

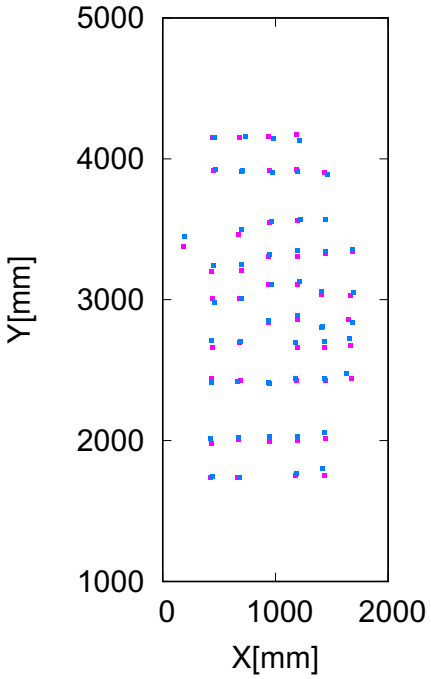

(b) Tag locations estimated by PF-SLAM

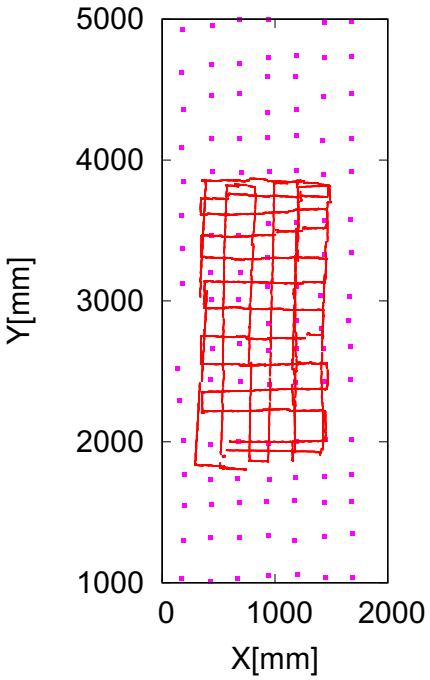

(c) Path estimated by FastSLAM

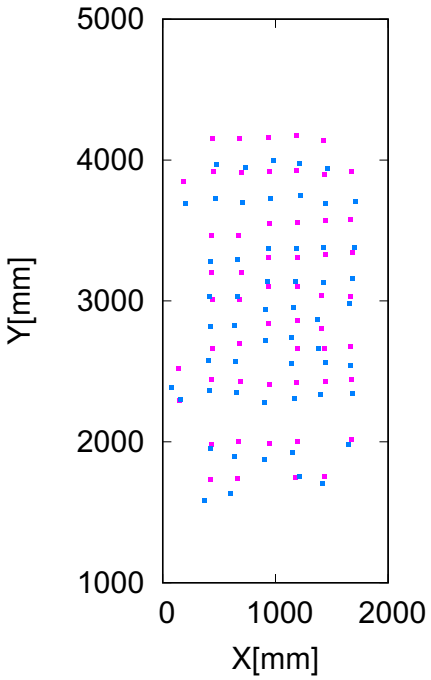

(d) Tag locations estimated by FastSLAM

FIGURE 3.17: Results obtained by PF-SLAM and FastSLAM on a random trajectory in the real environment. (a) and (c) show the path of the robot estimated by PF-SLAM and FastSLAM, respectively. (b) and (d) show the tag locations estimated by PF-SLAM and FastSLAM, respectively.

Chapter 4

SLAM Method utilizing Particle Smoother for Landmark Updating on RFID System

PF-SLAM is suitable to the RFID system used for an indoor mobile robot [84]. However, the accuracy of PF-SLAM is affected by the degeneracy problem of the particle filter for estimating tag locations. Especially, the effect increases with the detection range of RFID reader increases. Therefore, a particle smoother is proposed to estimate the tag location to avoid the influence of the degeneracy problem. The details of the SLAM method with particle smoother based landmark updating is explained in this chapter. We refer to it as PS-SLAM in the following description. Self-localization of PS-SLAM is based on MCL method, and the estimation of each landmark is based on a particle smoother. The fixed lag smoothing method is used to estimate the landmark location. PS-SLAM was evaluated in a simulated environment. The results of the experiments show the validity and superiority of PS-SLAM in the case of utilizing the large detection ranges. This chapter is organized as follows. Section 4.1 introduces the particle fixed lag smoother. The algorithm of PS-SLAM is explained in Section 4.2. Then, the computation cost of PS-SLAM is discussed in Section 4.3. The results of PS-SLAM in the simulated experimental environment are shown in Section 4.4. Summaries of PS-SLAM are drawn in Section 4.5.

4.1 Particle fixed lag smoother

The smoothing distribution of the particles in a sequential way is able to represent as:

$$p(\boldsymbol{x}_{0:t}|\boldsymbol{z}_{1:t}) \propto p(\boldsymbol{x}_{0:t-1}|\boldsymbol{z}_{1:t-1})h(\boldsymbol{z}_t|\boldsymbol{x}_t)f(\boldsymbol{x}_t|\boldsymbol{x}_{t-1}), \tag{4.1}$$

where $\boldsymbol{x}_{0:t}$ is the path of the robot, and $\boldsymbol{z}_{1:t}$ means the observations obtained during the robot movements. $f(\boldsymbol{x}_t|\boldsymbol{x}_{t-1})$ and $h(\boldsymbol{z}_t|\boldsymbol{x}_t)$ are specified state function and observation function. The sequential character appears clearly when this equation is decomposed into a predict step,

$$p(\boldsymbol{x}_{0:t}|\boldsymbol{z}_{1:t-1}) = p(\boldsymbol{x}_{0:t-1}|\boldsymbol{z}_{1:t-1})f(\boldsymbol{x}_t|\boldsymbol{x}_{t-1}), \tag{4.2}$$

and an analysis step,

$$p(\boldsymbol{x}_{0:t}|\boldsymbol{z}_{1:t}) \propto p(\boldsymbol{x}_{0:t}|\boldsymbol{z}_{1:t-1})h(\boldsymbol{z}_t|\boldsymbol{x}_t). \tag{4.3}$$

The particle fixed lag smoother was proposed by Kitagawa which can be achieved from a simple extension to the particle filter as shown in [54]. The difference lies in the size of the state vector to be estimated is kept stationary of last L time steps. Consequently, the oldest state is ruled out from the estimation process at each predict step. The predict step becomes:

$$p(\boldsymbol{x}_{t-L:t}|\boldsymbol{z}_{1:t-1}) = f(\boldsymbol{x}_t|\boldsymbol{x}_{t-1}) \int p(\boldsymbol{x}_{t-L-1:t-1}|\boldsymbol{z}_{1:t-1})d\boldsymbol{x}_{t-L-1}, \tag{4.4}$$

This smoother is straightforward to implement, exhibits a negligible CPU cost which almost the same as the particle filter. However, The diversity of the particles in the state vector representing the smoothing distribution decreases with a large L which leads to the smoothing distribution can not be approximated correctly. In order to avert this problem, L is constantly set at 20 to 30 based on [85].

4.2 Particle Smoother for Landmark Mapping of SLAM

PS-SLAM utilizes one particle filter to estimate the pose of the robot and N particle smothers to estimate the positions of the RFID tags. The form of the robot particle is the same as Equation (3.4). Each detected RFID tag is estimated by an independent particle smoother. Each tag particle in particle smoother is of the form

$$\boldsymbol{m}_{n,t}^{[j]} =< ^{w}\ \boldsymbol{m}_{n,t}^{[j]}, \hat{\boldsymbol{S}}_{n,t}^{[j]}, \omega_{n.t}^{[j]} > \tag{4.5}$$

The form of the particle in particle smoother is similar to Equation (3.5) excepts an addition element $\hat{\boldsymbol{S}}_{n,t}^{[j]}$. $\hat{\boldsymbol{S}}_{n,t}^{[j]}$ is the set which records the value from ${}^{w}\boldsymbol{m}_{n,t-L+1}^{[j]}$ to ${}^{w}\boldsymbol{m}_{n,t}^{[j]}$. The Equation (3.7) is also utilized as the likelihood function for the weight updates of both the robot particles and tag particles.

The algorithm of PS-SLAM is presented in **Algorithm 2**. The difference of the **Algorithm 2** with **Algorithm 1** is the updates of the detected tags. For instance, when the robot detects a RFID tag n, if the detection of the tag is the first time, a particle smoother set is initialized. The particles in the novel particle set are assigned with the importance weight 1, and these particles are distributed in the detection area of the reader that detected the tag. Especially, the initial state of each particle is also restored in $\hat{\boldsymbol{S}}_{n,1}^{j}$ of each particle for the smoothing procedure with the following step. Otherwise, the states of the tag particles are updated by adding a Gaussian random value based on $\boldsymbol{m}_{n,t-1}^{[j]}$. The importance weights of the updated robot particles are calculated by utilizing Equation (3.7). After the resampling step, the smoothed distribution of the tag particles is achieved by calculating the mean of $\boldsymbol{m}_{n}^{[j]}$ from $t+1-L$ to t which restored in $\hat{\boldsymbol{S}}_{n}^{j}$ of each particle. The position of the detected tag is updated based on the smoothed distribution $\tilde{\boldsymbol{S}}_{n,t}$. Then, the robot particles for estimating the robot self-localization is updated as **Algorithm 1**.

Algorithm 2: PS-SLAM:

Initialization of the robot particle set $\boldsymbol{S}_{r,t} = (\boldsymbol{x}_t^{[1]}, \boldsymbol{x}_t^{[2]}, \cdots, \boldsymbol{x}_t^{[I]})$
for $i = 1$ to I **do**
  Robot particles are updated by the motion model:
  ${}^{w}\boldsymbol{x}_t^{[i]} = MotionModel({}^{w}\boldsymbol{x}_{t-1}^{[i]})$
end for
if landmark n is detected **then**
  if landmark n never seen before **then**
    Initialize a new tag particle set $\boldsymbol{S}_{n,t} = (\boldsymbol{m}_{n,t}^{[1]}, \boldsymbol{m}_{n,t}^{[2]}, \cdots, \boldsymbol{m}_{n,t}^{[J]})$
    Store $\boldsymbol{m}_{n,t}^{[j]}$ in $\hat{\boldsymbol{S}}_{n,t}^{j}$
  else
    for from $j = 1$ to J **do**
      Obtain $\boldsymbol{m}_{n,t}^{[j]}$ based on $\boldsymbol{m}_{n,t-1}^{[j]}$ with a Gaussian random number
      Update $\omega_{n,t}^{[j]}$ for each particle in $\boldsymbol{S}_{n,t}$
      Store $\boldsymbol{m}_{n,t}^{[j]}$ in $\hat{\boldsymbol{S}}_{n,t}^{j}$
    end for
  end if
  for from $j = 1$ to J **do**
    Create particle $[k]$ with probability $\propto w_{n,t}^{[j]}$
    Add $\overline{m}_{n,t}^{[k]}$ to $\boldsymbol{S}_{n,t}$
  end for
  for From $j = 1$ to J **do**
    $\overline{m}_{n,t}^{[j]} = \sum_{i=t+1-L}^{t} \boldsymbol{m}_{n,i}^{[j]}/L$
    Add $\overline{m}_{n,t}^{[j]}$ to $\tilde{\boldsymbol{S}}_{n,t}$
  end for
  Update ${}^{w}\boldsymbol{x}_n$ based on $\tilde{\boldsymbol{S}}_{n,t}$
  for from $i = 1$ to I **do**
    Update $\omega_{r,t}^{[i]}$ based on the likelihood function
  end for
end if
for from $i = 1$ to I **do**
  Create particle o with probability $\propto w_{r,t}^{[i]}$
  Add $\overline{x}_{r,t}^{[o]}$ to $S_{r,t}$
end for
Return $\boldsymbol{S}_{r,t}$, $\boldsymbol{S}_{n,t}$

4.3 Computation cost of the proposed SLAM

To demonstrate the computational efficiency of the proposed PS-SLAM, it was compared with FastSLAM and PF-SLAM in a simulation environment. The RFID tags with a density of 4 tags/m^2 are set in the environment. PS-SLAM and PF-SLAM use 100 tag particles for estimating each detected tag position. By utilizing three SLAM methods, the mobile robot runs along a predetermined trajectory. The average time costs of the SLAM procedures are calculated after the movements. The average time costs of an update utilizing PS-SLAM and the other two SLAM methods with different numbers of the robot particles are shown in Figure 4.1(a). The robot particles are set from 100 to 5000. The time costs of three SLAM methods increase as the number of robot particles increase. However, the increase rate of the time cost utilizing FastSLAM is much larger than the increased rates obtained by our proposed PS-SLAM and PF-SLAM. Even PS-SLAM utilizes the particle smoother which needs more memory, the time cost is almost the same as PF-SLAM. We also surveyed the time cost by using these three SLAM methods with an update against the increase of the number of detected tags. Figure 4.1(b) shows the results of the average time costs of using three methods with an updating with different detected tag numbers. The time cost by utilizing FastSLAM increase obviously with the increase of the detected tags. The time costs of PS-SLAM and PF-SLAM are substantially unchanged and much smaller than that of FastSLAM. Although PS-SLAM needs additional memory to store the tag particle states in sequence, PS-SLAM also presents almost the same time cost as PF-SLAM. These data is capable of demonstrating the efficiency of PS-SLAM.

4.4 Experiment

The proposed SLAM method utilizes particle smoother for updating the landmark locations was evaluated in a simulated environment set with RFID tags. We tested PS-SLAM on the RFID detection model with two types of running

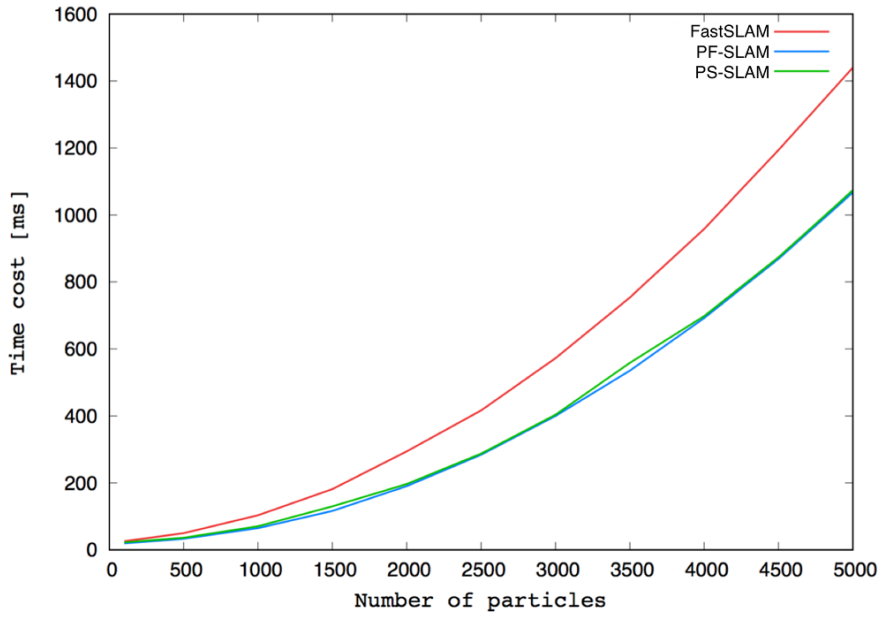

(a)

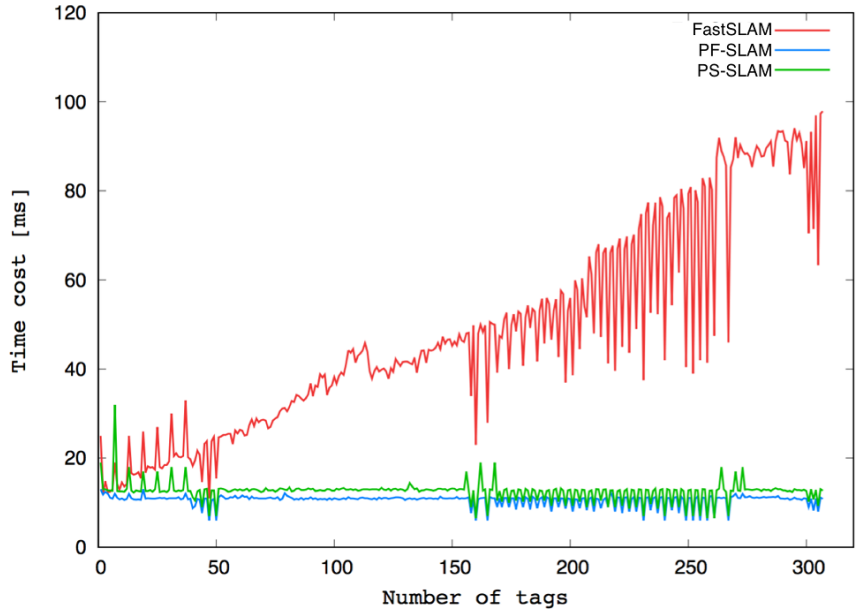

(b)

FIGURE 4.1: Average Time cost of the PS-SLAM, PF-SLAM and FastSLAM with an update along with the increase of (a) the robot particles and (b) the detected tags.

trajectories: predetermined trajectory and random trajectory. We also evaluate PF-SLAM and FastSLAM in the same experimental environment to compare with PS-SLAM. Moreover, five different trajectories are utilized in the predetermined trajectory experiments. The average errors of the robot and tag location are used to evaluate these three SLAM methods mentioned above. We employed 500 robot particles to these three SLAM methods and 100 tag particles to each detected RFID tag by using PS-SLAM and PF-SLAM.

Eight RFID readers are installed on the bottom of the mobile robot which is same as Chapter 3. The detection range of RFID reader is set at 300 by 300 mm^2 firstly. To prove the superiority of PS-SLAM, the performance of the proposed SLAM methods with different detection ranges are also evaluated. The RFID tags are arranged in the experimental environment with the density of 4 tags/m^2.

4.4.1 Predetermined Trajectory Experiment

TABLE 4.1: Errors of the robot and tag localization utilizing three SLAM methods on the predetermined trajectory.

Method	Robot location				Tag location		
	x [mm]	y [mm]	θ [rad]	dr [mm]	x [mm]	y [mm]	dt [mm]
PS-SLAM	25.4	45.1	0.006	53.8	50.3	51.2	79.0
PF-SLAM	41.4	66.6	0.003	82.1	66.1	80.1	110.5
FastSLAM	315.1	204.5	0.182	420.8	296.6	210.1	412.1

The robot equipped with RFID readers moved along five predetermined trajectories to estimate the robot self-localization and tag locations to evaluate the PS-SLAM, PF-SLAM, and FastSLAM. The robot runs on each predetermined trajectory three loops. We only show figures of the results of three SLAM methods on one predetermined trajectory here to avoid a lengthy article. The results on a predetermined trajectory generated by PS-SLAM, PF-SLAM, and FastSLAM are shown in Figure 4.2. Figure 4.2 shows that the path of the robot estimated by PS-SLAM is more accurate than that estimated by PF-SLAM and

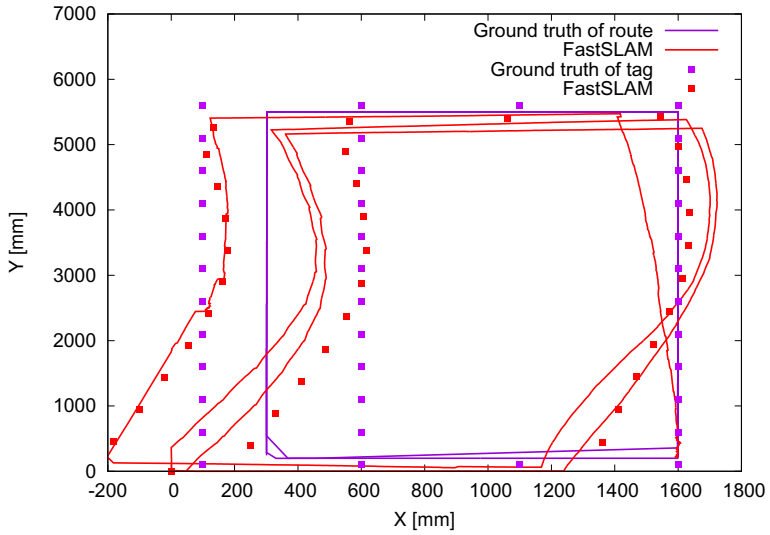

(a)

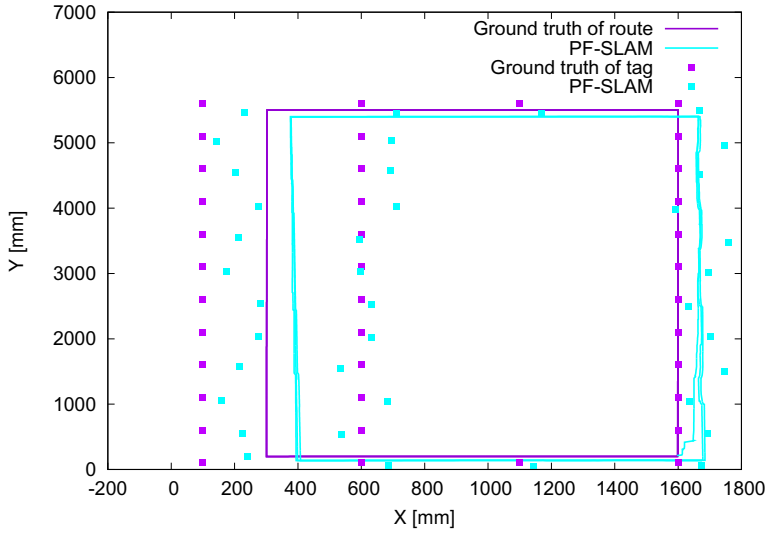

(b)

FIGURE 4.2: Results obtained by PS-SLAM, PF-SLAM and FastSLAM on a predetermined trajectory. (a) shows the results obtained by FastSLAM. (b) shows results obtained by PF-SLAM. (c) shows the results obtained by PS-SLAM.

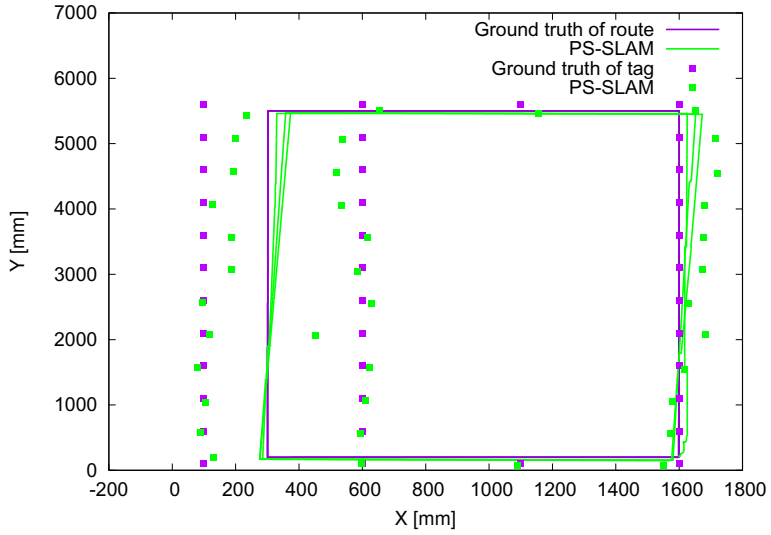

(c)

FIGURE 4.2: Results obtained by PS-SLAM, PF-SLAM and FastSLAM on a predetermined trajectory. (a) shows the results obtained by FastSLAM. (b) shows results obtained by PF-SLAM. (c) shows the results obtained by PS-SLAM.

FastSLAM. The path of the robot estimated by FastSLAM has incorrect estimations both on the position and orientation, as shown in Figure 4.2(a). The positions of the detected tags are also incorrectly estimated by the FastSLAM. Figure 4.2(b) presents the path of the robot and the tag locations estimated by PF-SLAM offsets to the right. Figure 4.2(c) shows the robot path estimated by the PS-SLAM almost coincides the trajectory and most of the tags overlap with the ground truth.

Table 4.1 lists the average errors of the robot self-localization and tag locations obtained by PS-SLAM, PF-SLAM, and FastSLAM on the five predetermined trajectories. The results obtained by PS-SLAM is sufficiently precise for the robot self-localization and the tag locations according to the detection range and the interval of the RFID tags. The average distance errors of the robot self-localization and tag locations are 54 mm and 79 mm by using PS-SLAM. The estimation errors generated by PF-SLAM are smaller than that generated by FastSLAM. However, comparing the result data with PS-SLAM, the errors generated by PF-SLAM are larger than that generated by PS-SLAM in the same

situation. PS-SLAM exhibits a better performance based on the RFID system with a large detection range.

4.4.2 Random Trajectory Experiment

As discussed in last chapter, by using PF-SLAM, the robot needs to detect a tag in additional locations to reduce the feasible region of the tag location to improve the accuracy of estimation for the localization of the robot and tag. The results become better when the robot moves along a random trajectory in Chapter 3. Particle smoother is also capable of narrowing the feasible region of the tag location by letting the robot detect the tag at more different locations. Due to the tag particles are updated by a pseudorandom value when a tag detected by plural times, the feasible region of the detected tag cannot be narrowed to a point through detecting the detected tag at different locations. However, this also preserves the possibility of a correct estimation when errors occur and avoids all of the particles convergence to unrecoverable wrong estimation.

We tested these three SLAM methods by moving the robot on a random trajectory to verify this hypothesis. Figure 4.3 shows the results obtained by FastSLAM, PF-SLAM and PS-SLAM. The localization results obtained by FastSLAM present a large deviation from the trajectory and tag real locations as shown in Figure 4.3(a). Figure 4.3(b) shows the comparisons of the results of PF-SLAM with the ground truth. Figure 4.3(c) presents the comparisons of the path of the robot and tag locations estimated by PS-SLAM with a random trajectory and the real tag positions. The estimations by PS-SLAM and PF-SLAM became better on a random trajectory than that on a predetermined trajectory according to Figures 4.3(b) and 4.3(c). However, the path of the robot and tag locations estimated by PS-SLAM got better overlaps than PF-SLAM.

Table 4.2 lists the errors of the localization of the robot and tags acquired by utilizing PS-SLAM, PF-SLAM and FastSLAM on the random trajectory. FastSLAM obtains a large error relative to the other two methods. PF-SLAM got a better result than that on the predetermined trajectory as proved in Chapter

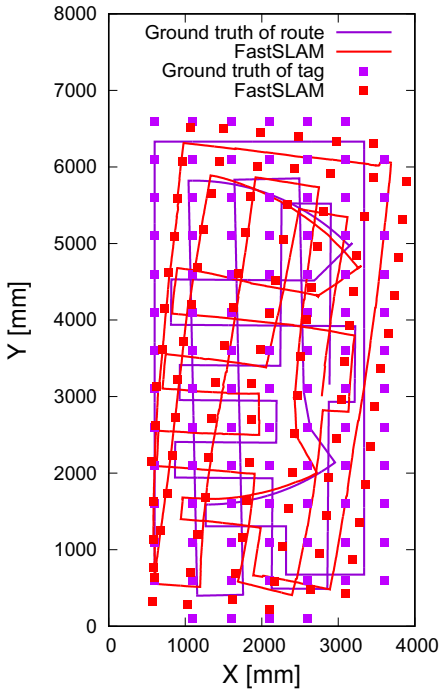

(a)

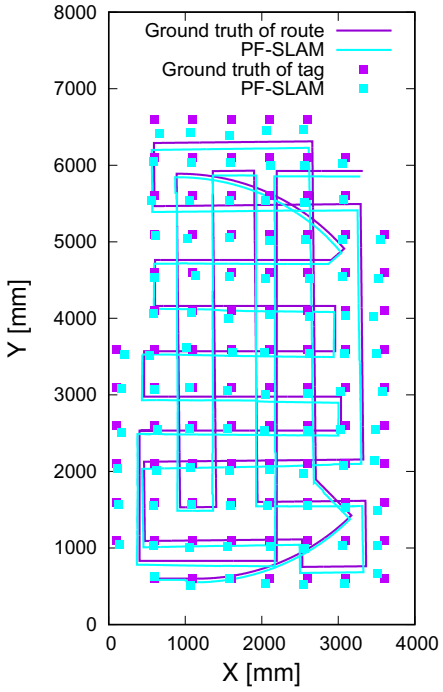

(b)

FIGURE 4.3: Results obtained by PS-SLAM, PF-SLAM and FastSLAM for the RFID detection model on a random trajectory. (a) shows the results obtained by FastSLAM. (b) shows results obtained by PF-SLAM. (c) shows the results obtained by PS-SLAM.

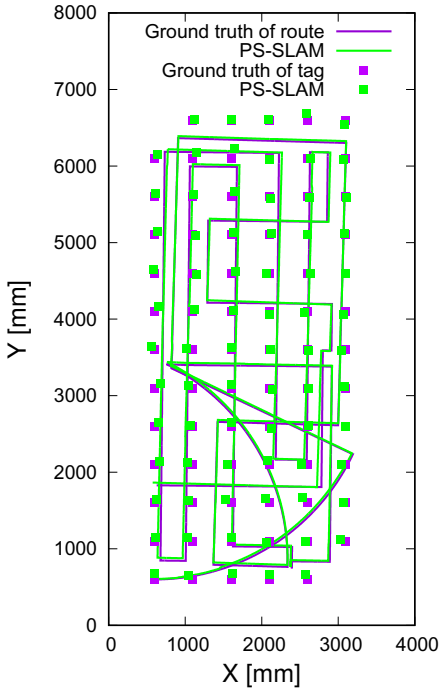

(c)

FIGURE 4.3: Results obtained by PS-SLAM, PF-SLAM and FastSLAM for the RFID detection model on a random trajectory. (a) shows the results obtained by FastSLAM. (b) shows results obtained by PF-SLAM. (c) shows the results obtained by PS-SLAM.

TABLE 4.2: Errors of the robot and tag localization utilizing three SLAM methods on the random trajectory.

Method	Robot localization				Tag localization		
	x [mm]	y [mm]	θ [rad]	d [mm]	x [mm]	y [mm]	d [cm]
PS-SALM	21.0	15.1	0.010	29.1	31.9	32.9	50.4
PF-SLAM	61.0	25.3	0.007	66.7	67.5	38.5	82.3
FastSLAM	110.4	198.6	0.131	245.7	122.5	234.1	280.0

3. The average distance errors of the robot and tag localization generated by utilizing PS-SLAM are about 30 mm and 50 mm. Both the results of the robot and tag locations obtained by PS-SLAM on the random trajectory are better than the results on the predetermined trajectory. Furthermore, our proposed PS-SLAM method also obtained a better performance on the random trajectory than PF-SLAM. This proves the validity of the hypothesis mentioned above. Although the particles for estimating the detected tag cannot be converged to a small range by using the smoothing method, the accuracy and stability are improved.

4.4.3 Performance of SLAM work with different detection range

To verify the superiority of the PS-SLAM method with the large detection range, PS-SLAM, PF-SLAM and FastSLAM were tested on the RFID detection model with different detection range. The robot moved on five predetermined trajectories with different detection ranges. The robot moved on each trajectory with three loops. The detection range was set from 100 to 500 mm. Figure 4.4 shows the average errors of robot and tag locations obtained by these three SLAM methods on the five predetermined trajectories with different detection ranges. The accuracy of the robot and tag locations reduces with the increase of the detection range. Because of the detection model of RFID is not belong to a Gaussian model, large detection range means a large uncertainty and noise. According to the results, the errors obtained by FastSLAM are much larger than the other two methods. Especially when the detection range increases. The accuracy of PS-SLAM and PF-SLAM is very similar when the detection range less than 180 mm. However, the performance of PS-SLAM becomes better than PF-SLAM as the detection range continues to increase. This proves PS-SLAM more suitable for the non-Gaussian detection model sensors with large detection range. By using the particle filter to estimate the tag location, particles easily converge to a wrong place with fast degeneracy. Particle smoother makes the particles converge slowly and obtains a stable estimation which improves the accuracy of full SLAM work.

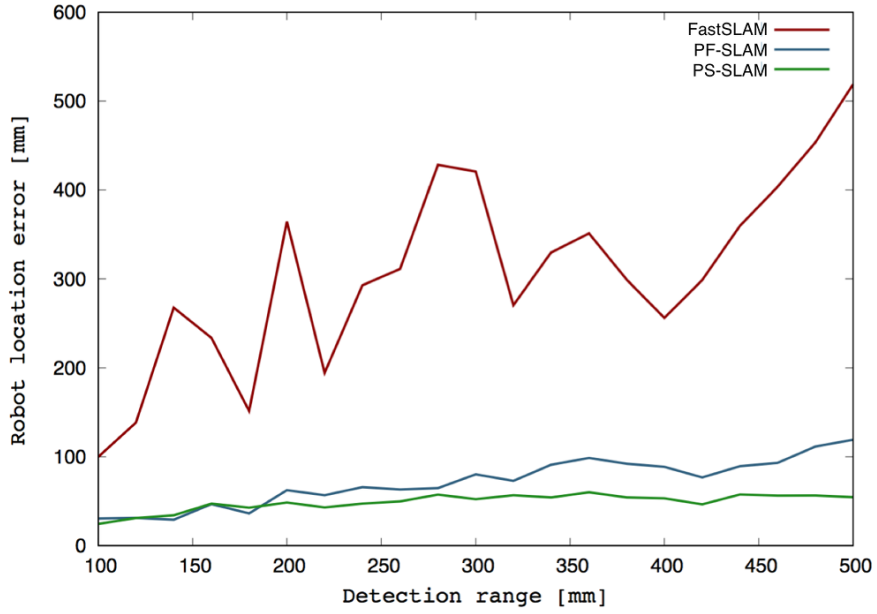

(a)

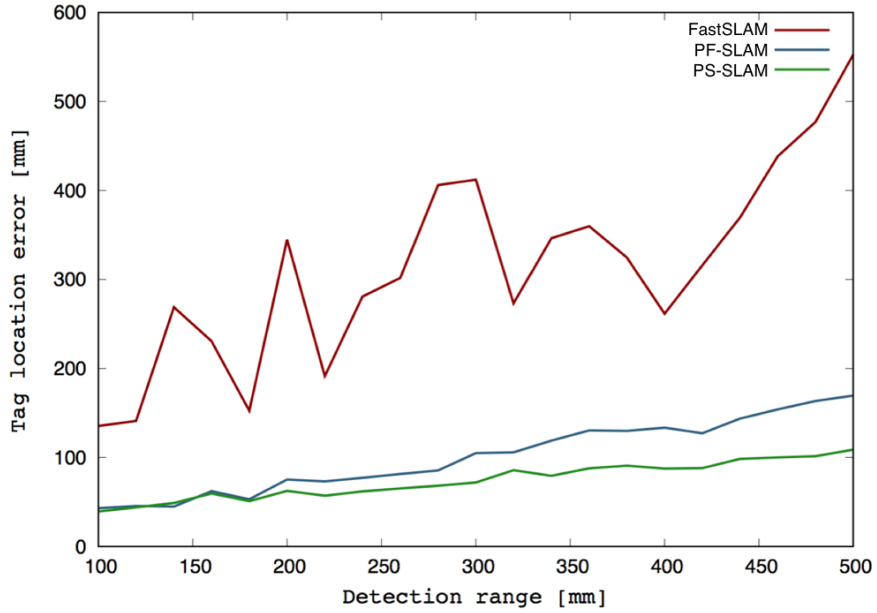

(b)

FIGURE 4.4: Localization errors as the detection range increases. (a) errors of the robot self-localization. (b) errors of the tag localization.

4.5 Summaries

SLAM method based on the particle smoother for the landmark mapping and particle filter for the self-localization of a mobile robot is proposed in this chapter. Although the particle filter is capable of processing the non-Gaussian detection model of the RFID system, the degeneracy problem becomes serious over time by using a particle filter to update the tag position. Therefore, the proposed PS-SLAM method utilizes particle smoother to update the position of the RFID tag and particle filter to update the position and orientation of the mobile robot. The particle smoother method reduces the degeneracy of particles, preserves the possibility of the correct estimation when errors occur and avoids all of the particles convergence to unrecoverable wrong estimation. The particle smoother improves the accuracy and stability of the estimation of the SLAM work. PS-SLAM is evaluated by the experiments based on the RFID detection model. Furthermore, PS-SLAM is compared with PF-SLAM and FastSLAM in the same experimental environments. The experimental results show the validity and superiority of the PS-SLAM method.

Chapter 5

A Low-cost IR-sensor-based Positioning System

The proposed IR-sensor-based positioning system is introduced in this chapter. The devices of the IR system used in our study is exhibited in Section 5.1. In Section 5.2, the algorithm of the self-localization method based on the proposed IR system is explained in detail. The performances of the robot self-localization by utilizing the proposed positioning system in the real experimental environment are shown in Sections 5.4. Last, we summarize this chapter in Section 5.5.

5.1 Proposed IR System

The illustration of the proposed IR-sensor-based positioning system is presented in Figure 5.1. The main components of the IR positioning system used in this study are the IR emitters and receivers. The IR emitters are installed on the ceiling used as landmarks. Different with RFID positioning system, the positions of the IR landmarks are known in advance for the IR positioning system. The proposed IR self-localization system consists of two types of emitters: the unique ID encoding emitter and repeated ID encoding emitter. The emitters are installed in a lattice pattern. One type of emitter is in the center of four the other type emitters. Two same type of emitters are separated by 80 cm. The robot is capable of frequently detecting the emitter and detecting one emitter at each time based on this interval. Two receivers equipped with an IR photodiode are

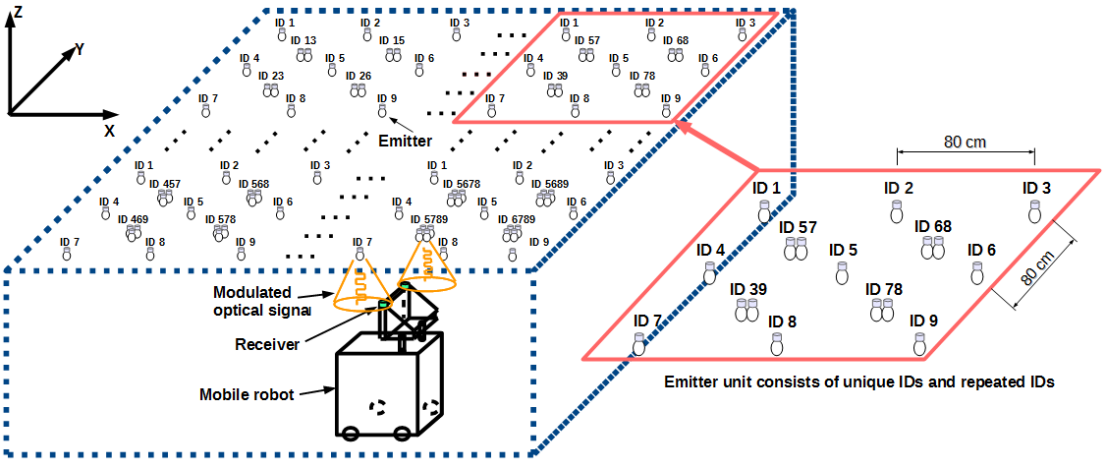

FIGURE 5.1: Illustration of the proposed IR-sensor-based positioning system

set on both sides of the robot top. The robot uses the receiver to obtain the signal transmitted from the IR emitter and recognize the detected IR emitter. Then, the self-localization of the robot can be achieved by using the location data of the detected emitters.

We use the frequency of the modulated signal as the IDs of the emitters. Because of the limitation of the available frequencies used as the IDs for the emitters, the mathematical combination method is utilized for generating the unique ID of the IR array. The IDs of the IR array in this type is obtained by a combination of different frequencies. The emitter encoded with unique ID is made up of an IR LED array which transmits the IR signals with multiple frequencies. One unique ID encoding emitter with four IR LEDs is shown in Figure 5.2(a). Four LEDs transmit the signal simultaneously and each LED transmits an independent signal with a frequency. The ID of this emitter is encoded by the four frequencies. In addition to using the combination method for solving the limited available IDs, the repeated ID encoding emitters are also applied in the system. The emitter encoded with repeated ID is just made up of a single LED which transmits the IR signals with a single frequency. Figure 5.2(b) shows a repeated ID encoding emitter. The IR LED with the part number OSI5LA5113A is used in the proposed system.

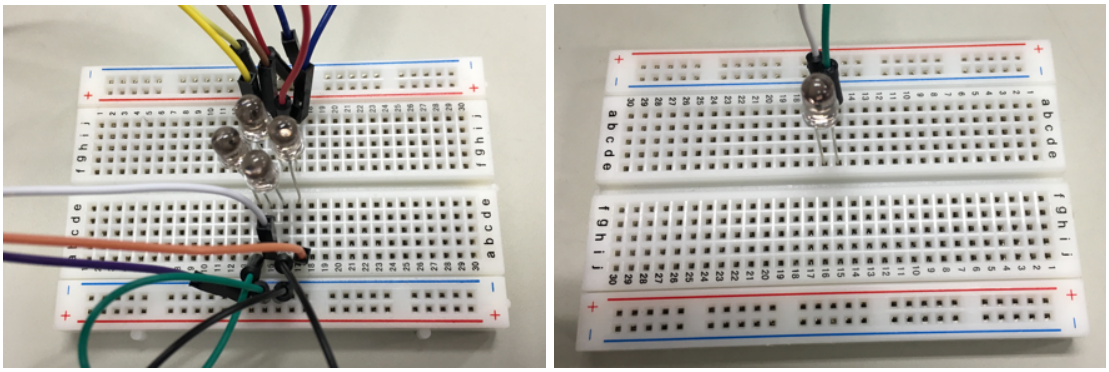

(a) (b)

FIGURE 5.2: Two types of the emitters: (a) unique ID encoding emitter with a LED array consists of four IR LEDs; (b) repeated ID encoding emitter with a single LED.

The modulated IR signals transmitted from the emitter are driven by a microcontroller connects with the IR LEDs. The on-off Keying (OOK) modulator is stored in the memory of the microcontroller for generating the IR signals with different frequencies. The circuit of the emitter is shown in Figure 5.3. Arduino UNO R3 is linked with the IR LEDs for generating the modulated optical signals. In this study, the IDs of the emitter are obtained by nine different frequencies. The nine frequencies with their corresponding code are listed in Table 5.1. The combination of the code generates the IDs of the emitters shown in Figure 5.1. For example, the emitter with ID 39 expresses that one of the LEDs transmits the IR signal with a frequency of 0.25 kHz and the other one is modulated by the frequency of 1.15 kHz.

TABLE 5.1: ID code and its corresponding frequency

Code	1	2	3	4	5	6	7	8	9
Frequency(kHz)	0.10	0.15	0.25	0.35	0.55	0.65	0.85	0.95	1.15

Two receivers with the photodiode and the configure of the receiver are shown in Figure 5.4. The receiver converts the detected IR signals to the electrical signal by utilizing the reverse bias circuit shown in Figure 5.5. A non-inverting amplifier is used in the receiver circuit to amplify the electrical signal

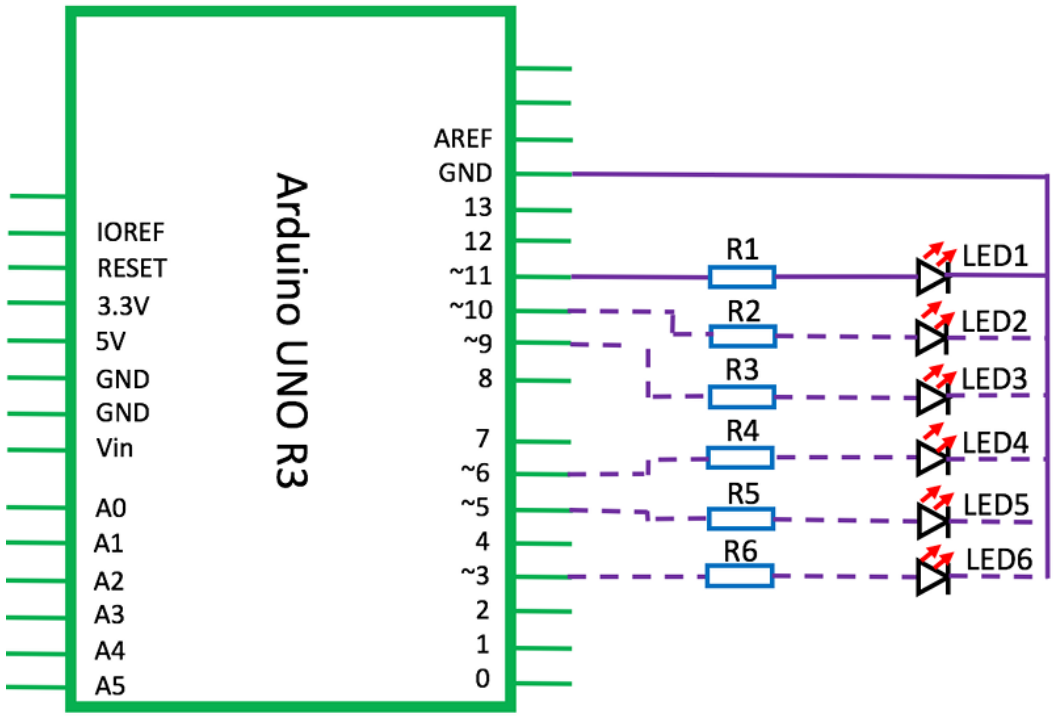

FIGURE 5.3: Emitter circuit.

to make the change of the signal more obvious. The photodiode with part number TPS 705 is used in the circuit of the receiver.

5.2 Self-localization of The Robot utilizing The IR-sensor-based Positioning System

MCL method is utilized to estimate the self-localization of the robot based on IR-sensor-based positioning system. A belief function is utilized to the MCL function for recognizing the emitter encoded with repeated ID. **Algorithm 3** shows the self-localization algorithm based on the positioning system. The form of the particles used to estimate the position and orientation of the robot is the same with Equation (3.4). The particles are initialized by randomly distributing in the environment. During the movement of the robot, these particles are updated based on the motion model which defined by Equation (3.6). Because the robot starts without known initialized position and orientation values, the belief of the repeated ID encoding emitters cannot be calculated at the

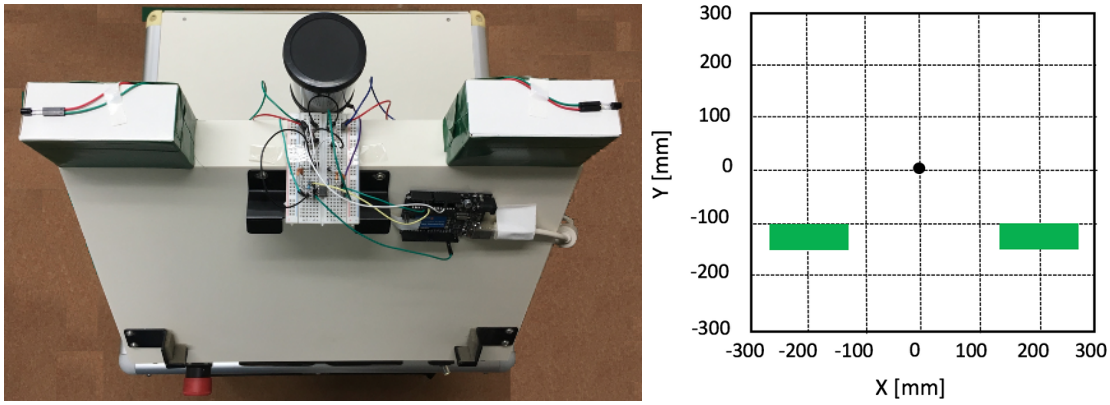

(a) (b)

FIGURE 5.4: The receiver: (a) top view of the receivers on the mobile robot; (b) the configuration of the receivers in 2D space.

beginning. The estimation of the robot localization starts when a unique ID encoding emitter is recognized.

As presented in line 6 of **Algorithm 3**, if an emitter is detected, we first determine whether it is encoded with a repeated ID. The recognition of the detected emitter is realized by analyzing the optical signals transmitted from the emitter. The ID of each emitter is encoded by using the frequencies of the transmitted IR signals. Therefore, we used the fast Fourier transform (FFT) method [86] to transform the signals obtained by the receiver in the time domain into the frequency domain. Figures 5.6(a) and 5.6(b) show the signals transmitted from a unique ID encoding emitter in the time domain and frequency domain, respectively. Figures 5.6(c) and 5.6(d) show the signals transmitted from a repeated ID encoding emitter in the time domain and frequency domain, respectively. The ID of the detected emitter can be obtained by resolving the frequencies of the received signals. If the detected emitter is encoded by a repeatedly used ID, a belief function is utilized to judge which emitter encoded with this repeated ID is being detected. This belief function is defined as:

$$bel_n^{[p]} = \exp(-\frac{1}{2\sigma^2}({}^w\boldsymbol{x}_n^{[p]} - {}^w\boldsymbol{x}_r)^{\mathrm{T}}({}^w\boldsymbol{x}_n^{[p]} - {}^w\boldsymbol{x}_r)). \tag{5.1}$$

Each emitter with the detected repeated ID obtains a belief value. The belief

Algorithm 3: Self-localization method based on the IR-sensor-based positioning system:

Initialization of the particle set $\boldsymbol{S}_{r,t} = (\boldsymbol{x}_{r,t}^{[1]}, \boldsymbol{x}_{r,t}^{[2]}, \cdots, \boldsymbol{x}_{r,t}^{[M]})$
for $i = 1$ to I **do**
  Particles are updated by the motion model: ${}^{w}\boldsymbol{x}_{r,t}^{[i]} = MotionModel({}^{w}\boldsymbol{x}_{r,t-1}^{[i]})$
end for
if emitter n is detected **then**
  if emitter n is encoded with a repeated ID **then**
    for $p = 1$ to P **do**
      $bel_n^{[p]}$ is calculated by utilizing the belief function
    end for
    $\boldsymbol{x}_e$ is equal to the location of the emitter that obtained the largest $bel_n^{[l]}$
  end if
  for $i = 1$ to I **do**
    $\omega_n^{[i]}$ is updated by utilizing the likelihood function
  end for
end if
for $i = 1$ to I **do**
  Create k with probability $\propto w_{r,t}^{[i]}$
  Add $\overline{x}_{r,t}^{[k]}$ to $\overline{S}_{r,t}$
end for
$\boldsymbol{S}_{r,t} \leftarrow \overline{\boldsymbol{S}}_{r,t}$
Return $\boldsymbol{S}_{,t}r$

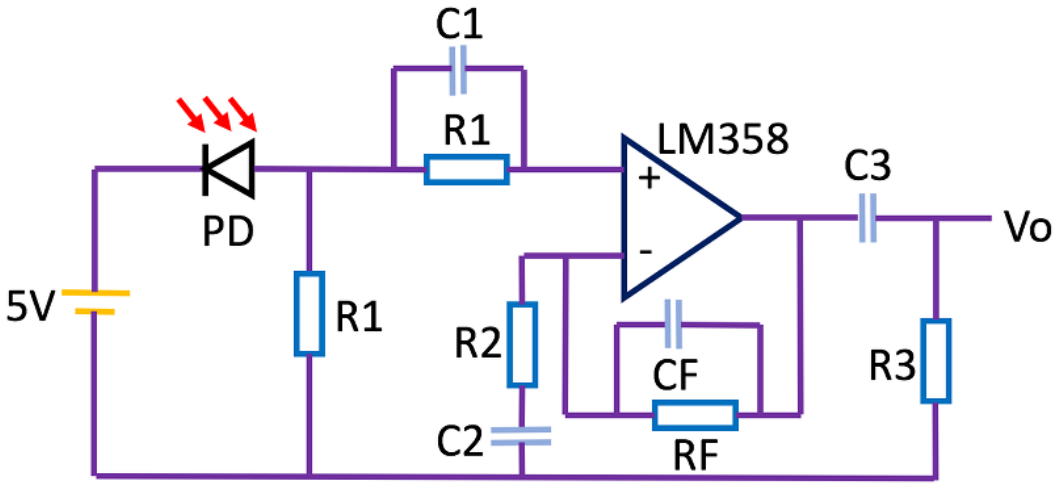

FIGURE 5.5: Receiver circuit consists of the reverse bias circuit and non-inverting amplifier. C1, C2, C3, and CF : 0.01 μF, R1 : 10 kΩ, R2 and R3 : 1 kΩ, RF : 680 kΩ, Vo : 8 V.

value of $bel_n^{[p]}$ is calculated by substituting the position value ${}^w\boldsymbol{x}_n^{[p]}$ of the emitter into the formula and comparing with the robot position ${}^w\boldsymbol{x}_r$. σ is set at 30 in this study. The emitter obtains the largest bel value is considered as the detected emitter and assign its location to $\boldsymbol{x}_e$ which is used for calculating the observation value.

The particles are updated after the detected emitter determined. The importance weight of each particle is updated by the likelihood function which is defined as:

$$\omega = \alpha \exp(-\frac{(V - \overline{V})^2}{2\sigma^2}), \tag{5.2}$$

where α is a constant value. V is the actual voltage obtained by the receiver. $\overline{V}$ is calculated by a function that expresses the relationship of the horizontal distance between the receiver and the detected emitter with the voltage obtained by the receiver. This function is obtained based on the experiment by keeping the distance between the receiver and the emitter at 1.2 m in the vertical direction and moving the receiver from the position right under the emitter to the 300 mm away in the horizontal direction. The voltage got from the receiver is recorded with 10-mm intervals. The approximation function is learned by

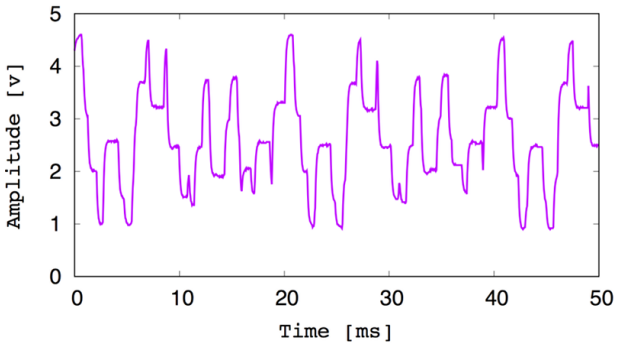

(a) Signals in time domain

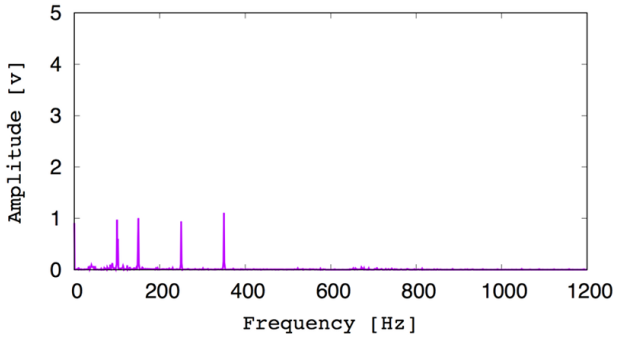

(b) Signals in frequency domain

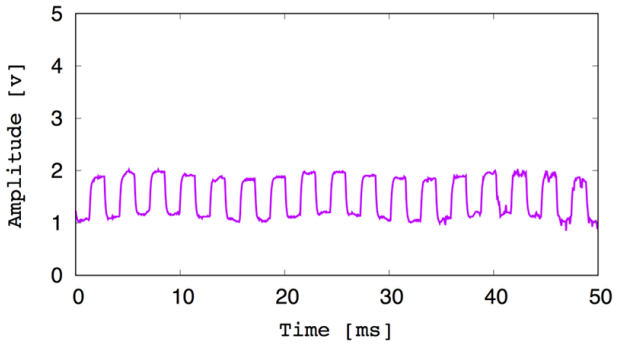

(c) Signals in time domain

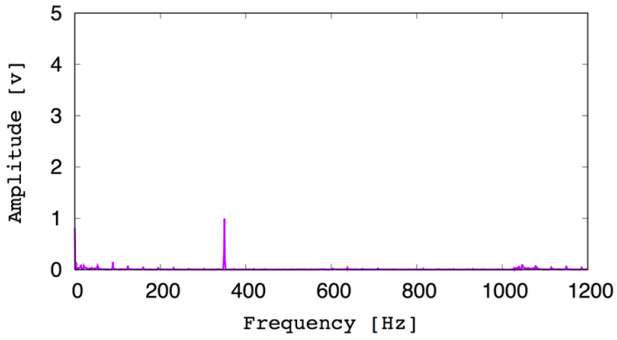

(d) Signals in frequency domain

FIGURE 5.6: Signals detected by receiver in the time and frequency domains: (a) and (b) signals transmitted from the unique ID encoding emitters; (c) and (d) signals transmitted from the repeated ID encoding emitters.

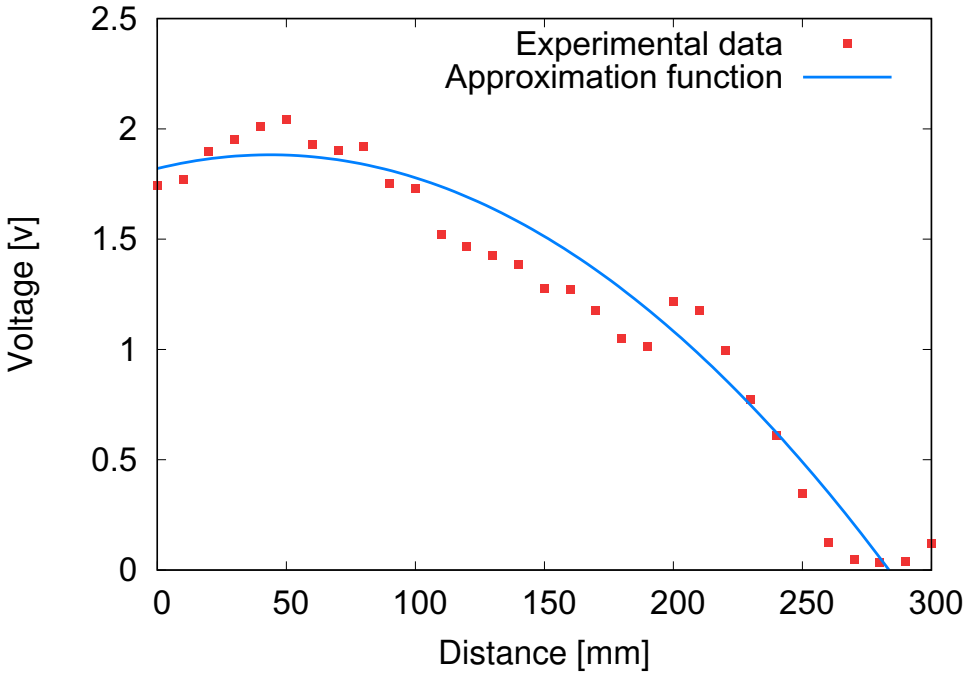

FIGURE 5.7: Experimental data (red points) recorded to obtain the observation function for the MCL method and the approximation function (blue line) achieved by utilizing the least-squares method.

using the least-square method. The learned function is defined as:

$$\overline{V} = -3.27 \times 10^{-5} e_d^2 + 2.855 \times 10^{-3} e_d + 1.81997, \tag{5.3}$$

$e_d = \sqrt{({}^w x_p - {}^w x_e)^2 + ({}^w y_p - {}^w y_e)^2}$. $({}^w x_p, {}^w y_p)$ presents the position of the receiver in the world coordinate. $({}^w x_e, {}^w y_e)$ is the position of the emitter with the largest bel. Figure 5.7 shows the learned function and the experimental data.

Then, the particles with the updated importance weights are resampled. The location and orientation of the robot are calculated by the resampled particles. The particles with larger important weights have a greater impact on the estimation of the robot self-localization. The function using the particles to estimate the position and orientation is expressed as:

$${}^w \boldsymbol{x}_{r,t} = \left(\frac{\sum_{i=1}^{I} {}^w \boldsymbol{x}_{r,t}^{[i]} \omega^{[i]}}{\sum_{i=1}^{I} \omega^{[i]}} \right) \tag{5.4}$$

5.3 Advantage of The Proposed IR System

The novel arrangement of emitter consists of utilizing the mathematical combination method to generate more unique IDs and the repeated ID encoding LED to make the proposed system suitable to a larger environment. To prove the validity of using the combination method, we assume that 30 frequencies are available to generate the IDs of the emitters, and six digital output pins of the microcontroller are provided. By using the combination method, $\sum_{n=1}^{6} {}_{30}C_n$ = 768,211 unique IDs which is approximately 25,000 times than the raw frequencies numbers can be obtained. In this study, 9 frequencies are applied to generate the IDs of the emitters. The proposed system is capable of obtaining $\sum_{n=1}^{9} {}_{9}C_n$ = 511 IDs by using 9 digital output pins of the microcontroller. Especially, the advantage of using the combination method for generating the IDs of the emitters becomes more obvious with the increase of the number of the available frequencies and the digital output pins of the microcontroller.

The validity of using the repeated ID encoding emitters as the landmarks in the environment for the self-localization of indoor mobile robot was demonstrated in [87]. In this study, we propose to combine the repeated ID encoding emitters and unique ID encoding emitters. By using this method, the limited IDs can be used to a larger environment. For instance, imaging 10 IDs are available to encode the emitters. The configurations of using the repeated ID encoding emitters and only using the unique ID encoding emitters are shown in Figures 5.8(a) and 5.8(b), respectively. The scale of the configuration combining the repeated ID encoding emitters and unique ID encoding emitters is approximate twice times more than the configuration which only uses the unique ID encoding emitters. Moreover, the production cost of the IR system is also reduced because of the emitter with the same ID driven by one microcontroller.

By using the emitter encoded by repeated ID, the memory size required for the system is fewer than only using the unique ID encoding emitter. Assuming L_r by W_r (L_r lines in the X-direction and W_r lines in the Y-direction) repeated ID

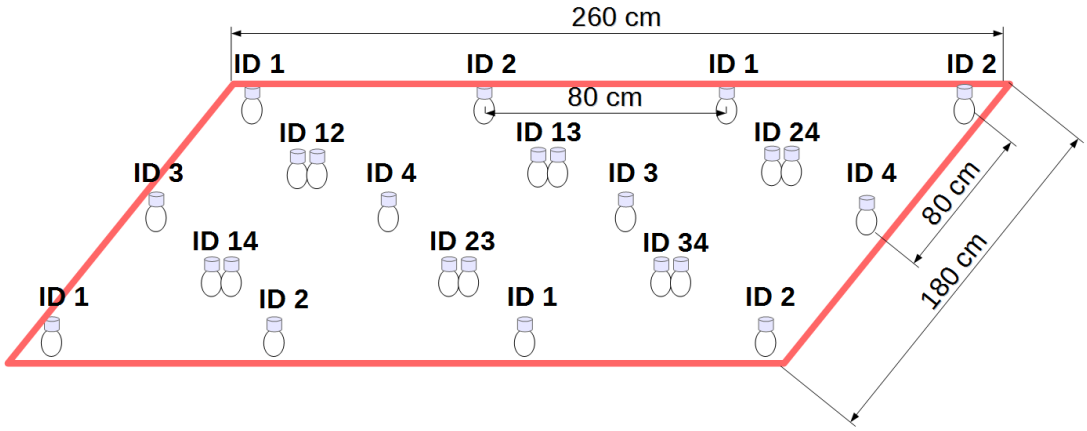

(a)

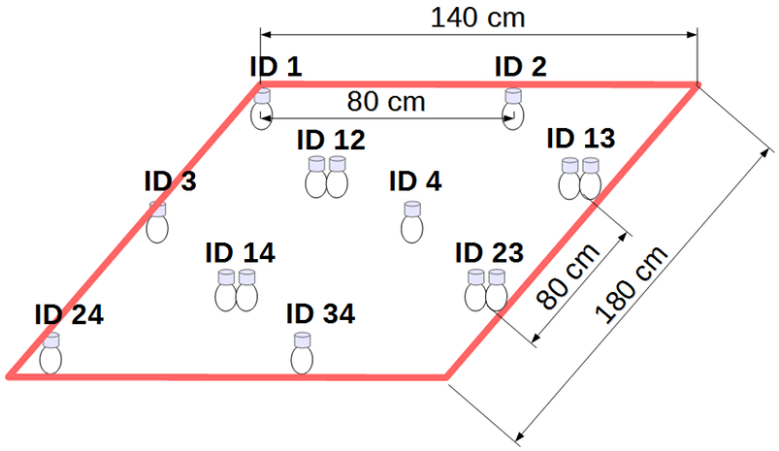

(b)

FIGURE 5.8: Available scale provided by two different emitter configurations: (a) utilizing the combination of the unique ID and repeated ID encoding emitters; (b) only utilizing the unique ID encoding emitters.

encoding emitters are used in the proposed system. According to the configuration shown in Figure 5.1, $(L_r - 1)$ by $(W_r - 1)$ unique ID encoding IR emitters are set in the proposed system. If 9 repeated IDs are used to the proposed system, the memory size of $(L_r - 1)(W_r - 1) + 9$ is needed. In the same scale of the environment, the system only uses the unique ID encoding emitters needs the memory size of $(L_r - 1)(W_r - 1) + L_r W_r$. For instance, let L_r = 600 and W_r = 400, memory sizes of $(L_r - 1)(W_r - 1) + 9$ = 239,010 and $(L_r - 1)(W_r - 1) + L_r W_r$ = 479,001 are needed for the proposed system and the system with unique ID encoding emitter only, respectively. The memory needed by the positioning system only using the unique ID encoding emitters is more than twice times than that of the proposed positioning system. Moreover, this superiority of the proposed positioning system becomes more obvious with the increase of L_r and W_r.

5.4 Experiment

The proposed IR-sensor-based positioning system was installed in the real environment and evaluated by several types of experiments. The experimental environment is shown in Figure 5.9(b). To make it clear, the illustration of the experimental environment is also presented in Figure 5.9(a). Because of the limitation of the real experimental environment, four IDs were repeatedly used in the experimental environment which is different with the emitter arrangements shown in Figure 5.1. The emitter encoded by the repeated ID was installed with a single LED. The unique ID encoding emitters were set in the center of four repeated ID encoding emitter. An LED array with four LEDs was used as the emitter encoded by the unique ID. The interval between two same type emitter was 80 cm. The height between the emitter and the receiver was 120 cm. Two receivers were set on two sides of the top of the robot. The emitter can be detected by the receiver within 280 cm from the center of the emitter in the horizontal direction. Seven microcontrollers were used for the emitters to generate the modulated IR signals. The emitters encoded by a same ID were driven by

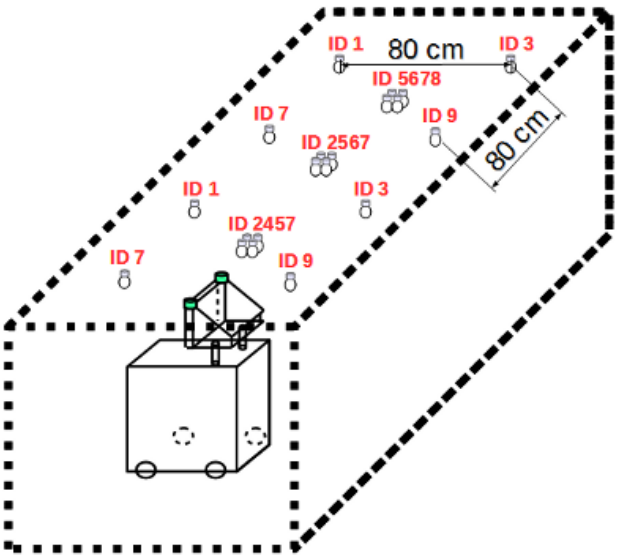

(a)

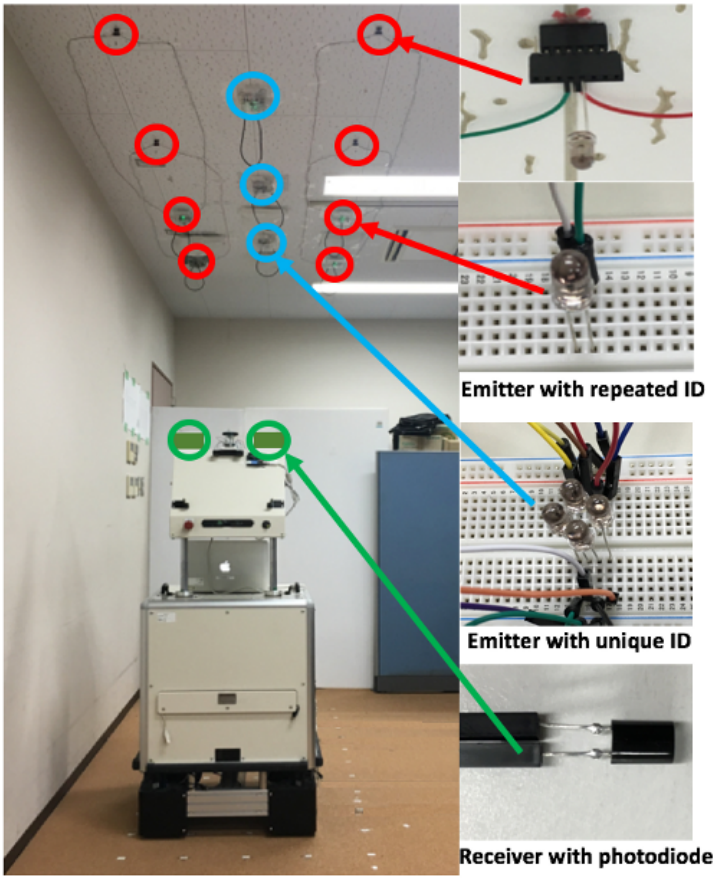

(b)

FIGURE 5.9: The IR-sensor-based positioning system in the Experimental environment: (a) illustration of positioning system and the experimental environment; (b) the real positioning system and experimental environment.

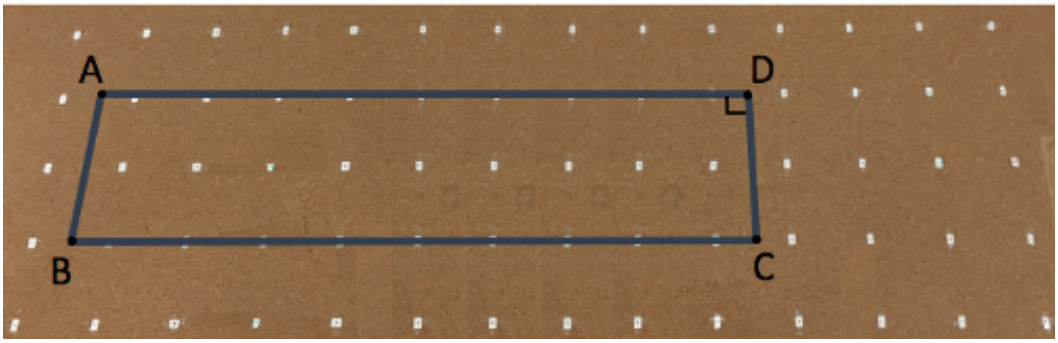

FIGURE 5.10: Experimental environment for estimating the real-time localization on a trajectory (represented by the blue line).

one microcontroller. One microcontroller was used for the receivers to analyze the received signals.

The proposed IR sensor based self-localization system was evaluated by a mobile robot in the experimental environment. We compared the performance of the robot self-localization utilizing the proposed emitter arrangement with that based on other arrangements. Moreover, the robot were performed at different speeds by using the proposed positioning system. At last, the proposed system was also evaluated in some special situations: the failure of some emitters and the change of the height between the receiver and the emitter. The number of particles used for the estimation of the robot self-localization is 1,000 in the environments.

5.4.1 Experiment with Different Emitter Configurations

The self-localization performances based on the proposed system and other two configurations of the emitters are evaluated on a predetermined trajectory. The predetermined trajectory is shown in Figure 5.10. The proposed system combines 3 unique ID encoding emitters and 8 repeated ID encoding emitters as shown in Figure 5.9. The other two configurations use 11 unique ID encoding emitters and no emitters, respectively. In the case of no emitters, the estimation of the position and orientation of the robot only rely on the odometry. The speed of the robot moved on the predetermined trajectory is set at 200 mm/s.

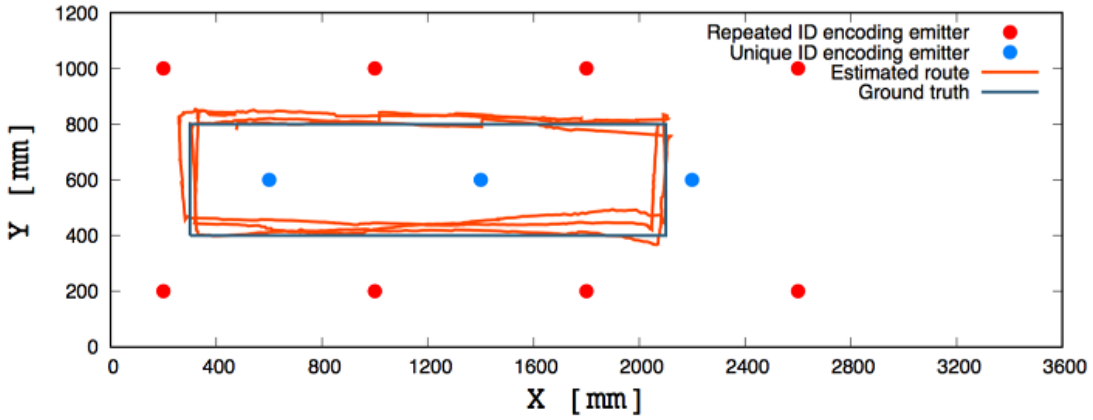

(a)

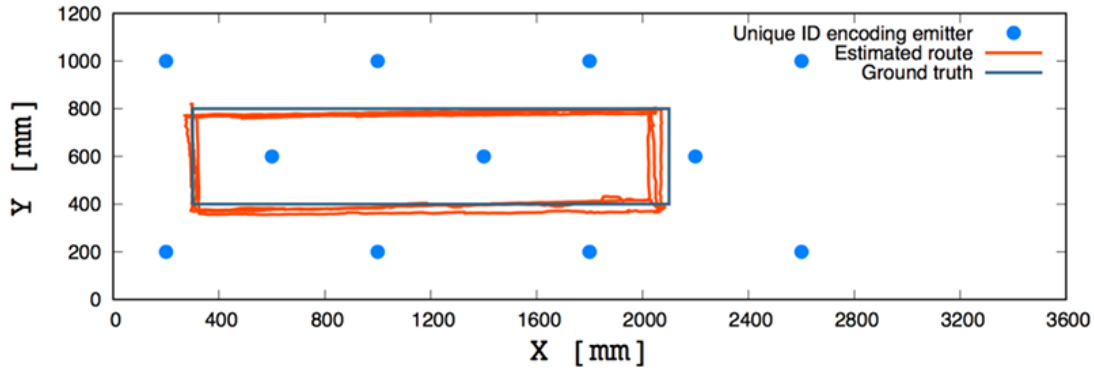

(b)

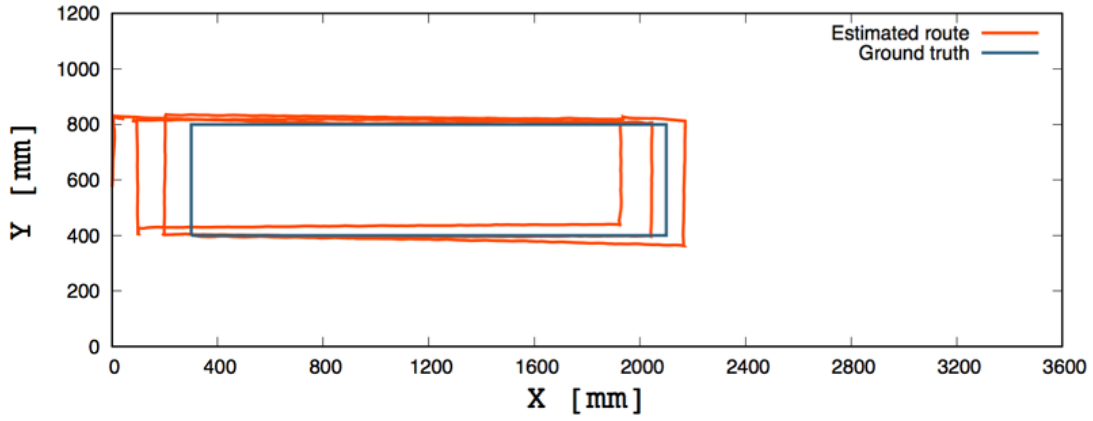

(c)

FIGURE 5.11: Results of the self-localization based on different configurations: (a) configuration of combining the unique ID and repeated ID encoding emitters; (b) configuration of using 11 unique ID encoding emitters; (c) no emitter.

Figure 5.11 presents the results obtained on the three configurations on the predetermined trajectory. The robot stated from the position of (300, 800) and moved along the trajectory 3 times. Figure 5.11(a) shows the result of the path estimated by the proposed positioning system on the predetermined trajectory. Most of the path estimated by using the proposed positioning system is consistent with the actual trajectory. Figure 5.11(b) shows the result of the path estimated by utilizing the configuration of 11 unique ID encoding emitters. The estimation based on the configuration with 11 emitters encoded by the unique IDs is accurate as the estimation obtained by the proposed system. The configuration of utilizing 11 unique ID encoding emitters has the same interval between the emitters as the proposed system. The robot is capable of detecting the emitters frequently during the movements on the predetermined trajectory with both configurations so that the calculated motor errors can be modified effectively. However, the result only relies on the odometry seriously deviates from the actual trajectory in the X direction as shown in Figure 5.11(c). The errors generated by the motors are accumulated without the adjustment based on the landmarks.

Comparing the results obtained by the three configurations, the accuracy of the self-localization of the robot based proposed positioning system and the configuration applies 11 unique ID encoding emitters much better than only relies on odometry. However, 11 IDs and microcontrollers are needed for the self-localization system only utilizes the unique ID encoding emitters. The proposed system only utilizes 7 IDs and microcontrollers for supporting an accurate performance. Therefore, the proposed system combines the repeated and unique ID encoding emitters reduces the ID and production costs than the existed IR self-localization system.

5.4.2 Experiment at The Marked Spots

To obtain the quantitative precision of the proposed system, 70 spots are marked in the experimental environment as shown in Figure 5.12. The performances of positioning by utilzing the configuration with 11 unique ID encoding emitters

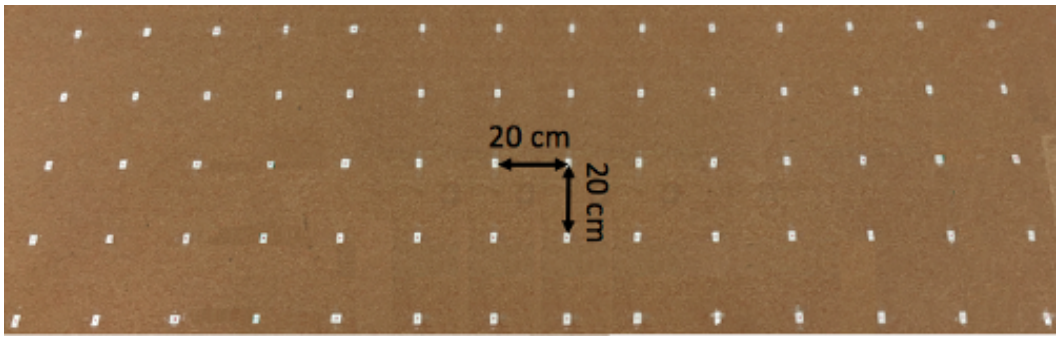

FIGURE 5.12: Experimental environment for estimating the location accuracy at 70 spots (the white points are the chosen positions).

and odometry are also verified at the 70 marked spots. The robot stays 5 seconds at the marked spot when passing by to record the estimated position and orientation data of the robot. The orientation of the robot was maintained at 0 [rad] during the experiments. The errors are calculated by comparing the recorded data with the ground truth of the marked spots.

TABLE 5.2: Errors of the self-localization at the 70 spots

Emitter configuration	Average error				Maximum error			
	x [mm]	y [mm]	θ [rad]	dr [mm]	x [mm]	y [mm]	θ [rad]	dr [mm]
Proposed system	22	29	0.06	36	69	79	0.23	105
11 unique IDs	30	25	0.04	39	87	91	0.10	126
Odometery	94	55	0.03	108	161	99	0.08	189

Table 5.2 lists the errors of the robot self-localization obtained by three different configurations at the 70 marked spots. The average distance error of the self-localization based on the proposed system is 36 mm and the orientation error is 0.06 [rad]. The accuracy of the estimation based on the configuration with 11 unique ID encoding emitters is close to that obtained by the proposed system. However, the error generated by the odometery is three times more than the proposed system. The performances of the robot self-localization on the discrete spots are same with the performances on the predetermined trajectory. The proposed system obtained an accurate estimation with fewer IDs and microcontrollers. Figure 5.13 shows the results of the self-localization at the 70 marked spots by utilizing the proposed positioning system. Considering

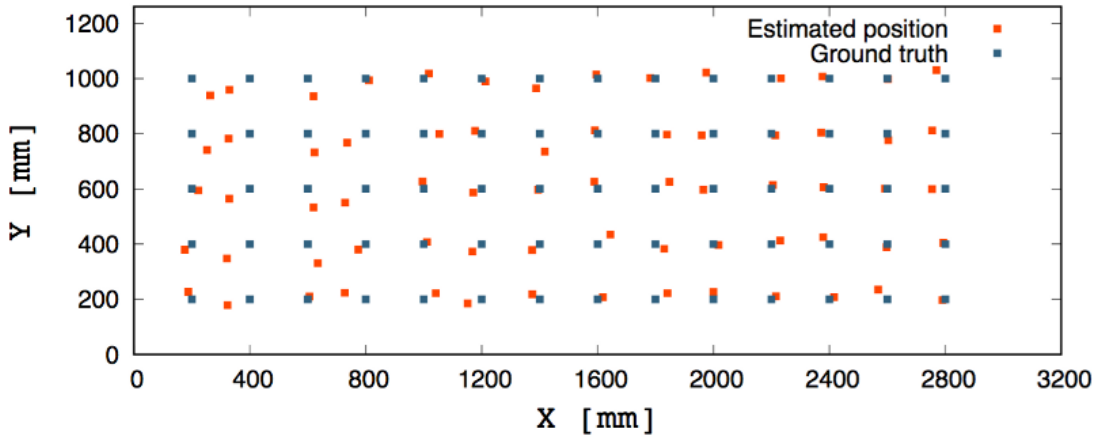

FIGURE 5.13: Results at 70 spots based on the proposed system.

the interval and installation errors in the emitters, the results obtained by the proposed system are accurate.

5.4.3 Experiment on Trajectory with Rotation

The proposed system supported an precise estimation for the robot self-localization on the trajectory without rotation. The path will obviously deviate with the trajectory when the orientation of the robot incorrectly estimated. To prove the validity of the system for the orientation estimation of the robot, we also tested the proposed system on a predetermined trajectory with rotations. The predetermined trajectory with different rotations is shown in Figure 5.14(a). The robot moved from E point to K point. The orientation of the robot changed five times at the marked points during the movements.

The path of the robot estimated by utilizing the proposed system on the predetermined trajectory with rotations is shown in Figure 5.14(b). The robot started without prior known initial position and orientation information so that the estimation at the beginning possibly cannot overlap with E point. However, the estimation was modified during the movements and the estimated path almost coincides with the trajectory. The validity of the proposed positioning system for the estimation of the robot orientation is proved by the experiment result.

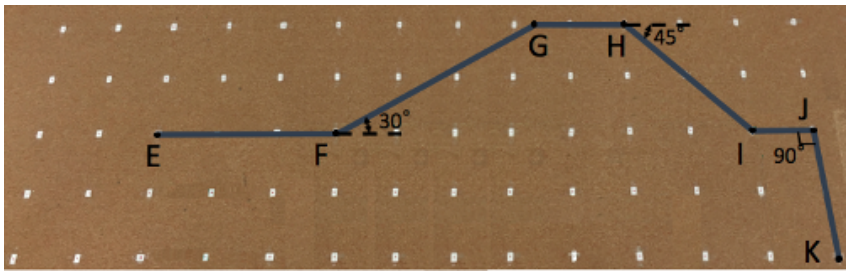

(a)

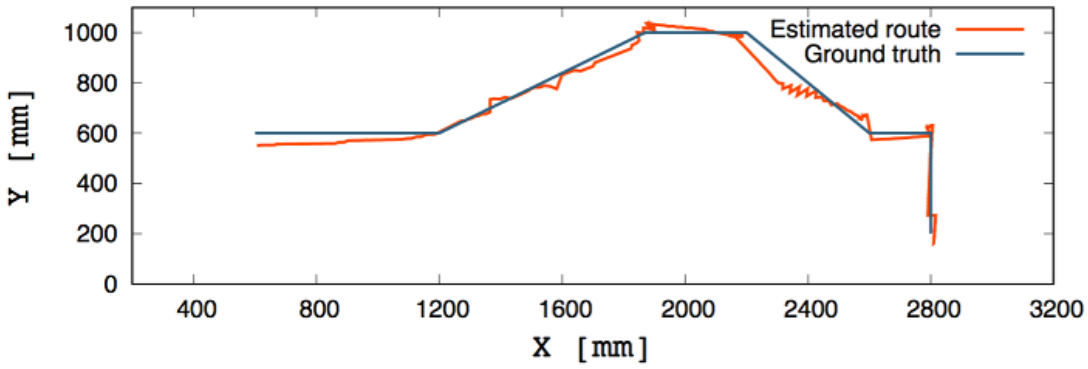

(b)

FIGURE 5.14: Result of the robot self-localization on the trajectory with orientations: (a) experimental environment and the trajectory (blue line) with different orientations; (b) Path of the robot estimated by utilizing the IR-sensor-based positioning system.

5.4.4 Experiment with Different Robot Speeds

The proposed system for the self-localization of the mobile robot also tested in the experimental environment by setting the robot at different speeds. The robot moved on the predetermined trajectory three times at speeds of 100, 150, 250, and 300 mm/s, respectively. The routes estimated by using the proposed system at these speeds are shown in Figure 5.15. All of the estimated routes almost overlap with the predetermined trajectory. The increase or decrease of the robot speed does not affect the accuracy of the robot self-localization by using the proposed system. The rapid communication property of the IR sensor makes the proposed system is capable of supporting an accurate estimation at a high speed.

5.4.5 Performances of The Proposed System with Emitter Failure and Height Alteration

Some particular cases possibly occur during the utilization of the proposed system. For instance, the light decay of the IR LED with a long utilization, the signals of some emitters obscured by some obstacles, and the bumps and depressions on the floor lead to the height between the receiver and emitter changed. In this section, the proposed system was evaluated in the situations of emitter failure and height alterations between the receiver and emitter.

The electricity of different ID encoding emitters is provided by independent powers in the proposed system so that there will not be a lot of emitter failures. Therefore, we removed the power of the two emitters encoded with the same ID to simulate the emitter failure. The configuration of the rest emitter is shown in Figure 5.16. Comparing with Figure 5.11(a), two emitters are eliminated in the configuration. The robot also moved on the predetermined trajectory without rotation three times. Figure 5.16 shows the path of the robot estimated in this particular situation. Although the instability increases, the accuracy of the estimation is acceptable for the indoor mobile robot.

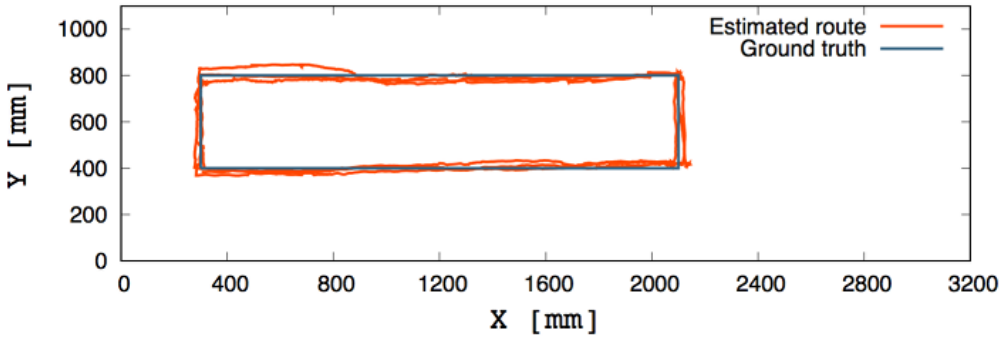

(a)

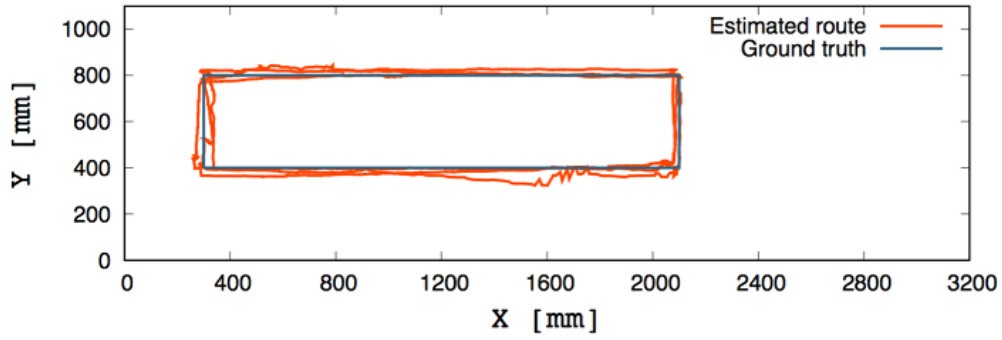

(b)

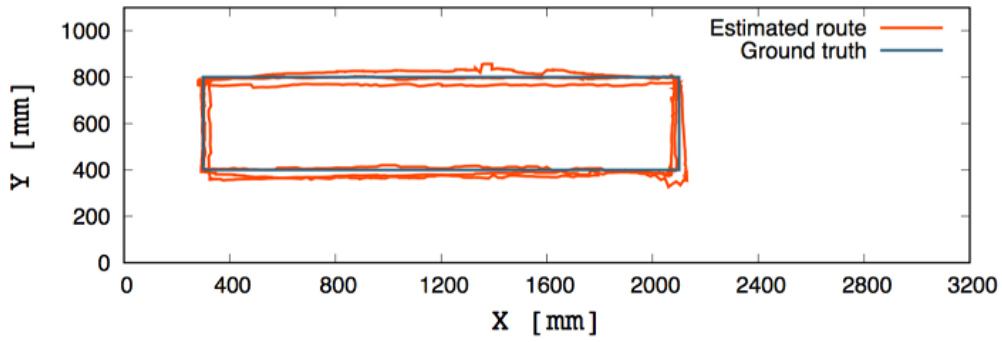

(c)

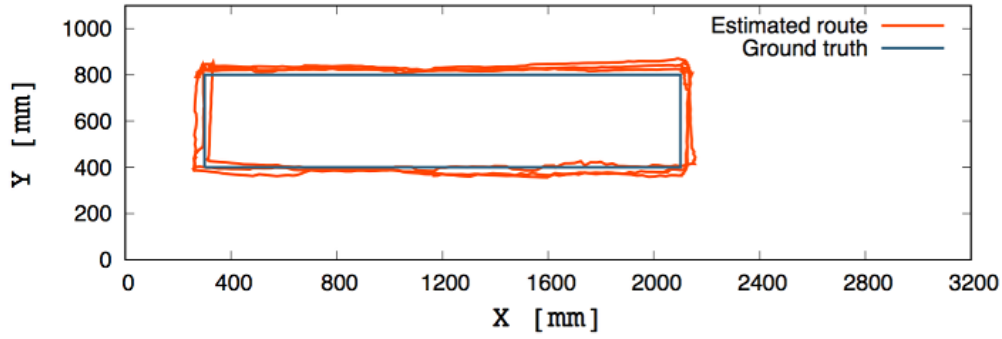

(d)

FIGURE 5.15: Real-time self-localization at different speeds: (a) 100 mm/s; (b) 150 mm/s; (c) 250 mm/s; (d) 300 mm/s.

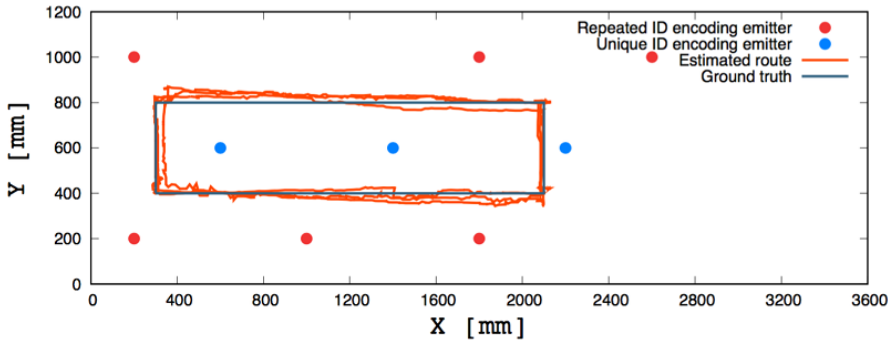

FIGURE 5.16: Path of the robot estimated by the proposed system with two emitter failures.

The undulation of the floor and the installation errors of the emitter in vertical direction occur in indoor environments. Equation (5.3) used for calculating the observation value is obtained based on the experimental data by keeping the height between the receiver and the emitter at a fixed value of 1.2 m. The undulation of the floor and the installation errors in emitter change the height between the receiver and the emitter. To evaluate the effect of the height change on the estimation of the positioning system, the height between the receiver and the emitter is adjusted from 1.1 to 1.3 m in the experiments. The performances of the self-localization under these heights are evaluated at the 70 marked spots shown in Figure 5.12. The robot stayed 5 seconds at each marked spot when passing by and recorded the estimated position and orientation of the robot.

Table 5.3 presents the average and maximum errors of the self-localization at the marked spots under different heights. The errors of the robot self-localization becomes larger with the increase of the height alteration. The average distance error of the robot is approximately 50 mm when the height alteration within 60 mm. If the height alteration exceeds 60 mm, the accuracy of the proposed system is not suitable for the indoor mobile robot self-localization. The propagation model of IR LED in 3D space makes Equation (5.3) will not lose its function immediately, but become less precise with the increase of the height alteration. Therefore, the alteration of the height between the emitter and receiver affects the accuracy of the proposed system. However, the accuracy is acceptable when the alteration within 60 mm. Especially, the undulation of the

floor and the installation errors of the emitters in the vertical direction are commonly less than 60 mm, in which case the proposed system is unaffected by these conditions.

TABLE 5.3: Errors of the robot self-localization with different heights

	Average error				Maximum error			
Height [m]	x [mm]	y [mm]	θ [rad]	dr [mm]	x [mm]	y [mm]	θ [rad]	dr [mm]
1.10	54	60	0.20	80	129	216	0.22	251
1.12	74	42	0.12	85	141	96	0.16	171
1.14	38	30	0.10	49	103	76	0.16	128
1.16	29	38	0.11	47	56	88	0.15	105
1.18	25	26	0.04	36	45	38	0.08	59
1.20	**22**	**29**	**0.07**	**36**	**69**	**79**	**0.23**	**105**
1.22	26	28	0.05	39	53	47	0.07	70
1.24	36	30	0.01	47	63	74	0.02	97
1.26	22	36	0.06	42	50	72	0.08	88
1.28	87	21	0.04	90	122	39	0.05	128
1.30	56	51	0.07	76	98	77	0.11	124

5.5 Summaries

In this study, an low-cost IR sensor based positioning system utilizing a novel emitter arrangement is proposed. The IR LED arrays used as the unique ID encoding emitters and the single LEDs used as the repeated ID encoding emitters are installed on the ceiling. The ID of the emitter is encoded by the frequency values of the signals transmitted from the emitter. The mathematical combination method is used for obtaining more available IDs for unique ID encoding emitters. With same number of available IDs, using the repeated ID encoding emitters makes the system can be used for larger environment. Two receivers are set on two sides of the robot top to scan the signals transmitted from the emitters.

The self-localization of the robot is estimated by the MCL method embedded with a belief function. Because the multiple applied ID encoding emitters used in the environment, this belief function is utilized to recognize the detected emitters. The IR-sensor-based positioning system is evaluated in several

types of experimental environments. The validity of this positioning system is also tested in some particular situations. The proposed IR system is capable of supporting an accurate estimation in the experiments.

Chapter 6

Conclusions and Future works

The self-localization systems for an indoor mobile robot based on the HF-band RFID system and IR system were proposed in this paper. RFID system based positioning system commonly needs the map of the RFID tags as a prior knowledge. However, the preparation work for recording the ID and measuring the positions of the RFID tags by human takes a long time. To solve this problem, the SLAM method is chosen to replace human labor. The non-Gaussian detection model of the RFID reader makes the classical FastSLAM with the Kalman filter based landmark updating is not suitable. Especially, RFID self-localization system always needs to set a huge amount of tags in the environment to realize an accurate performance for the self-localization of the robot. However, the time cost of FastSLAM increase obviously with the increase of the detected tags. Therefore, two novel SLAM methods: PF-SLAM and PS-SLAM respectively using the particle filter and particle smoother for the tag localization were proposed in this paper. Particle filter and particle smoother do not need any parametric model so that they are suitable to the HF-band RFID system with the non-Gaussian detection model.

PF-SLAM utilizes the particle filter for both the self-localization of the robot and the tag localization. By using the independent particle filter for each tag localization makes the update of the tag localization less affected by the increase of the detected tags. The superiority of PF-SLAM was proved in time cost with the increases of the numbers of the particles and the detected tags by comparing with FastSLAM in a simulation. The accuracy of PF-SLAM and FastSLAM were also evaluated in the simulated and real experimental environments by using

the RFID reader with the detection range of 60 $\times$ 60 mm^2. PF-SLAM showed a better performance than FastSLAM in both environments, and the accuracy of the PF-SLAM is enough to a real environment.

PF-SLAM is suitable to the RFID system for an indoor mobile robot by using the RFID reader with the detection range of 60 $\times$ 60 mm^2. However, the degeneracy of the particle filter for estimating the tag location becomes serious with the increase of the detection range which is capable of reducing the number of the RFID readers so that reduces the production cost. PS-SLAM utilizes the particle filter for the self-localization of the robot and particle smoother for the tag localization. By utilizing the particle smoother, novel states of the particles are generated by adding a Gaussian random value during the update and the tag localization relies on the sequential states of the particles which makes the estimation much more smoothing. Comparing with PF-SLAM, PS-SLAM only needs a slightly larger memory size. The time cost of PS-SLAM almost the same with PF-SLAM. However, the accuracy of PS-SLAM is much better than PF-SLAM and FastSLAM when using an RFID reader with a large detection range according to the results of the experiments in a simulated environment.

The algorithms of the two proposed SLAM methods are analyzed in Chapter 3 and Chapter 4. The superiority and validity of the two SLAM methods are discussed and evaluated in kinds of experiments. PF-SLAM is capable of using for the RFID self-localization system with a small detection range within 180 mm. Exceeding this range, PS-SLAM shows a better performance.

Chapter 5 introduced the proposed IR sensor based self-localization system for the indoor mobile robot. Most current IR sensor based self-localization techniques only use unique IDs to encode the emitters. Because the limited available IDs, some systems are not suitable for a large environment. To solve this problem, we proposed to utilize the mathematical combination method to obtain more available IDs and use the repeated ID encoding emitters and unique ID encoding emitters simultaneously in the environment. An IR LED array and a single LED are applied as the unique ID encoding emitter and repeated ID encoding emitter, respectively. The proposed system with the novel emitter

arrangement was evaluated in the real experimental environment. The experiments results confirm that the proposed system reduces the ID, storage, and production costs. Moreover, the proposed arrangement can be also used to the arrangement of the landmarks based on other sensors for the self-localization of the robot.

Comparing with the conventional positioning system based on RFID and IR sensors, the proposed methods improve the accuracy and reduce the calculation and production costs. The proposed PS-SLAM is tested in a simulated environment. In the future, this method is expected to be evaluated in the real experimental environment with the RFID system. The production of the RFID system also can be reduced by setting the configuration of the RFID tags and readers based on the proposed method with particle smoother based landmark updating. Especially, we plan to evaluate the two proposed SLAM methods on other sensors, for instance, the range and bearing sensor. We also intend to obtain the prior knowledge of the proposed IR self-localization system by using the SLAM method. The proposed SLAM methods are considered to combine with the received signal strength fingerprints method for a more accurate estimation. Especially, by using this method, the proposed IR system is capable of supporting the self-localization of the robot in a 3D space and the effect by the height alteration also can be solved. In addition to the estimation for the robot self-localization, the proposed IR system is also expected to the positioning of the people in the indoor environment.

Bibliography

[1] H. S. Dulimart and A. K. Jain, "Mobile robot localization in indoor environment", *Pattern Recognition*, vol. 30, no. 1, pp. 99 –111, 1997, ISSN: 0031-3203. DOI: https://doi.org/10.1016/S0031-3203(96)00064-7. [Online]. Available: http://www.sciencedirect.com/science/article/pii/S0031320396000647.

[2] C. Zhou, Y. Wei, and T. Tan, "Mobile robot self-localization based on global visual appearance features", *2003 IEEE International Conference on Robotics and Automation (Cat. No.03CH37422)*, vol. 1, pp. 1271–1276, 2003, ISSN: 1050-4729. DOI: 10.1109/ROBOT.2003.1241767.

[3] H. Surmann, A. Nüchter, and J. Hertzberg, "An autonomous mobile robot with a 3d laser range finder for 3d exploration and digitalization of indoor environments", *Robotics and Autonomous Systems*, vol. 45, no. 3, pp. 181 –198, 2003, ISSN: 0921-8890. DOI: https://doi.org/10.1016/j.robot.2003.09.004. [Online]. Available: http://www.sciencedirect.com/science/article/pii/S0921889003001556.

[4] A. A. Panchpor, S. Shue, and J. M. Conrad, "A survey of methods for mobile robot localization and mapping in dynamic indoor environments", *2018 Conference on Signal Processing And Communication Engineering Systems (SPACES)*, pp. 138–144, 2018. DOI: 10.1109/SPACES.2018.8316333.

[5] S. H. Cho and S. Hong, "Map based indoor robot navigation and localization using laser range finder", *2010 11th International Conference on Control Automation Robotics Vision*, pp. 1559–1564, 2010. DOI: 10.1109/ICARCV.2010.5707420.

[6] Z. Wang, Y. S. Hwang, Y. k. Kim, D. H. Lee, and J. Lee, "Mobile robot indoor localization using surf algorithm based on lrf sensor", *2015 54th Annual Conference of the Society of Instrument and Control Engineers of Japan (SICE)*, pp. 1122–1125, 2015. DOI: 10.1109/SICE.2015.7285500.

[7] U. Yayan, H. Yucel, and A. Yazıcı, "A low cost ultrasonic based positioning system for the indoor navigation of mobile robots", *Journal of Intelligent & Robotic Systems*, vol. 78, no. 3, pp. 541–552, 2015. DOI: 10.1007/s10846-014-0060-7. [Online]. Available: http://dx.doi.org/10.1007/s10846-014-0060-7.

[8] K. h. Hwang, D. e. Kim, D. h. Lee, and T. y. Kuc, "A simple ultrasonic gps system for indoor mobile robot system using kalman filtering", *2006 SICE-ICASE International Joint Conference*, pp. 2915–2918, 2006. DOI: 10.1109/SICE.2006.314996.

[9] C. E. Galvan, I. Galvan-Tejada, E. I. Sandoval, and R. Brena, "Wifi bluetooth based combined positioning algorithm", *Procedia Engineering*, vol. 35, pp. 101 –108, 2012.

[10] A. N. Raghavan, H. Ananthapadmanaban, M. S. Sivamurugan, and B. Ravindran, "Accurate mobile robot localization in indoor environments using bluetooth", *2010 IEEE International Conference on Robotics and Automation*, pp. 4391–4396, 2010, ISSN: 1050-4729. DOI: 10.1109/ROBOT.2010.5509232.

[11] G. Jekabsons, V. Kairish, and V. Zuravlyov, "An analysis of wi-fi based indoor positioning accuracy", *Scientific Journal of Riga Technical University Computer Science. Applied Computer Systems*, vol. 47, no. 6, Nov. 2011.

[12] J. Biswas and M. Veloso, "Wifi localization and navigation for autonomous indoor mobile robots", *2010 IEEE International Conference on Robotics and Automation*, pp. 4379–4384, 2010, ISSN: 1050-4729. DOI: 10.1109/ROBOT.2010.5509842.

[13] N. Akai and K. Ozaki, "Gaussian processes for magnetic map-based localization in large-scale indoor environments", pp. 4459–4464, 2015. DOI: 10.1109/IROS.2015.7354010.

[14] D. Navarro and G. Benet, "Magnetic map building for mobile robot localization purpose", pp. 1–4, 2009, ISSN: 1946-0740. DOI: 10.1109/ETFA.2009.5347181.

[15] J. Lee, C.-H. Hyun, and M. Park, "A vision-based automated guided vehicle system with marker recognition for indoor use", *Sensors*, vol. 13, no. 8, pp. 10 052–10 073, 2013, ISSN: 1424-8220. DOI: 10.3390/s130810052. [Online]. Available: http://www.mdpi.com/1424-8220/13/8/10052.

[16] J. Mi and Y. Takahashi, "Performance analysis of mobile robot self-localizaiton based on different configurations of rfid system", *2015 IEEE International Conference on Advanced Intelligent Mechatronics(AIM), July 7-11, 2015, Busan, Korea*, pp. 1591 –1596, 2015.

[17] S. Park and S. Hashimoto, "Indoor localization for autonomous mobile robot based on passive rfid", *2008 IEEE International Conference on Robotics and Biomimetics*, pp. 1856–1861, 2009. DOI: 10.1109/ROBIO.2009.4913284.

[18] S. Hijikata, K. Terabayashi, and K. Umeda, "A simple indoor self-localization system using infrared leds", *2009 Sixth International Conference on Networked Sensing Systems (INSS)*, pp. 1–7, 2009. DOI: 10.1109/INSS.2009.5409955.

[19] J. Bae, S. Lee, and J.-B. Song, "Use of coded infrared light for mobile robot localization", *Journal of Mechanical Science and Technology*, vol. 22, no. 7, pp. 1279 –1286, 2008.

[20] L. Mao, J. Chen, Z. Li, and D. Zhang, "Relative localization method of multiple micro robots based on simple sensors", *International Journal of Advanced Robotic Systems*, vol. 10, no. 2, p. 128, 2013. DOI: 10.5772/55587. eprint: https://doi.org/10.5772/55587. [Online]. Available: https://doi.org/10.5772/55587.

[21] T. Taketomi, H. Uchiyama, and S. Ikeda, "Visual slam algorithms: A survey from 2010 to 2016", *IPSJ Transactions on Computer Vision and Applications*, vol. 9, no. 1, pp. 1–16, 2017, ISSN: 1882-6695. DOI: 10.1186/s41074-017-0027-2. [Online]. Available: https://doi.org/10.1186/s41074-017-0027-2.

[22] T. Bailey, J. Nieto, J. Guivant, M. Stevens, and E. Nebot, "Consistency of the ekf-slam algorithm", *2006 IEEE/RSJ International Conference on Intelligent Robots and Systems*, pp. 3562–3568, 2006, ISSN: 2153-0858. DOI: 10.1109/IROS.2006.281644.

[23] D. M. Cole and P. M. Newman, "Using laser range data for 3d slam in outdoor environments", *Proceedings 2006 IEEE International Conference on Robotics and Automation, 2006. ICRA 2006.*, pp. 1556–1563, 2006, ISSN: 1050-4729. DOI: 10.1109/ROBOT.2006.1641929.

[24] G. Dissanayake, H. Durrant-Whyte, and T. Bailey, "A computationally efficient solution to the simultaneous localisation and map building (slam) problem", *Proceedings 2000 ICRA. Millennium Conference. IEEE International Conference on Robotics and Automation. Symposia Proceedings (Cat. No.00CH37065)*, vol. 2, pp. 1009–1014, 2000, ISSN: 1050-4729. DOI: 10.1109/ROBOT.2000.844732.

[25] A. Doucet, N. de Freitas, K. P. Murphy, and S. J. Russell, "Rao-blackwellised particle filtering for dynamic bayesian networks", *CoRR*, vol. abs/1301.3853, 2013. arXiv: 1301.3853. [Online]. Available: http://arxiv.org/abs/1301.3853.

[26] S. Thrun, "A probabilistic on-line mapping algorithm for teams of mobile robots", *The International Journal of Robotics Research*, vol. 20, no. 5, pp. 335–363, 2001. DOI: 10.1177/02783640122067435. eprint: https://doi.org/10.1177/02783640122067435. [Online]. Available: https://doi.org/10.1177/02783640122067435.

[27] R. Want, "An introduction to rfid technology", *IEEE Pervasive Computing*, vol. 5, pp. 25–33, 2006.

[28] A. Shibata, *Basics of rfid*, https://www.japia.or.jp/only/iinkai/RFID-081202kiso.pdf, Japan Auto Parts Industries Association, 2008.

[29] Y. Takahashi, Y. Ii, M. Jian, W. Jun, Y. Maeda, M. Takeda, R. Nakamura, H. Miyoshi, H. Takeuchi, Y. Yamashita, H. Sano, and A. Masuda, "Mobile robot self localization based on multi-antenna-rfid reader and ic tag textile", *2013 IEEE Workshop on Advanced Robotics and its Social Impacts*, pp. 106–112, 2013, ISSN: 2162-7568. DOI: 10.1109/ARSO.2013.6705514.

[30] S. Schneegans, P. Vorst, and A. Zell, "Using rfid snapshots for mobile robot self-localization", *European Conference on Mobile Robots*, pp. 241–246, 2007.

[31] K. Yamano, K. Tanaka, M. Hirayama, E. Kondo, Y. Kimuro, and M. Matsumoto, "Self-localization of mobile robots with rfid system by using support vector machine", *Proceedings of 2004 IEEE/RSJ International Conference on Intelligent Robots and Systems*, pp. 3756 –3761, 2004.

[32] S. Park and S. Hashimot, "Autonomous mobile robot navigation using passive rfid in indoor environment", *IEEE TRANSACTIONS ON INDUSTRIAL ELECTRONICS*, vol. 56, no. 7, pp. 2366–2373, 2009.

[33] N. A. Sabto and K. A. Mutib, "Autonomous mobile robot localization based on rssi measurements using an rfid sensor and neural network bpann", *Journal of King Saud University - Computer and Information Sciences*, vol. 25, no. 2, pp. 137 –143, 2013, ISSN: 1319-1578. DOI: https://doi.org/10.1016/j.jksuci.2012.10.001. [Online]. Available: http://www.sciencedirect.com/science/article/pii/S1319157812000377.

[34] K. Chawla, G. Robins, and L. Zhang, "Efficient rfid-based mobile object localization", *2010 IEEE 6th International Conference on Wireless and Mobile Computing, Networking and Communications*, pp. 683–690, 2010, ISSN: 2160-4886. DOI: 10.1109/WIMOB.2010.5644853.

[35] G. H. Lee, F. Fraundorfer, and M. Pollefeys, "Structureless pose-graph loop-closure with a multi-camera system on a self-driving car", *2013 IEEE/RSJ International Conference on Intelligent Robots and Systems*, pp. 564–571, 2013, ISSN: 2153-0858. DOI: 10.1109/IROS.2013.6696407.

[36] R. W. Wolcott and R. M. Eustice, "Visual localization within lidar maps for automated urban driving", *2014 IEEE/RSJ International Conference on Intelligent Robots and Systems*, pp. 176–183, 2014, ISSN: 2153-0858. DOI: 10.1109/IROS.2014.6942558.

[37] G. Bresson, Z. Alsayed, L. Yu, and S. Glaser, "Simultaneous localization and mapping: A survey of current trends in autonomous driving", *IEEE Transactions on Intelligent Vehicles*, vol. 2, no. 3, pp. 194–220, 2017, ISSN: 2379-8904. DOI: 10.1109/TIV.2017.2749181.

[38] M. N. Dailey, "Landmark-based simultaneous localization and mapping with stereo vision", 2005.

[39] M. Montemerlo, S. Thrun, D. Koller, and BenWegbreit, "Fastslam: A factored solution to the simultaneous localization and mapping problem", *AAAI-02 Proceedings*, 2002.

[40] M. Montemerlo, S. Thrun, D. Koller, and B. Wegbreit, "Fastslam 2.0: An improved particle filtering algorithm for simultaneous localization and mapping that provably converges", *Proc. IJCAI Int. Joint Conf. Artif. Intell.*, Jun. 2003.

[41] J. Wang and Y. Takahashi, "Simultaneous localization and mapping on hf-band rfid system for omni-direction vehicle", *The Robotics and Mechatronics Conference*, no. 2A2-M04, 2015.

[42] S. Thrun, "Particle filters in robotics", *Proceedings of the Eighteenth Conference on Uncertainty in Artificial Intelligence*, UAI'02, pp. 511–518, 2002. [Online]. Available: http://dl.acm.org/citation.cfm?id=2073876.2073937.

[43] H. R. Künsch, "Particle filters", *Bernoulli*, vol. 19, no. 4, pp. 1391–1403, Sep. 2013. DOI: 10.3150/12-BEJSP07. [Online]. Available: https://doi.org/10.3150/12-BEJSP07.

[44] X. Wang, T. Li, S. Sun, and J. M. Corchado, "A survey of recent advances in particle filters and remaining challenges for multitarget tracking", *Sensors*, 2017.

[45] C. KWOK, D. FOX, and M. MEILA, "Real-time particle filters", *Proceedings of the IEEE*, vol. 92, no. 3, pp. 469–484, 2004, ISSN: 0018-9219. DOI: 10.1109/JPROC.2003.823144.

[46] D. Fox, W. Burgard, F. Dellaert, and S. Thrun, "Monte carlo localization: Efficient position estimation for mobile robots", 1999.

[47] F. Dellaert, D. Fox, W. Burgard, and S. Thrun, "Monte carlo localization for mobile robots", *Proceedings 1999 IEEE International Conference on Robotics and Automation (Cat. No.99CH36288C)*, vol. 2, pp. 1322–1328, 1999, ISSN: 1050-4729. DOI: 10.1109/ROBOT.1999.772544.

[48] A. Doucet and A. M. Johansen, "A tutorial on particle filtering and smoothing: Fifteen years later", *Nonlinear Filtering Handbook*, D. Crisan and B. Rozovsky, Eds., pp. 656–704, 2011.

[49] F. Daum and J. Huang, "Particle degeneracy: Root cause and solution", *Proceedings of SPIE - The International Society for Optical Engineering*, vol. 8050, May 2011.

[50] T. Li, S. Sun, T. P. Sattar, and J. M. Corchado, "Fighting against sample degeneracy and impoverishment in particle filters: Particularly on intelligent choices", *CoRR*, vol. abs/1308.2443, 2013. arXiv: 1308.2443. [Online]. Available: http://arxiv.org/abs/1308.2443.

[51] C. M. Carvalho, M. S. Johannes, H. F. Lopes, and N. G. Polson, "Particle learning and smoothing", *Statist. Sci.*, vol. 25, no. 1, pp. 88–106, Feb. 2010. DOI: 10.1214/10-STS325. [Online]. Available: https://doi.org/10.1214/10-STS325.

[52] M. Klaas, M. Briers, N. de Freitas, A. Doucet, S. Maskell, and D. Lang, "Fast particle smoothing: If i had a million particles", *Proceedings of the 23rd International Conference on Machine Learning*, ICML '06, pp. 481–488, 2006. DOI: 10.1145/1143844.1143905. [Online]. Available: http://doi.acm.org/10.1145/1143844.1143905.

[53] C. M. Carvalho, M. S. Johannes, H. F. Lopes, and N. G. Polson, "Particle learning and smoothing", *Statistical Science*, vol. 25, no. 1, pp. 88–106, 2010, ISSN: 08834237. [Online]. Available: http://www.jstor.org/stable/41058999.

[54] G. Kitagawa, "Monte carlo filter and smoother for non-gaussian nonlinear state space models", *Journal of Computational and Graphical Statistics*, vol. 5, no. 1, pp. 1–25, 1996, ISSN: 10618600. [Online]. Available: http://www.jstor.org/stable/1390750.

[55] A. Cuzol and E. Mémin, "Monte Carlo fixed-lag smoothing in state-space models", *Nonlinear Processes in Geophysics*, vol. 21, pp. 633–643, 2014. DOI: 10.5194/npg-21-633-2014. arXiv: 1310.1267 [stat.AP].

[56] E. Aitenbichler and M. Muhlhauser, "An ir local positioning system for smart items and devices", *23rd International Conference on Distributed Computing Systems Workshops, 2003. Proceedings.*, pp. 334–339, 2003. DOI: 10.1109/ICDCSW.2003.1203576.

[57] S. S. Ghidary, T. Tani, T. Takamori, and M. Hattori, "A new home robot positioning system (hrps) using ir switched multi ultrasonic sensors", *IEEE SMC'99 Conference Proceedings. 1999 IEEE International Conference on Systems, Man, and Cybernetics (Cat. No.99CH37028)*, vol. 4, pp. 737–741, 1999, ISSN: 1062-922X. DOI: 10.1109/ICSMC.1999.812496.

[58] T. Raharijaona, R. Mawonou, T. V. Nguyen, F. Colonnier, M. Boyron, J. Diperi, and S. Viollet, "Local positioning system using flickering infrared leds", *Sensors*, 2017.

[59] M. Cikowskii, "A prototype of static ir beacon-receiver positioning system based on triangulation method", *Measurement*, vol. 128, pp. 149 – 159, 2018, ISSN: 0263-2241. DOI: https://doi.org/10.1016/j.measurement.2018.06.039. [Online]. Available: http://www.sciencedirect.com/science/article/pii/S0263224118305657.

[60] J. Krejsa and S. Vechet, "Infrared beacons based localization of mobile robot", *Elektronika ir Elektrotechnika*, vol. 117, no. 1, 2012, ISSN: 2029-5731. [Online]. Available: http://eejournal.ktu.lt/index.php/elt/article/view/1046.

[61] C.-H. Chen and K.-T. Song, "Complete coverage motion control of a cleaning robot using infrared sensors", *IEEE International Conference on Mechatronics*, pp. 543–548, 2005. DOI: 10.1109/ICMECH.2005.1529316.

[62] J. H. Oh, D. Kim, and B. H. Lee, "An indoor localization system for mobile robots using an active infrared positioning sensor", *Journal of Industrial and Intelligent Information*, vol. 2, no. 1, pp. 35 –38, Mar. 2014.

[63] S. Lee, "Use of infrared light reflecting landmarks for localization", *Industrial Robot: An International Journal*, vol. 36, no. 2, pp. 138–145, 2009. DOI: 10.1108/01439910910932595. eprint: https://doi.org/10.1108/01439910910932595. [Online]. Available: https://doi.org/10.1108/01439910910932595.

[64] M. Forzati, "Phase modulation techniques for on-off keying transmission", *2007 9th International Conference on Transparent Optical Networks*, vol. 1, pp. 24–29, 2007, ISSN: 2162-7339. DOI: 10.1109/ICTON.2007.4296022.

[65] K. Mishina, S. Kitagawa, and A. Maruta, "All-optical modulation format conversion from on-off-keying to multiple-level phase-shift-keying based on nonlinearity in optical fiber", *Opt. Express*, vol. 15, no. 13, pp. 8444–8453, 2007. DOI: 10.1364/OE.15.008444. [Online]. Available: http://www.opticsexpress.org/abstract.cfm?URI=oe-15-13-8444.

[66] S. Thrun, W. Burgard, and D. Fox, *Probabilistic Robotics*. Cambridge and Massachusetts: The MIT Press, 2006.

[67] N. B. F. da Silva, D. B. Wilson, and K. R.L. J. Branco, "Performance evaluation of the extended kalman filter and unscented kalman filter", *2015 International Conference on Unmanned Aircraft Systems (ICUAS)*, pp. 733–741, 2015. DOI: 10.1109/ICUAS.2015.7152356.

[68] Q. Li, R. Li, K. Ji, and W. Dai, "Kalman filter and its application", *2015 8th International Conference on Intelligent Networks and Intelligent Systems (ICINIS)*, pp. 74–77, 2015.

[69] K. P. Murphy, "Bayesian map learning in dynamic environments", *Neural Information Processing Systems (NIPS)*, pp. 1015–1021, 1999.

[70] G. Grisetti, G. D. Tipaldi, C. Stachniss, W. Burgard, and D. Nardi, "Fast and accurate slam with raoblackwellized particle filters", *Robotics and Autonomous Systems*, vol. 55, no. 1, pp. 30 –38, 2007, Simultaneous Localisation and Map Building, ISSN: 0921-8890. DOI: https://doi.org/10.1016/j.robot.2006.06.007. [Online]. Available: http://www.sciencedirect.com/science/article/pii/S092188900600145X.

[71] A. Eliazar and R. Parr, "Dp-slam: Fast, robust simultaneous localization and mapping without predetermined landmarks", *International Joint Conference on Artificial Intelligence*, 2003.

[72] C. Forster, D. Sabatta, R. Siegwart, and D. Scaramuzza, "Rfid-based hybrid metric-topological slam for gps-denied environments", *IEEE International Conference on Robotics and Automation*, pp. 5228 –5234, 2013.

[73] D. Joho, C. Plagemann, and W. Burgard, "Modeling rfid signal strength and tag detection for localization and mapping", *IEEE International Conference on Robotics and Automation*, pp. 3160 –3165, 2009.

[74] T. Deyle, C. C. Kemp, and M. S. Reynolds, "Probabilistic uhf rfid tag pose estimation with multiple antennas and a multipath rf propagation model", *IEEE/RSJ International Conference on Intelligent Robots and Systems*, pp. 1379 –1384, Sep. 2008.

[75] K. Berntorp and J. Nordh, "Rao-blackwellized particle smoothing for occupancy-grid based slam using low-cost sensors", *IFAC Proceedings Volumes*, vol. 47, no. 3, pp. 10174 –10 181, 2014, 19th IFAC World Congress, ISSN: 1474-6670. DOI: https://doi.org/10.3182/20140824-6-ZA-1003.00649. [Online]. Available: http://www.sciencedirect.com/science/article/pii/S1474667016432283.

[76] D. E. Clark, C. S. Lee, and S. Nagappa, "Single-cluster phd filtering and smoothing for slam applications", *International Conference on Robotics and Automation*, 2012.

[77] robotshop, *Hagisonic stargazer rs robot localization system*, http://www.robotshop.com/en/hagisonic-stargazer-rs-localization-system.html, Hagisonic.

[78] I. Ul-Haque and E. Prassler, "Experimental evaluation of a low-cost mobile robot localization technique for large indoor public environments", *ISR 2010 (41st International Symposium on Robotics) and ROBOTIK 2010 (6th German Conference on Robotics)*, pp. 1–7, 2010.

[79] E. M. Gorostiza, J. L. Lázaro Galilea, F. J. Meca Meca, D. Salido Monzú, F. Espinosa Zapata, and L. Pallarés Puerto, "Infrared sensor system for mobile-robot positioning in intelligent spaces", *Sensors*, vol. 11, no. 5, pp. 5416–5438, 2011, ISSN: 1424-8220. DOI: 10.3390/s110505416. [Online]. Available: http://www.mdpi.com/1424-8220/11/5/5416.

[80] U. Tomohiro, M. Yasushi, I. Kenji, A. Tatsuo, and Y. Jun-ichi, "Pose estimation of objects using multiple id devices", *Journal of the Robotics Society of Japan*, vol. 23, no. 1, pp. 84–94, 2005.

[81] S. Masahiro, K. Takayuki, E. Daniel, I. Hiroshi, and H. Norihiro, "Communication robot for science museum with rfid tags", *Journal of the Robotics Society of Japan*, vol. 24, no. 4, pp. 489–496, 2006.

[82] D. Yu, Y. Ma, and Z. Zhang, "Uhf band tag antenna design in rfid system", *2009 Asia Pacific Microwave Conference*, pp. 512–515, 2009, ISSN: 2165-4727. DOI: 10.1109/APMC.2009.5384188.

[83] I. Mayordomo, A. Ubarretxena, D. Valderas, R. Berenguer, and I. Gutierrez, "Design and analysis of a complete rfid system in the uhf band focused on the backscattering communication and reader architecture", *3rd European Workshop on RFID Systems and Technologies*, pp. 1–6, 2007.

[84] J. Wang and Y. Takahashi, "Slam method based on independent particle filters for landmark mapping and localization for mobile robot based on hf-band rfid system", *Journal of Intelligent & Robotic Systems*, vol. 92, no. 3, pp. 413–433, 2018, ISSN: 1573-0409. DOI: 10.1007/s10846-017-0701-8. [Online]. Available: https://doi.org/10.1007/s10846-017-0701-8.

[85] K. Yano, "A tutorial on particle filters: Filters, smoothing, and parameter estimation", *Journal of the Japan Statistical Society, Japanese Issue*, vol. 44, no. 1, pp. 189–216, 2014. DOI: 10.11329/jjssj.44.189.

[86] W. T. Cochran, J. W. Cooley, D. L. Favin, H. D. Helms, R. A. Kaenel, W. W. Lang, G. C. Maling, D. E. Nelson, C. M. Rader, and P. D. Welch, "What is the fast fourier transform?", *Proceedings of the IEEE*, vol. 55, no. 10, pp. 1664–1674, 1967, ISSN: 0018-9219. DOI: 10.1109/PROC.1967.5957.

[87] J. Wang and Y. Takahashi, "A low-cost light based self-localization system with repeated landmark id for the indoor mobile robot", *The 5th International Workshop on Advanced Computational Intelligence and Intelligent Informatics (IWACIII 2017)*, 2017.